

IP
Flight distance

muon

muon

pion

kaon

$B_{\{s,d\}} \rightarrow \ell^+ \ell^-$ and $b \rightarrow \{s,d\} \ell^+ \ell^-$ process

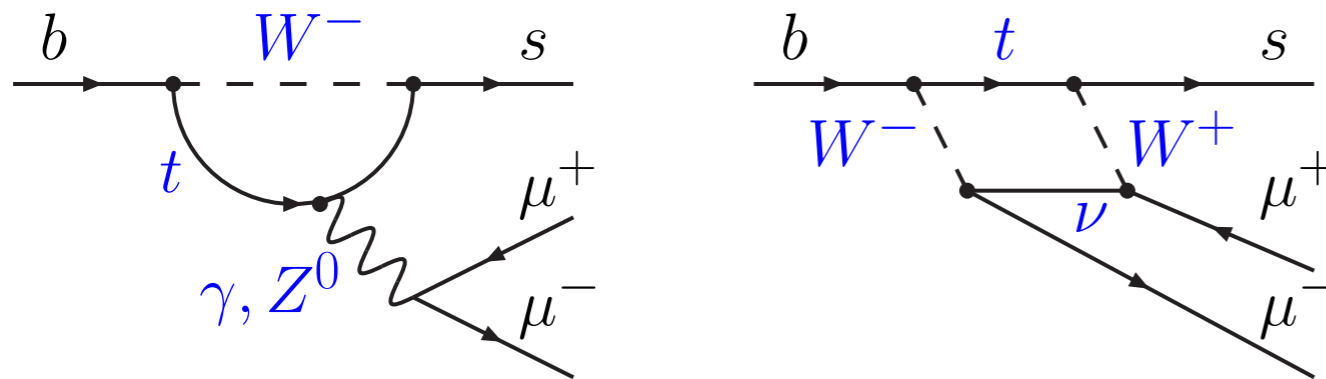
What have we measured and how will these results evolve?

T. Blake

Towards the ultimate precision in flavour physics, Warwick 2018

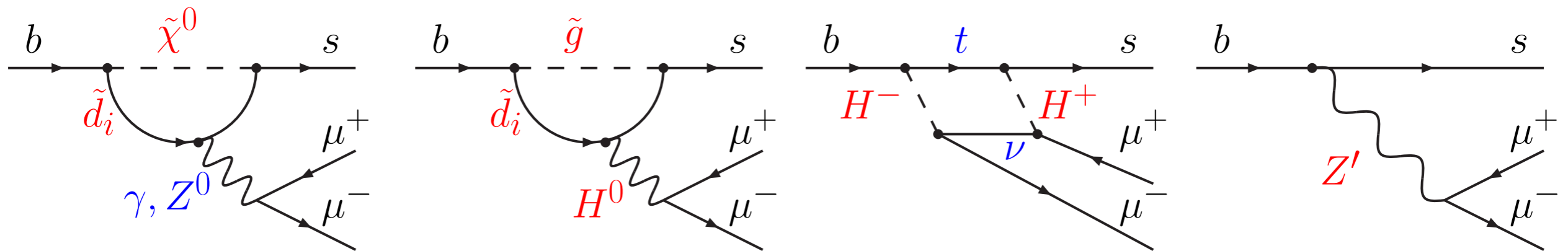
Rare FCNC decays

- Flavour changing neutral current transitions only occur at loop order (and beyond) in the SM.



SM diagrams involve the charged current interaction.

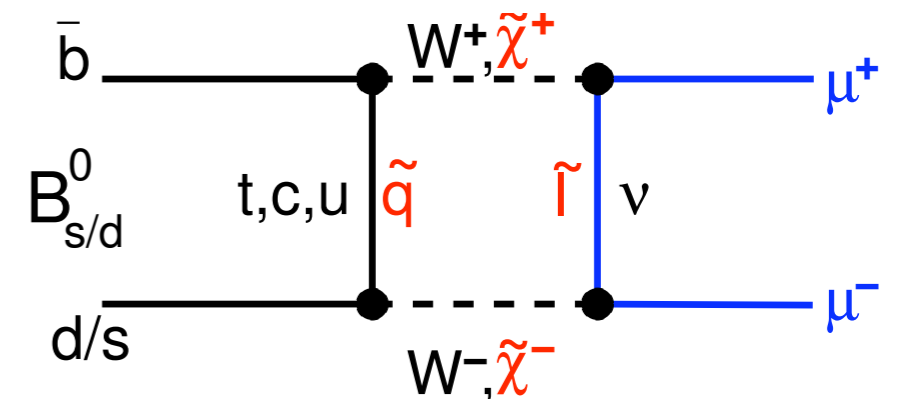
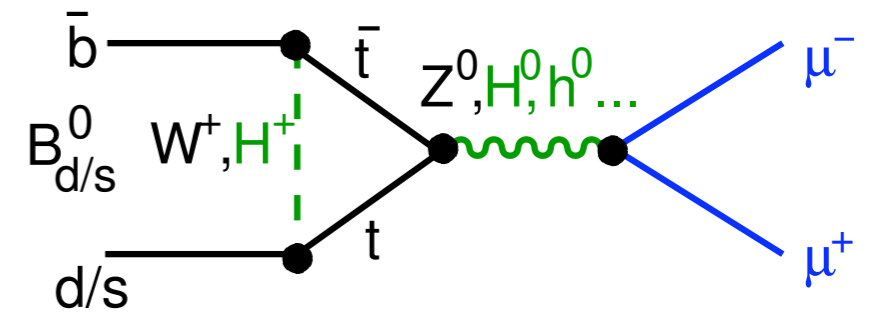
- New particles can also contribute:



Enhancing/suppressing decay rates, introducing new sources of CP violation or modifying the angular distribution of the final-state particles.

Rare leptonic decays

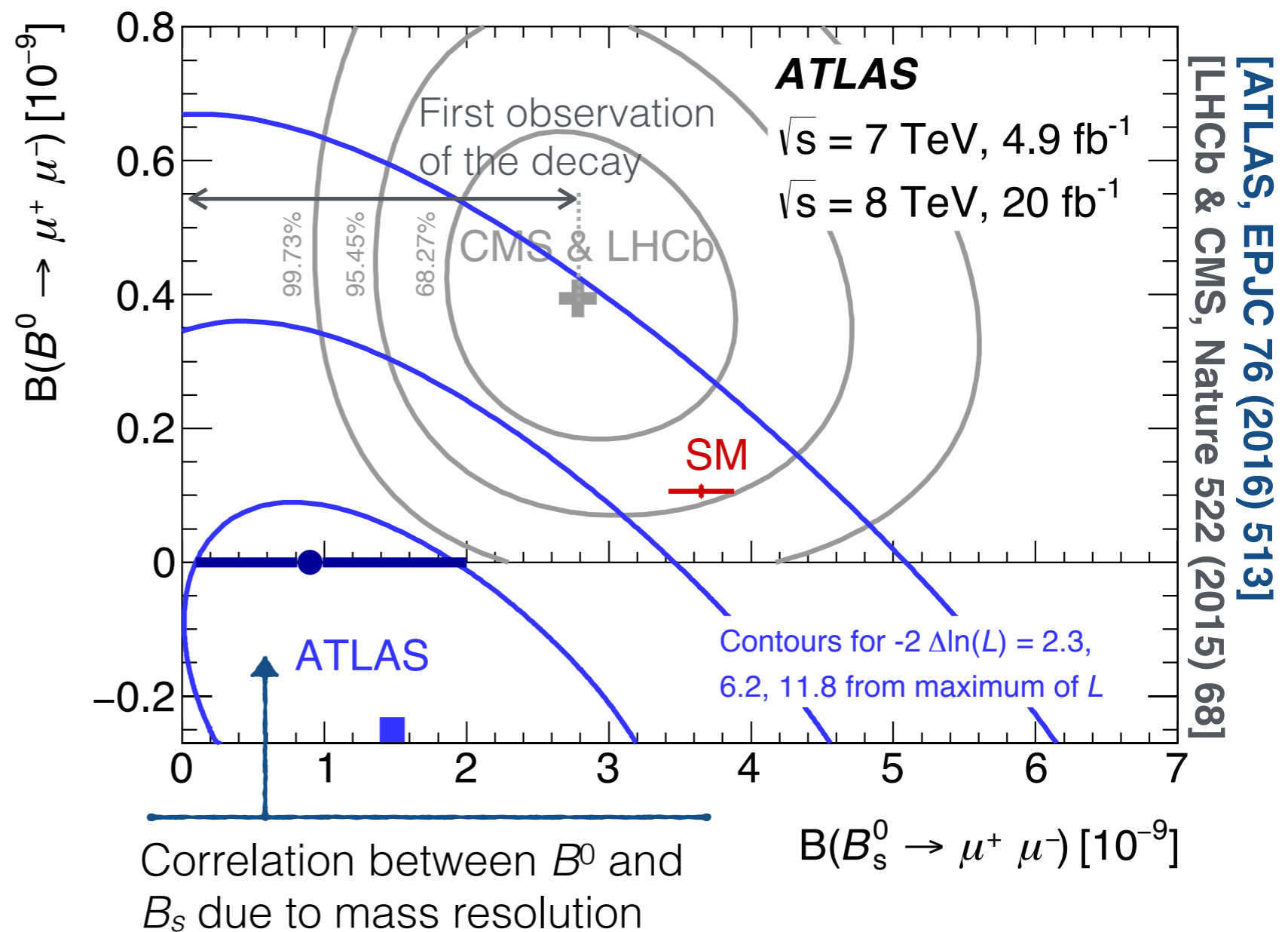
- $B_{\{s,d\}} \rightarrow \mu^+ \mu^-$ are golden modes to study at the LHC.
 - ➔ SM contribution is CKM, loop and helicity suppressed.
 - ➔ Powerful probe of models with new enhanced (pseudo)scalar interactions, e.g. SUSY at high $\tan\beta$.



$$\frac{\mathcal{B}(B_q \rightarrow \ell^+ \ell^-)_{\text{NP}}}{\mathcal{B}(B_q \rightarrow \ell^+ \ell^-)_{\text{SM}}} = \frac{1}{|C_{10}^{\text{SM}}|^2} \left\{ \left(1 - 4 \frac{m_\ell^2}{m_{B_q}} \right) \left| \frac{m_{B_q}}{2m_\ell} (C_S - C'_S) \right|^2 + \left| \frac{m_{B_q}}{2m_\ell} (C_P - C'_P) + (C_{10} - C'_{10}) \right|^2 \right\}$$

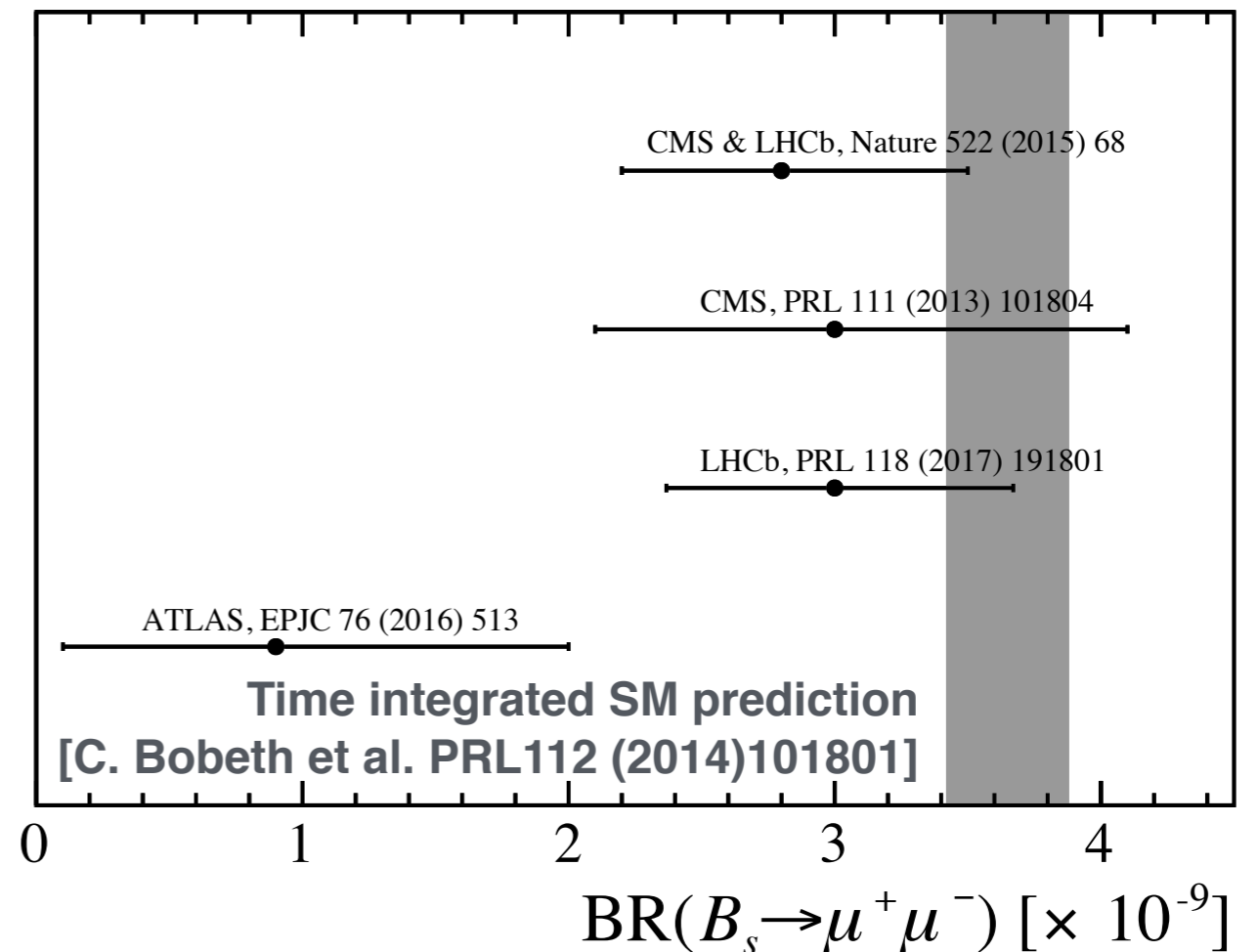
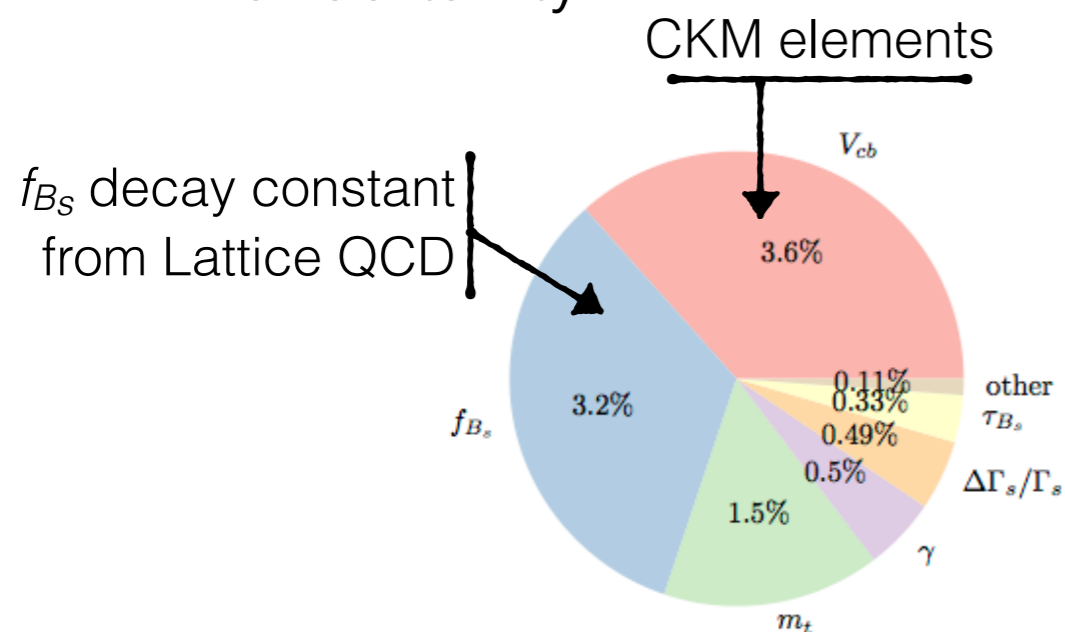
$B_s \rightarrow \mu^+ \mu^-$ results

- Experiments perform a simultaneous fits to determine the B^0 and B_s branching fractions.
- Signal normalised to $B^+ \rightarrow J/\psi K^+$ ($B^0 \rightarrow K^+ \pi^-$ and $B_s \rightarrow J/\psi \phi$ in LHCb), with input on the b -meson production fractions.



$B_s \rightarrow \mu^+ \mu^-$

- Recent LHCb analysis using Run 1 and 2 data ($3\text{fb}^{-1} + 1.4\text{fb}^{-1}$) provides the first single experiment observation of the $B_s \rightarrow \mu^+ \mu^-$ decay at more than 7σ [LHCb, PRL 118 (2017) 191801].
- Measurements are all consistent with the SM expectation.
 - ➔ Can exclude large scalar contributions.
- Branching fraction predicted precisely in the SM with a $\sim 6\%$ uncertainty.

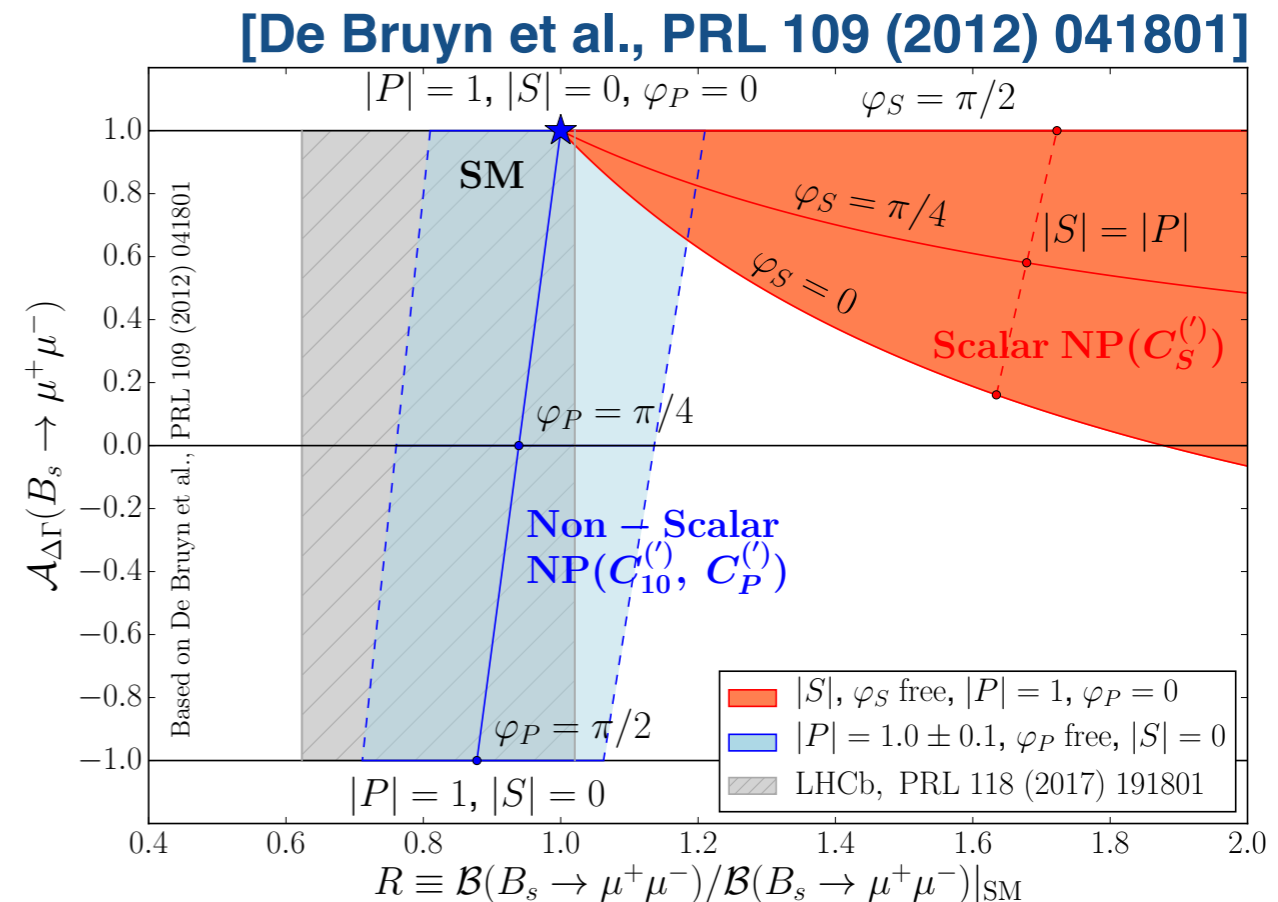


Effective lifetime

- The untagged time dependent decay rate is

$$\Gamma[B_s(t) \rightarrow \mu^+ \mu^-] + \Gamma[\bar{B}_s(t) \rightarrow \mu^+ \mu^-] \propto e^{-t/\tau_{B_s}} \left\{ \cosh\left(\frac{\Delta\Gamma_s}{2}t\right) + A_{\Delta\Gamma} \sinh\left(\frac{\Delta\Gamma_s}{2}t\right) \right\}$$

- $A_{\Delta\Gamma}$ provides additional separation between scalar and pseudoscalar contributions.
- In the SM $A_{\Delta\Gamma} = 1$ such that the system evolves with the lifetime of the heavy B_s mass eigenstate.



$B_s \rightarrow \mu^+ \mu^-$ effective lifetime

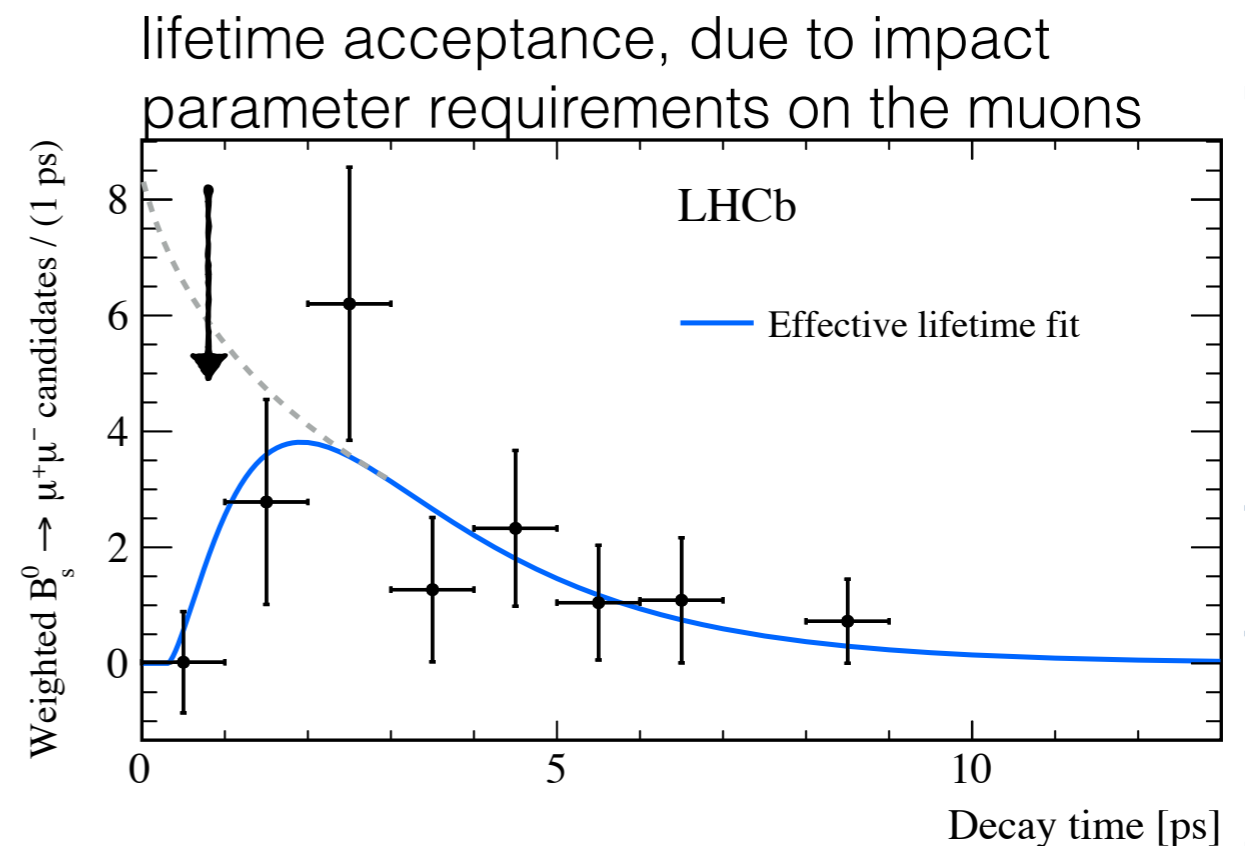
- The $A_{\Delta\Gamma}$ parameter modifies the effective lifetime of the decay:

$$\tau_{\text{eff}} = \frac{\tau_{B_s}}{1 - y_s^2} \left(\frac{1 + 2A_{\Delta\Gamma} y_s + y_s^2}{1 + A_{\Delta\Gamma} y_s} \right) \quad \text{where } y_s = \tau_{B_s} \frac{\Delta\Gamma}{2}$$

- LHCb have performed a first measurement of τ_{eff} , giving

$$\tau[B_s^0 \rightarrow \mu^+ \mu^-] = 2.04 \pm 0.44 \pm 0.05 \text{ ps}$$

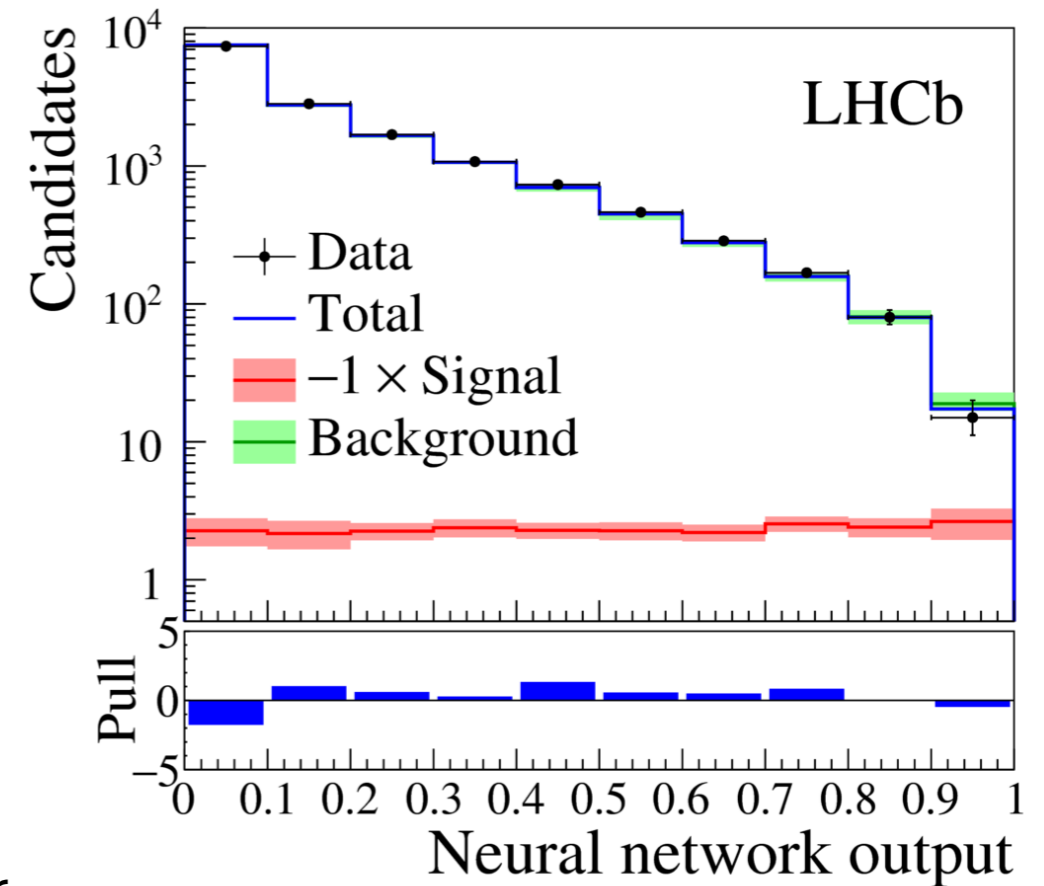
NB Not yet sensitive to $A_{\Delta\Gamma}$ (the stat. uncertainty is larger than the change in the lifetime from $\Delta\Gamma_s$). This will become more interesting during Run 3 and 4.



[LHCb, PRL 118 (2017) 191801]

$B_{\{s,d\}} \rightarrow \tau^+ \tau^-$

- LHCb performs a search for $B_{\{s,d\}} \rightarrow \tau^+ \tau^-$ decays using $\tau^- \rightarrow \pi^- \pi^+ \pi^- \nu_\tau$.
 - ➔ Exploit the $\tau^- \rightarrow a_1(1260)^- \nu_\tau$ and $a_1(1260)^- \rightarrow \rho(770)^0 \pi^-$ decays to select signal/control regions of dipion mass.
- Fit Neural network response to discriminate signal from background.
 - ➔ Ditaup mass is not a good discriminator due to missing neutrino energy.
- LHCb sets limits on:
 - $\mathcal{B}(B_s^0 \rightarrow \tau^+ \tau^-) < 6.8 \times 10^{-3}$ (95% CL)
 - $\mathcal{B}(B^0 \rightarrow \tau^+ \tau^-) < 2.1 \times 10^{-3}$ (95% CL)

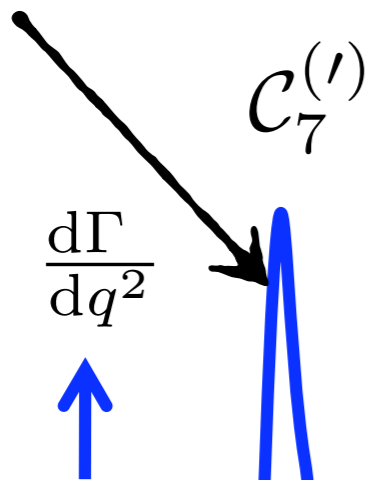


[LHCb, PRL 118 (2017) 251802]

First limit on $B_s \rightarrow \tau^+ \tau^-$ and best limit on $B^0 \rightarrow \tau^+ \tau^-$

$b \rightarrow \{s, d\} \ell^+ \ell^-$ mass spectrum

Photon pole enhancement
(for $B \rightarrow V \ell \ell$ decays)



Spectrum dominated by narrow charmonium resonances. (vetoed in data)

$J/\psi(1S)$

$\psi(2S)$

$C_7^{(l)} C_9^{(l)}$
interference

$C_9^{(l)}$ and $C_{10}^{(l)}$

Long distance contributions from $c\bar{c}$ above open charm threshold

Form-factors from LCSR calculations

Form-factors from Lattice QCD

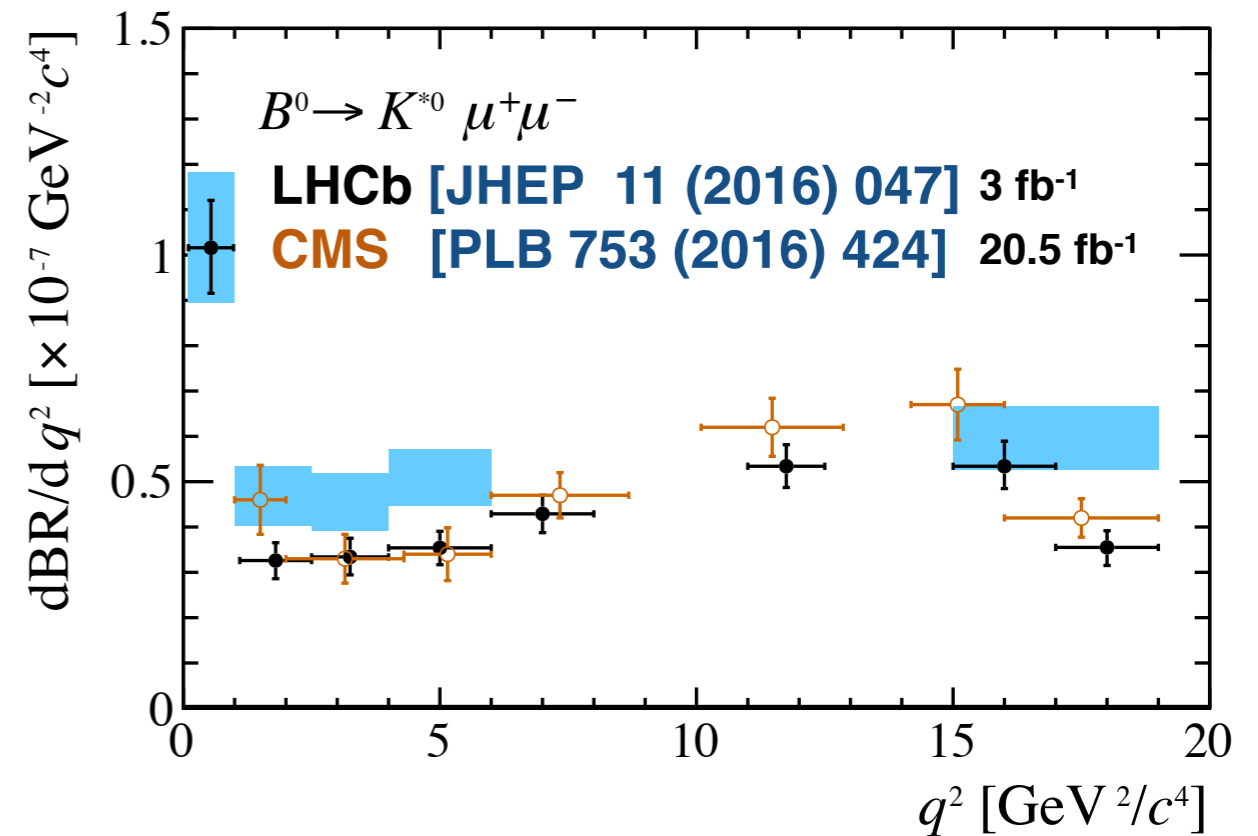
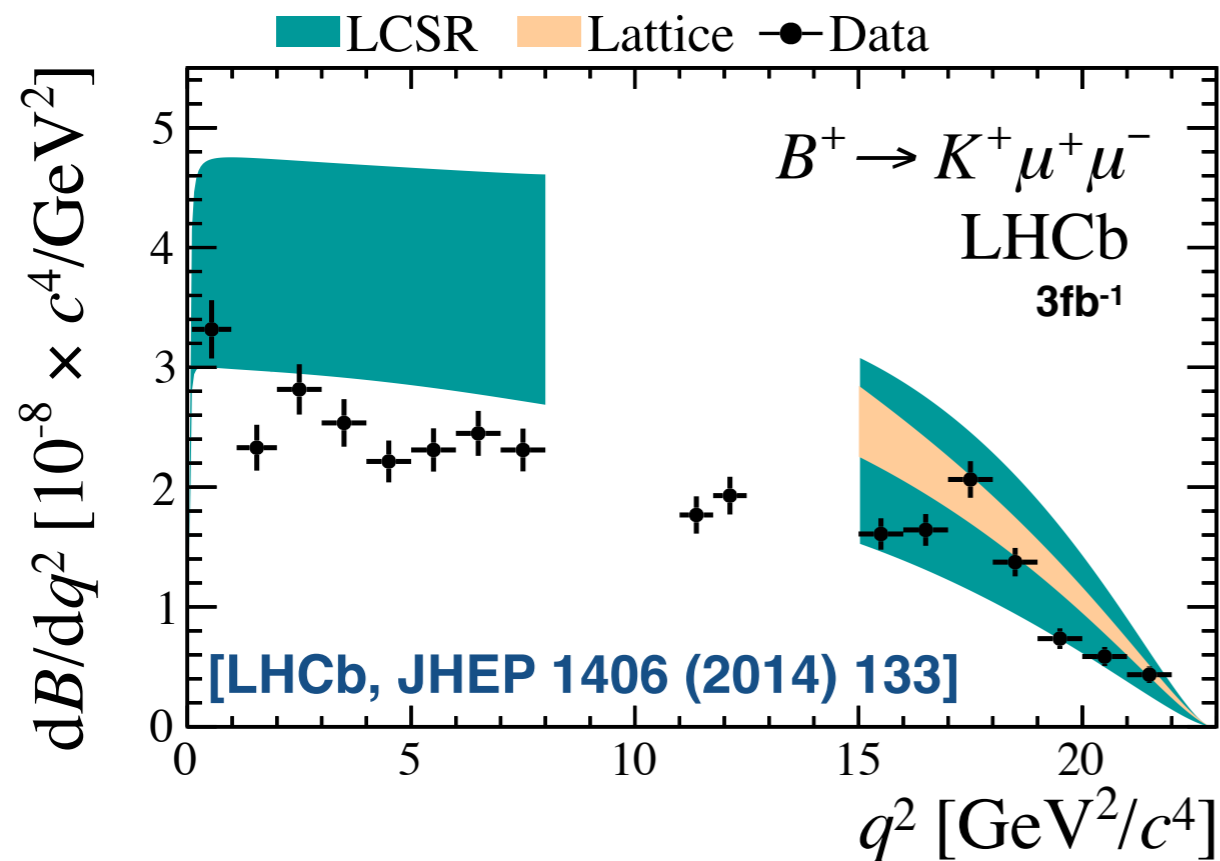
parameterisation

$4 [m(\mu)]^2$

q^2 (mass squared)

Branching fraction measurements

- We already have precise measurements of branching fractions in the run1 datasets with at least comparable precision to SM expectations:

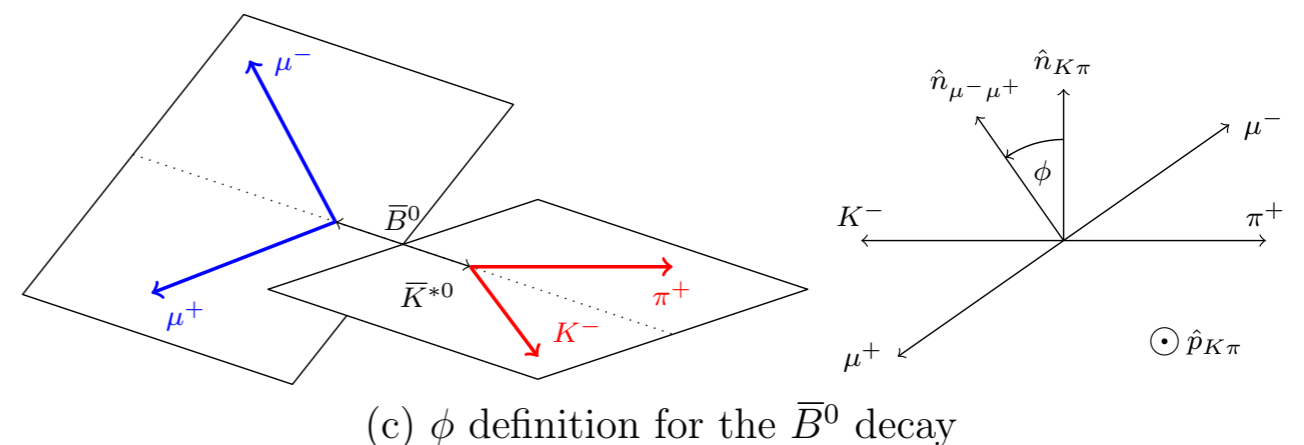
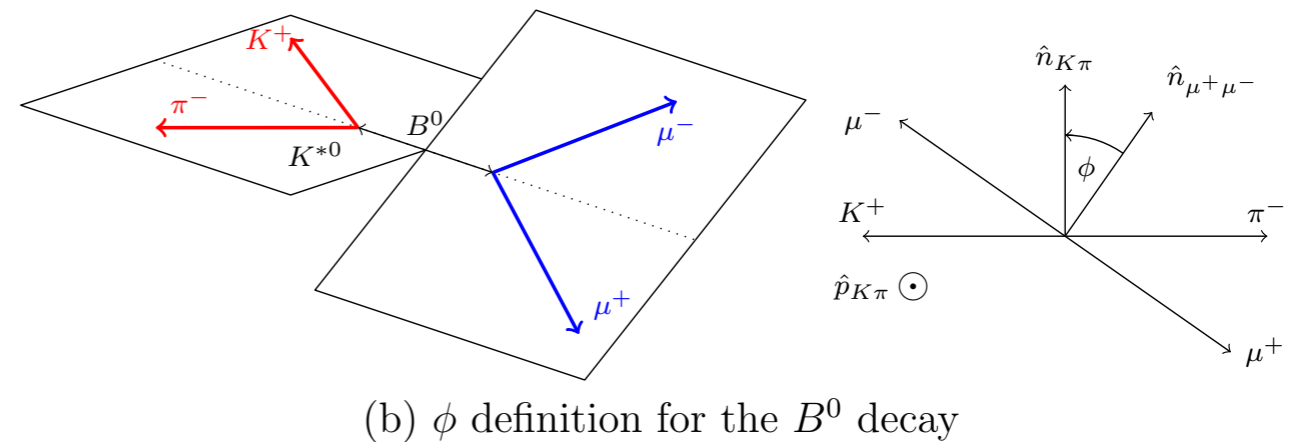
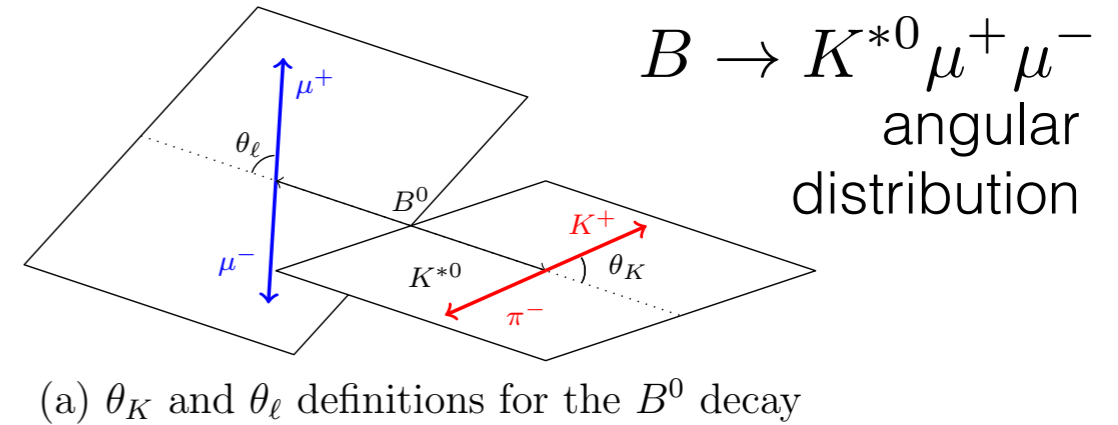


- SM predictions have large theoretical uncertainties from hadronic form factors (3 for $B \rightarrow K$ and 7 for $B \rightarrow K^*$ decays). For details see [Bobeth et al JHEP 01 (2012) 107] [Bouchard et al. PRL111 (2013) 162002] [Altmannshofer & Straub, EPJC (2015) 75 382].

Angular observables

- Multibody final-states:
 - ➔ Angular distribution provides many observables that are sensitive to BSM physics.
 - ➔ Constraints are orthogonal to branching fraction measurements, both in their impact in global fits and in terms of experimental uncertainties.


eg $B \rightarrow K^{*0} \ell^+ \ell^-$ system described by three angles and the dimuon invariant mass squared, q^2 .




$B^0 \rightarrow K^{*0} \mu^+ \mu^-$ angular distribution

Complex angular distribution:

$$\frac{1}{d(\Gamma + \bar{\Gamma})/dq^2} \frac{d^3(\Gamma + \bar{\Gamma})}{d\vec{\Omega}} \Big|_P = \frac{9}{32\pi} \left[\frac{3}{4} (1 - F_L) \sin^2 \theta_K + F_L \cos^2 \theta_K + \right. \\ \left. + \frac{1}{4} (1 - F_L) \sin^2 \theta_K \cos 2\theta_l - F_L \cos^2 \theta_K \cos 2\theta_l + S_3 \sin^2 \theta_K \sin^2 \theta_l \cos 2\phi \right. \\ \left. + S_4 \sin 2\theta_K \sin 2\theta_l \cos \phi + S_5 \sin 2\theta_K \sin \theta_l \cos \phi \right. \\ \left. + \frac{4}{3} A_{FB} \sin^2 \theta_K \cos \theta_l + S_7 \sin 2\theta_K \sin \theta_l \sin \phi \right. \\ \left. + S_8 \sin 2\theta_K \sin 2\theta_l \sin \phi + S_9 \sin^2 \theta_K \sin^2 \theta_l \sin 2\phi \right]$$

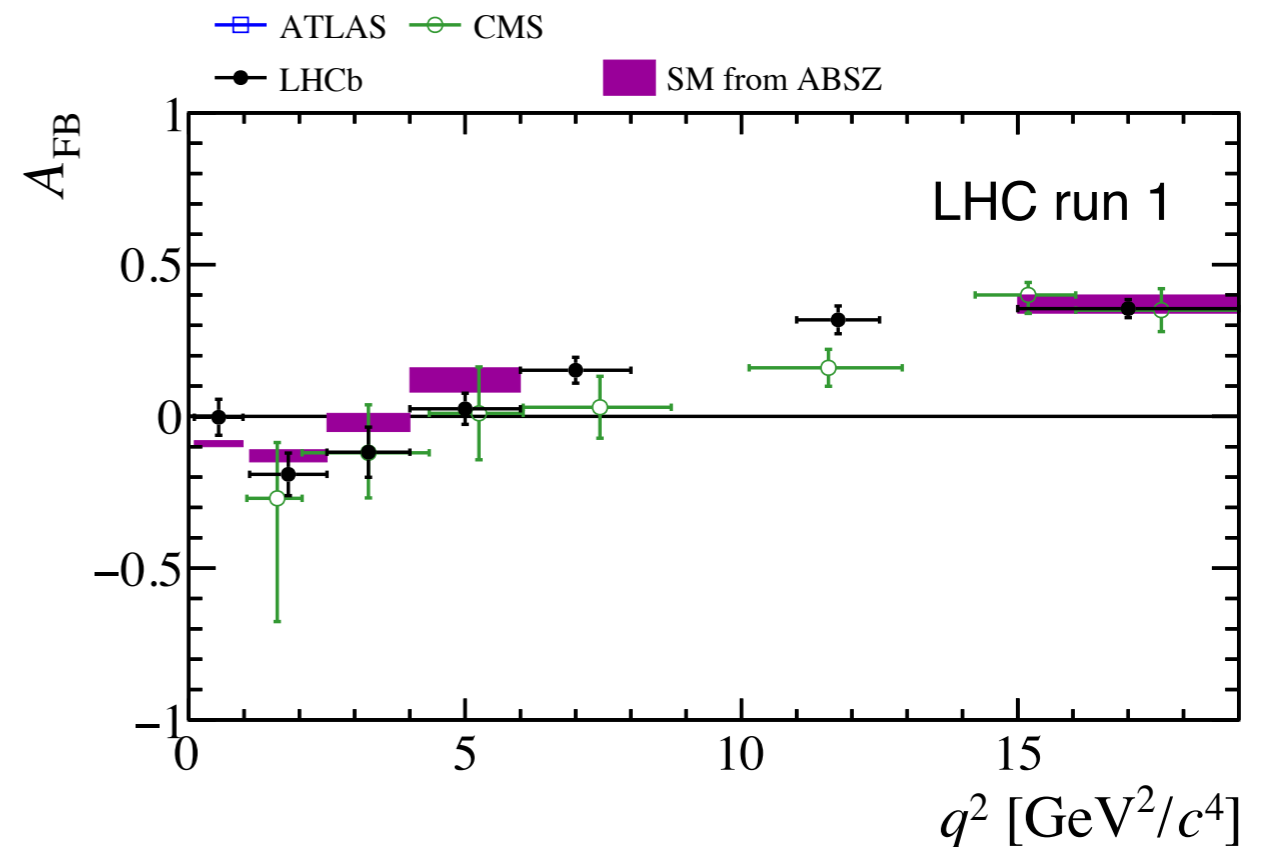
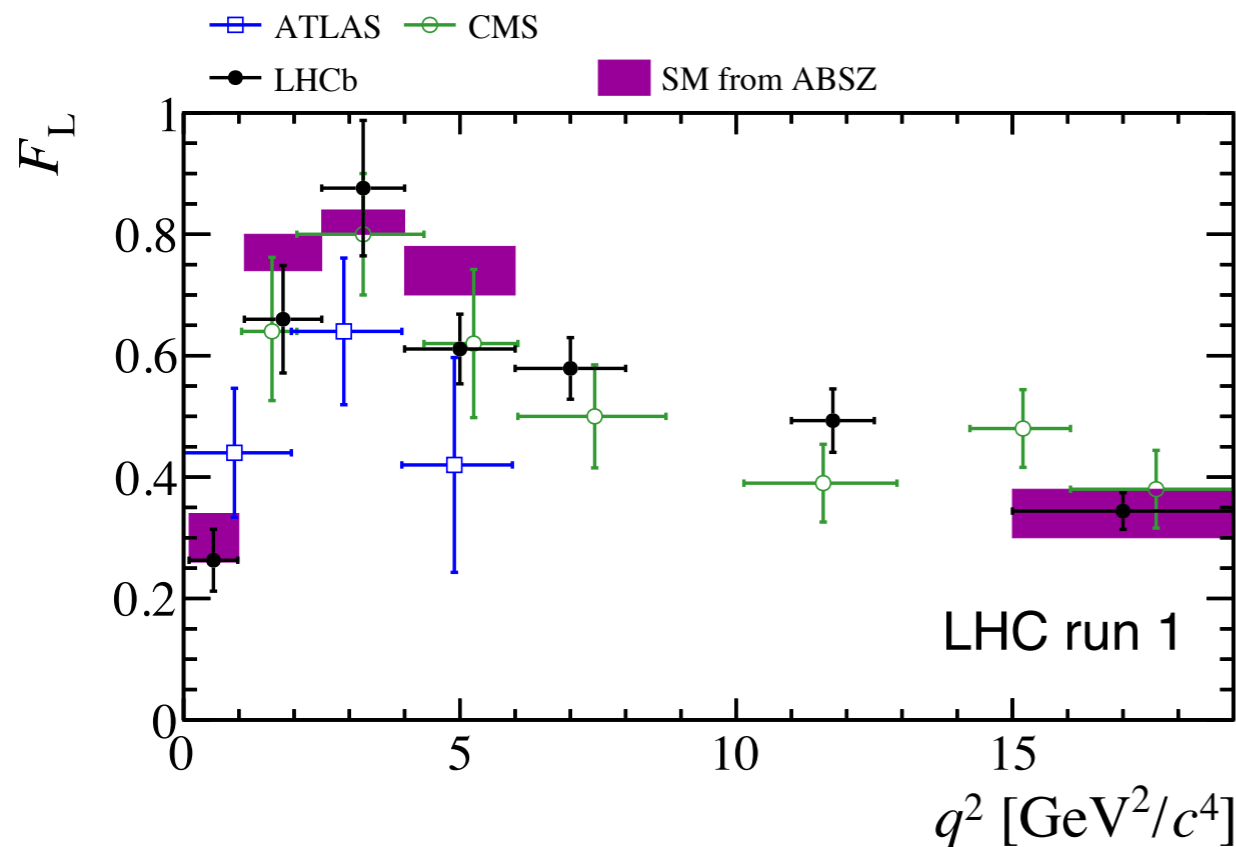
fraction of longitudinal polarisation of the K^* 

forward-backward asymmetry of the dilepton system 

The observables depend on form-factors for the $B \rightarrow K^*$ transition plus the underlying short distance physics (Wilson coefficients).

Experiments can reduce the complexity by folding the angular distribution, see **[LHCb, PRL 111 (2013) 191801]**

$B^0 \rightarrow K^{*0} \mu^+ \mu^-$ angular observables

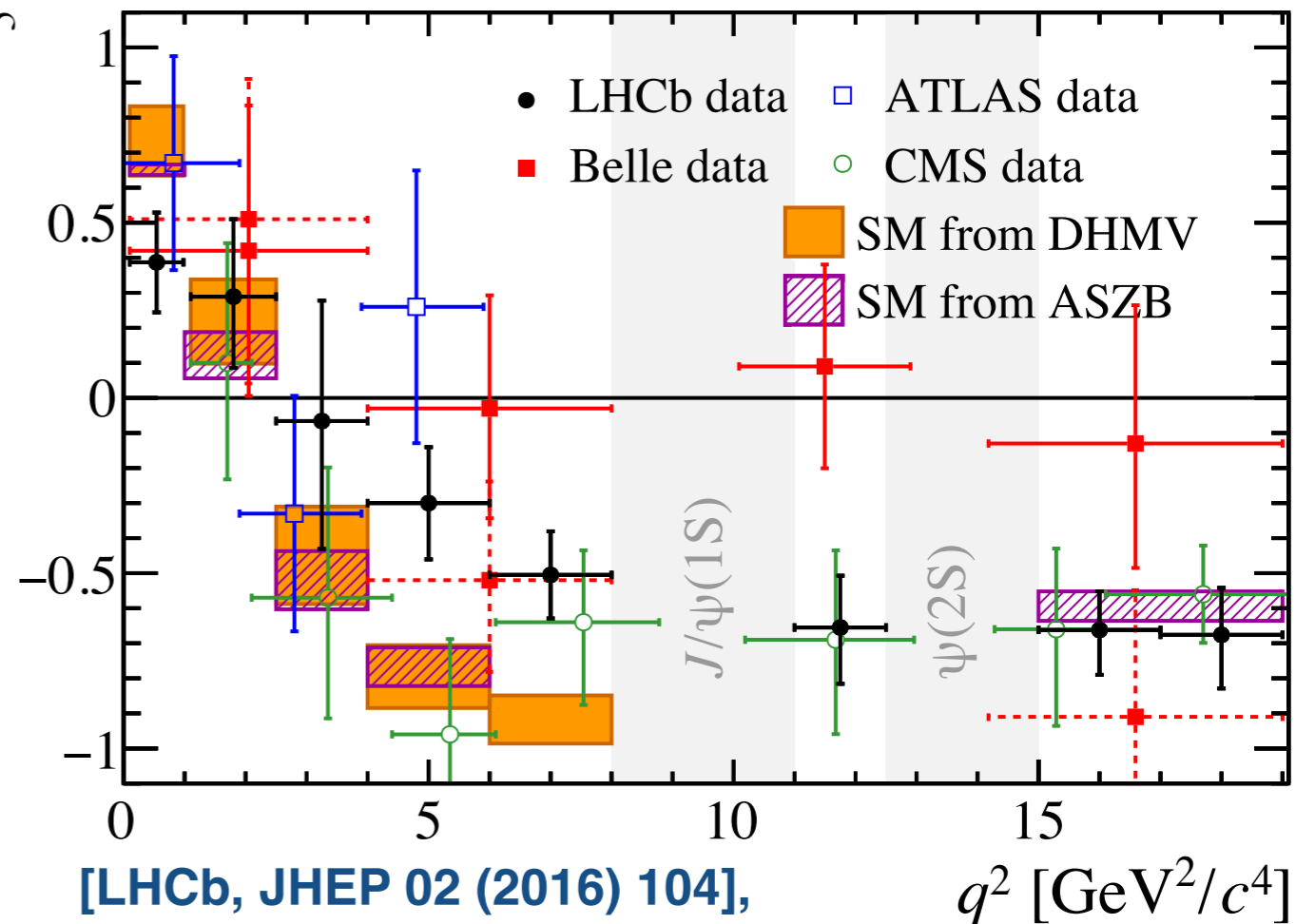


- Overlaying results for F_L and A_{FB} from LHCb [[JHEP 02 \(2016\) 104](#)], CMS [[PLB 753 \(2016\) 424](#)] and ATLAS [[ATLAS-CONF-2017-023](#)].
- SM predictions based on
 - [[Altmannshofer & Straub, EPJC 75 \(2015\) 382](#)]
 - [[LCSR form-factors from Bharucha, Straub & Zwicky, JHEP 08 \(2016\) 98](#)]
 - [[Lattice form-factors from Horgan, Liu, Meinel & Wingate arXiv:1501.00367](#)]
 } Joint fit performed

Form-factor “free” observables

- In QCD factorisation/SCET there are only two form-factors
 → One is associated with A_0 and the other $A_{||}$ and A_{\perp} .
- Can then construct ratios of observables which are independent of these soft form-factors at leading order, e.g.

$$P'_5 = S_5 / \sqrt{F_L(1 - F_L)}$$



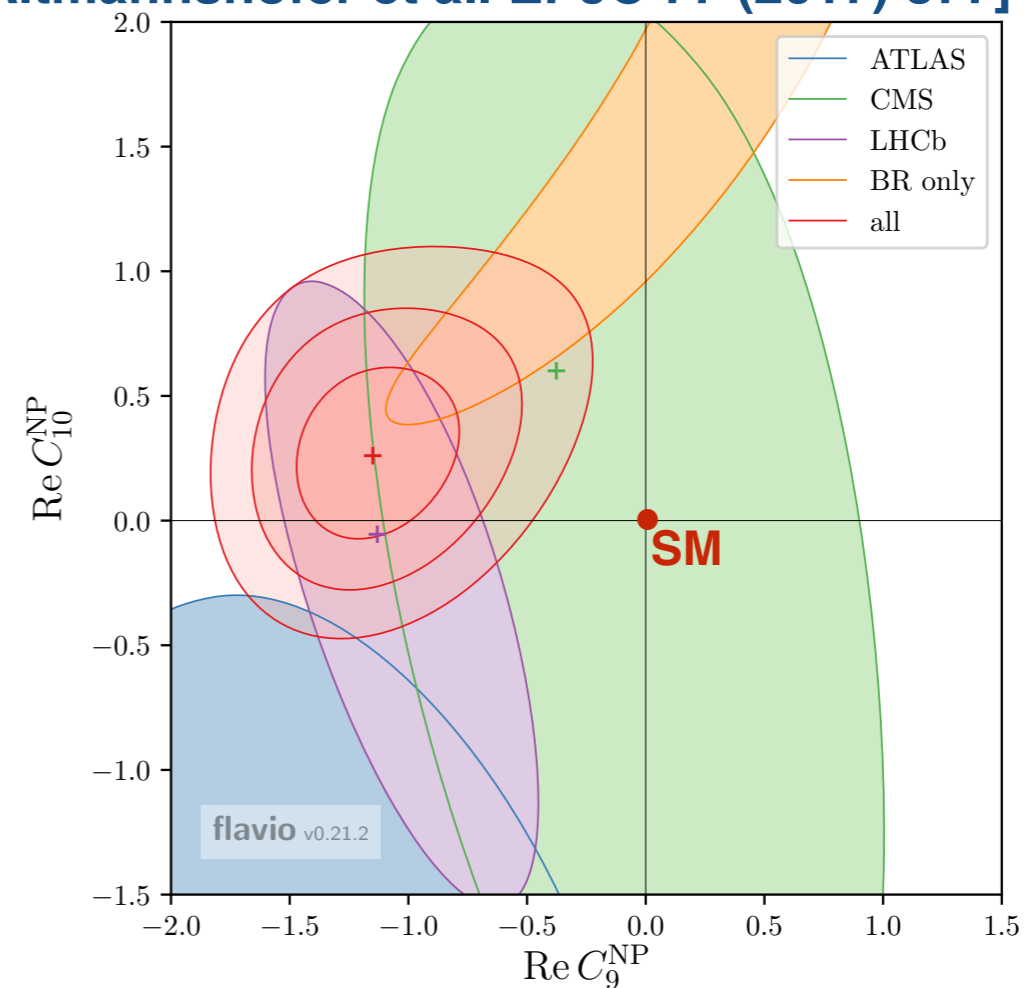
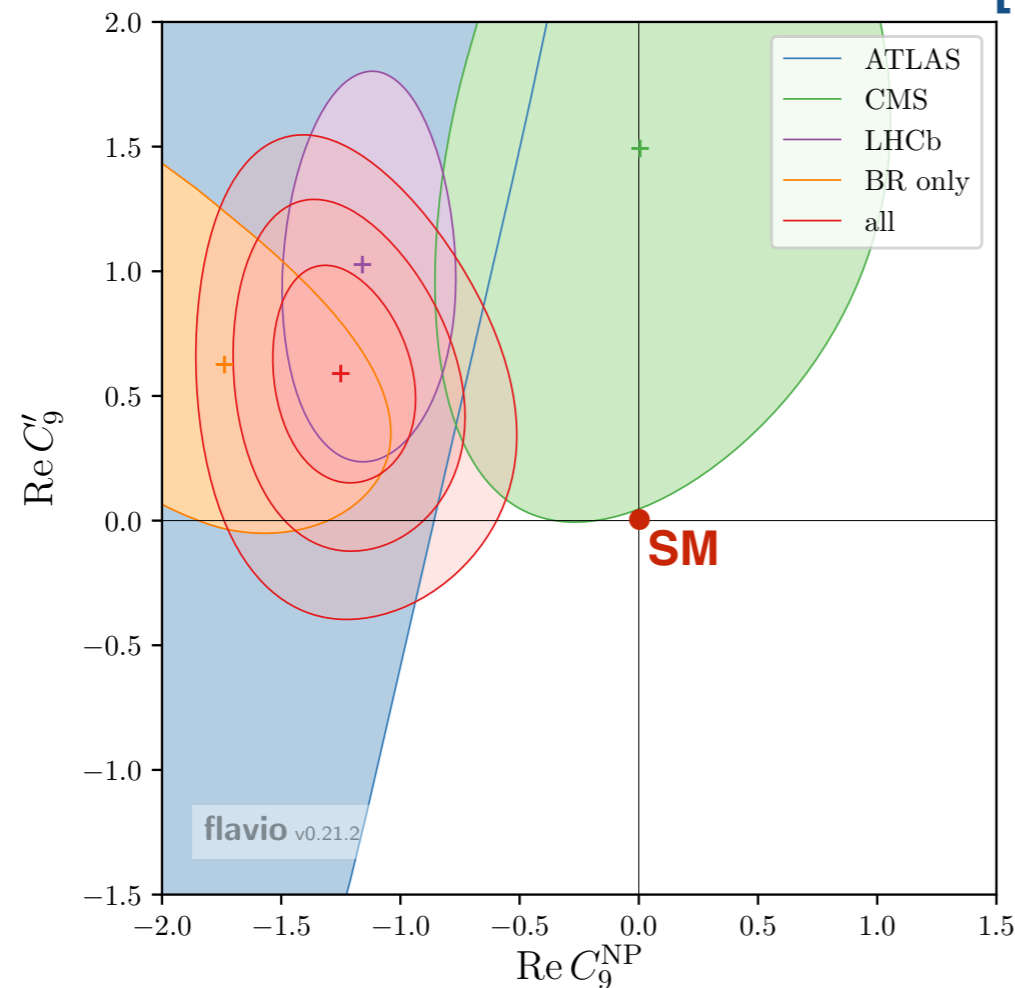
[LHCb, JHEP 02 (2016) 104],
 [Belle, PRL 118 (2017) 111801],
 [ATLAS-CONF-2017-023],
 [CMS-PAS-BPH-15-008]

- P'_5 is one of a set of so-called form-factor free observables that can be measured [Descotes-Genon et al. JHEP 1204 (2012) 104].

Global fits

- Several attempts to interpret our results through global fits to $b \rightarrow s$ data.

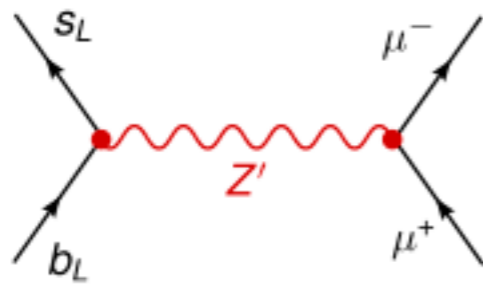
[W. Altmannshofer et al. EPJC 77 (2017) 377]



- General pattern of consistency between experiments/measurements.
Data favours a modified vector coupling ($C_9^{NP} \neq 0$) at 4-5 σ .

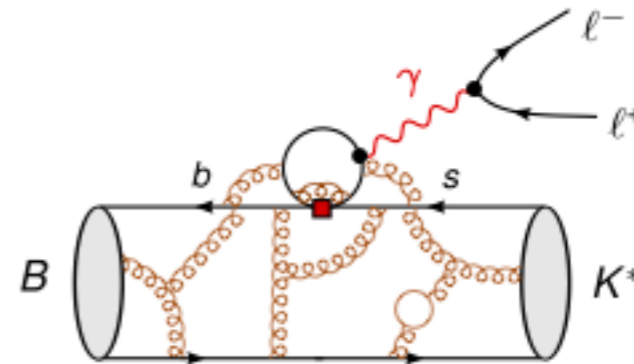
Interpretation of global fits

Optimist's view point



Vector-like contribution could come from e.g. new tree level contribution from a Z' with a mass of a few TeV.

Pessimist's view point



Vector-like contribution could point to a problem with our understanding of QCD, e.g. are we correctly estimating the contribution for charm loops that produce dimuon pairs via a virtual photon?

More work needed from experiment/theory to disentangle the two

Lepton universality tests

- In the SM, ratios

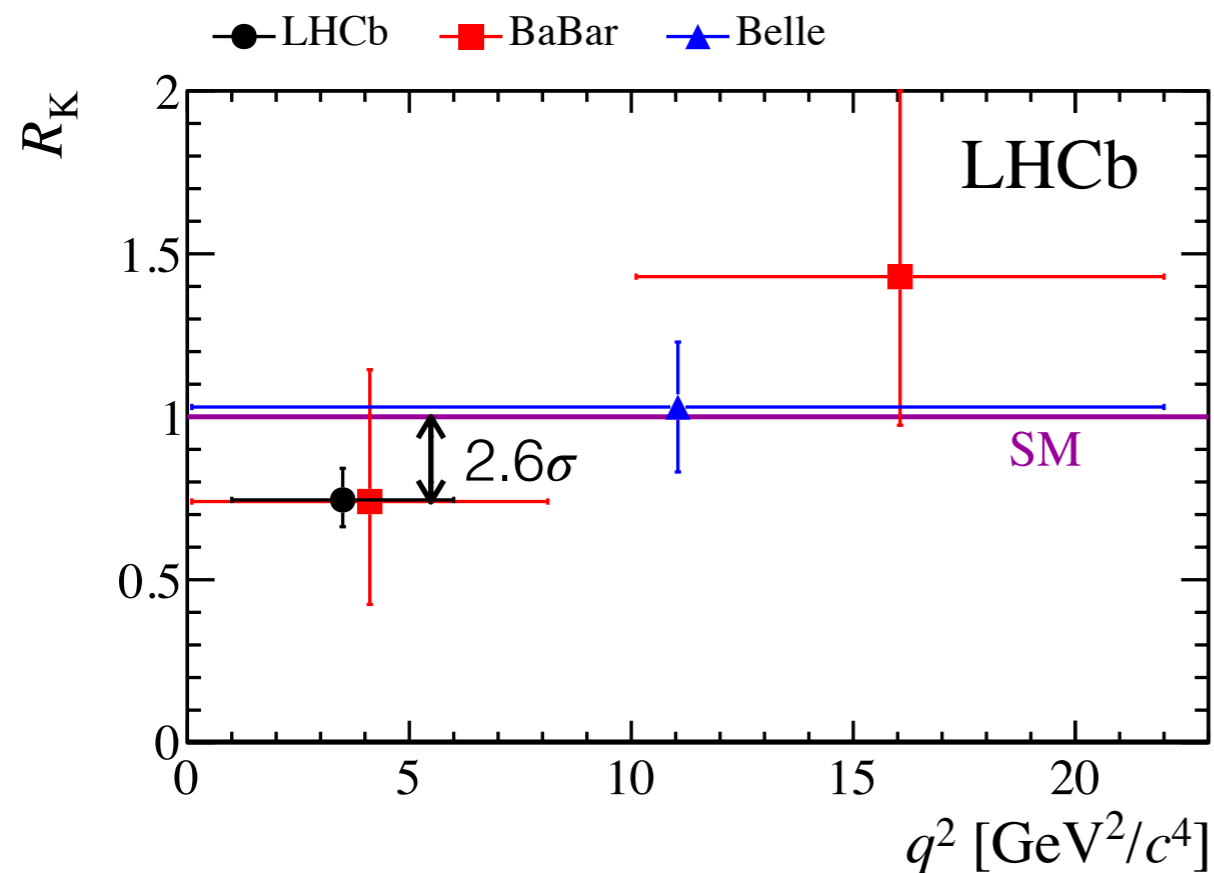
$$R_K = \frac{\int d\Gamma[B^+ \rightarrow K^+ \mu^+ \mu^-]/dq^2 \cdot dq^2}{\int d\Gamma[B^+ \rightarrow K^+ e^+ e^-]/dq^2 \cdot dq^2}$$

only differ from unity by phase space — the dominant SM processes couple equally to the different lepton flavours.

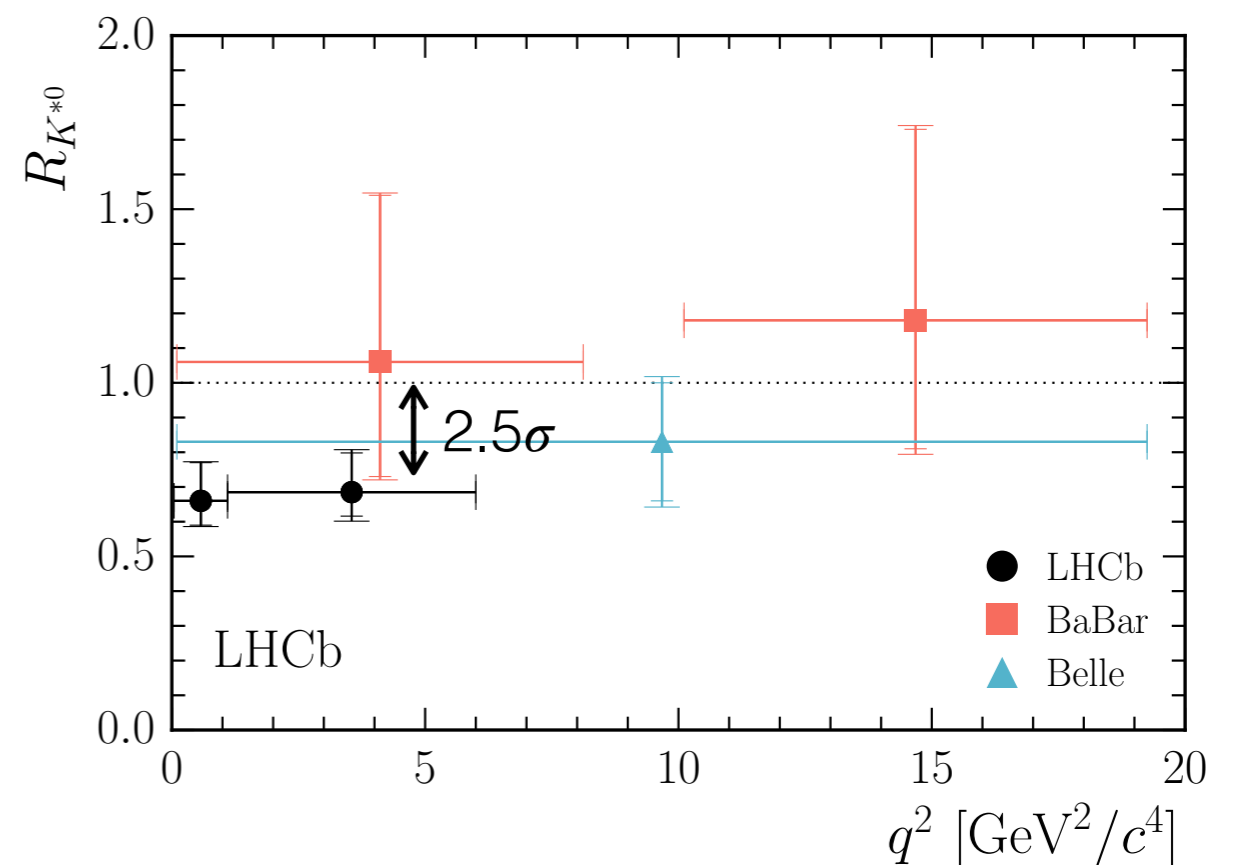
- Theoretically clean since hadronic uncertainties cancel in the ratio.
- Experimentally challenging due to differences in muon/electron reconstruction (in particular Bremsstrahlung from the electrons).
 - ➔ Take double ratios with $B \rightarrow J/\psi X$ decays to cancel possible sources of systematic uncertainty.
 - ➔ Correct for migration of events in q^2 due to FSR/Bremsstrahlung using MC (with PHOTOS).

Lepton universality tests

- We have interesting hints of non-universal lepton couplings in LHCb run 1 dataset:



[LHCb, PRL 113 (2014) 151601]
 [LHCb, JHEP 08 (2017) 055]
 [BaBar, PRD 86 (2012) 032012]
 [Belle, PRL 103 (2009) 171801]



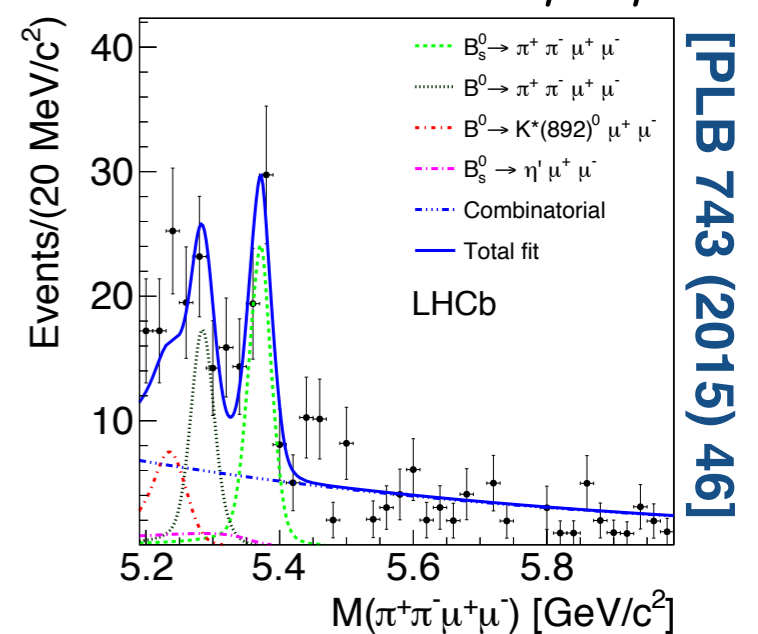
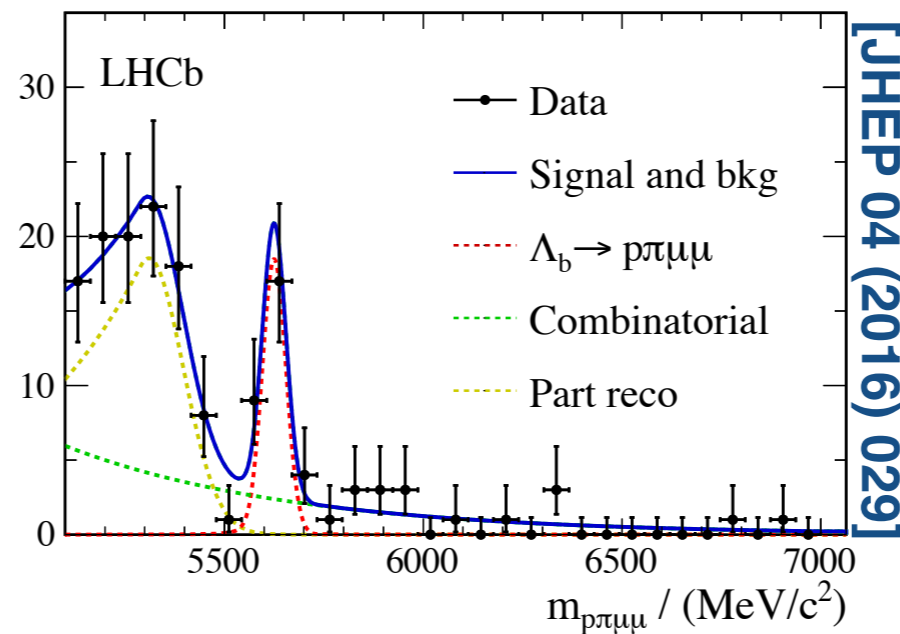
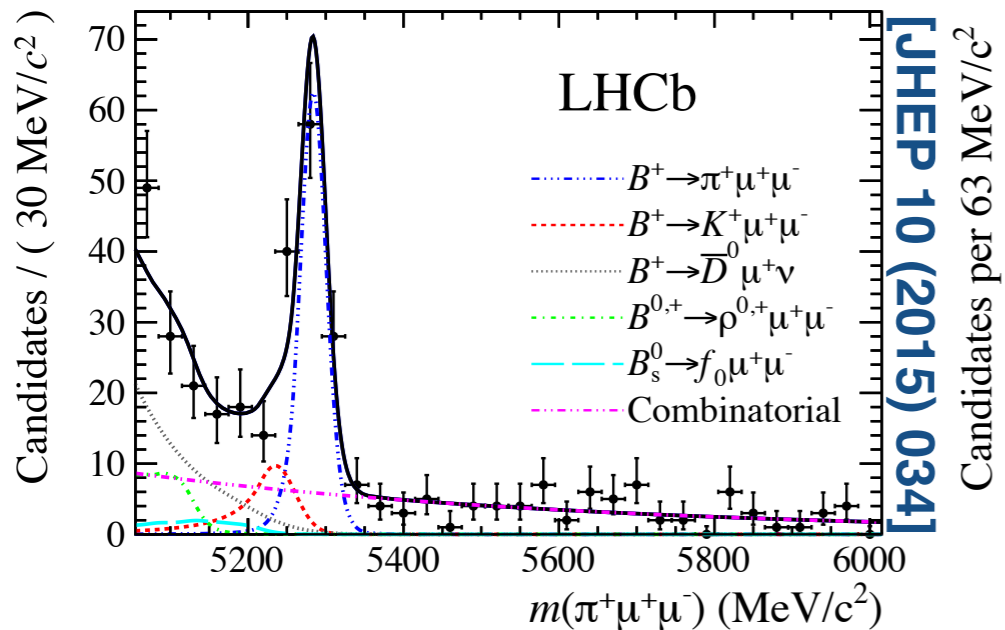
NB $R_K \approx 0.8$ is a prediction of one class of model explaining the $B^0 \rightarrow K^{*0} \mu^+ \mu^-$ angular observables, see $L_\mu - L_\tau$ models
W. Altmannshofer et al. [PRD 89 (2014) 095033]

$b \rightarrow d \ell^+ \ell^-$ processes

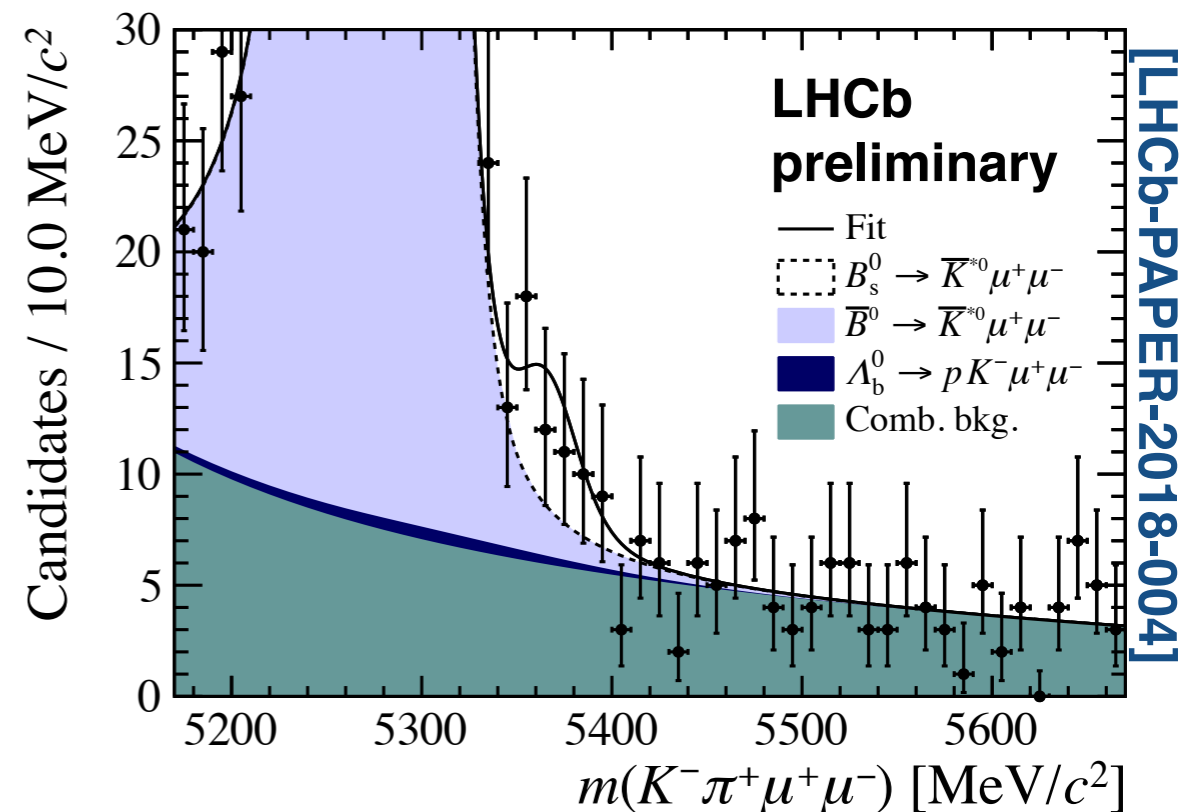
$$B^+ \rightarrow \pi^+ \mu^+ \mu^-$$

$$\Lambda_b \rightarrow N^* \mu^+ \mu^-$$

$$B^0 \rightarrow \pi^+ \pi^- \mu^+ \mu^-$$

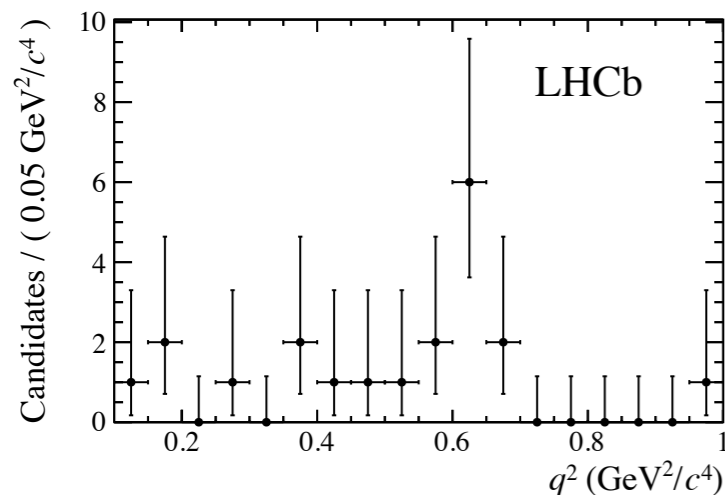
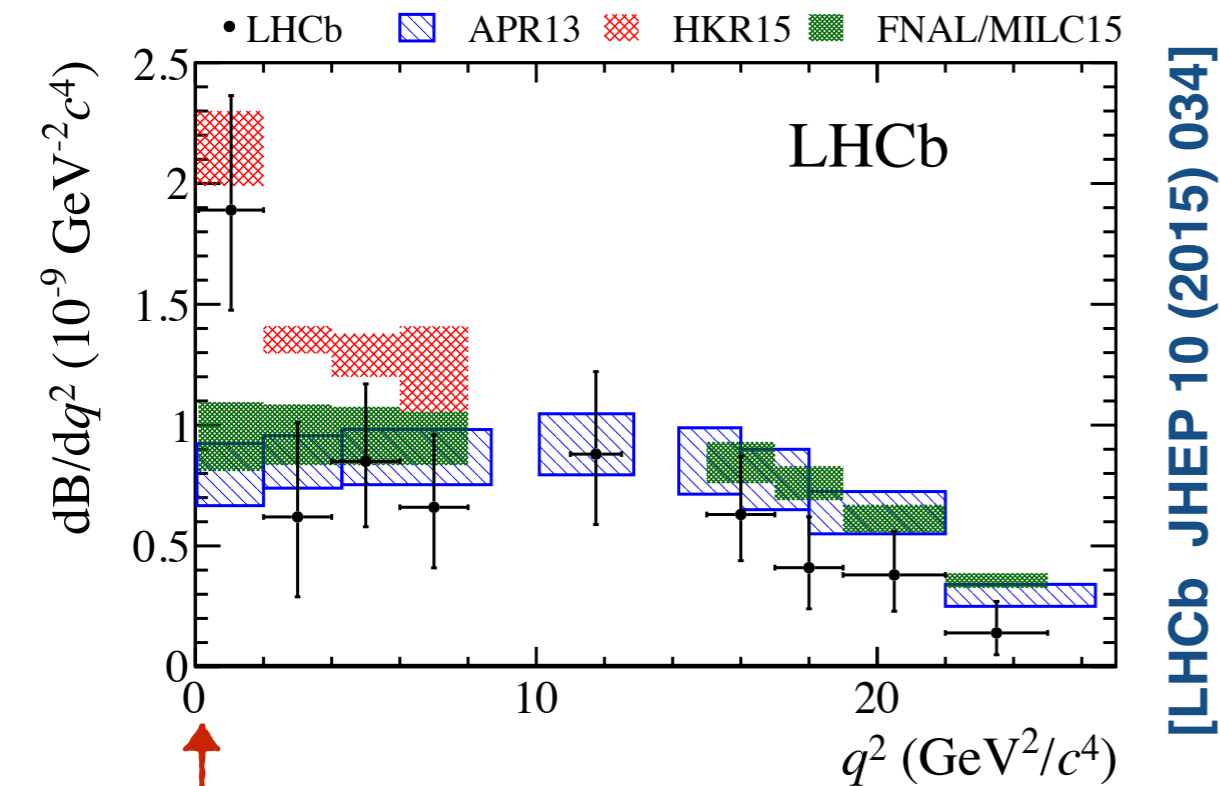


- We also have access to $b \rightarrow d \mu^+ \mu^-$ processes in the LHC Run 1 and 2 datasets.
- First observation of $B^+ \rightarrow \pi^+ \mu^+ \mu^-$ and $\Lambda \rightarrow N^* \mu^+ \mu^-$ and first evidence for $B_s \rightarrow K^{*0} \mu^+ \mu^-$ and $B^0 \rightarrow \pi^+ \pi^- \mu^+ \mu^-$ (in the ρ resonance region).



$B^+ \rightarrow \pi^+ \mu^+ \mu^-$ branching fraction

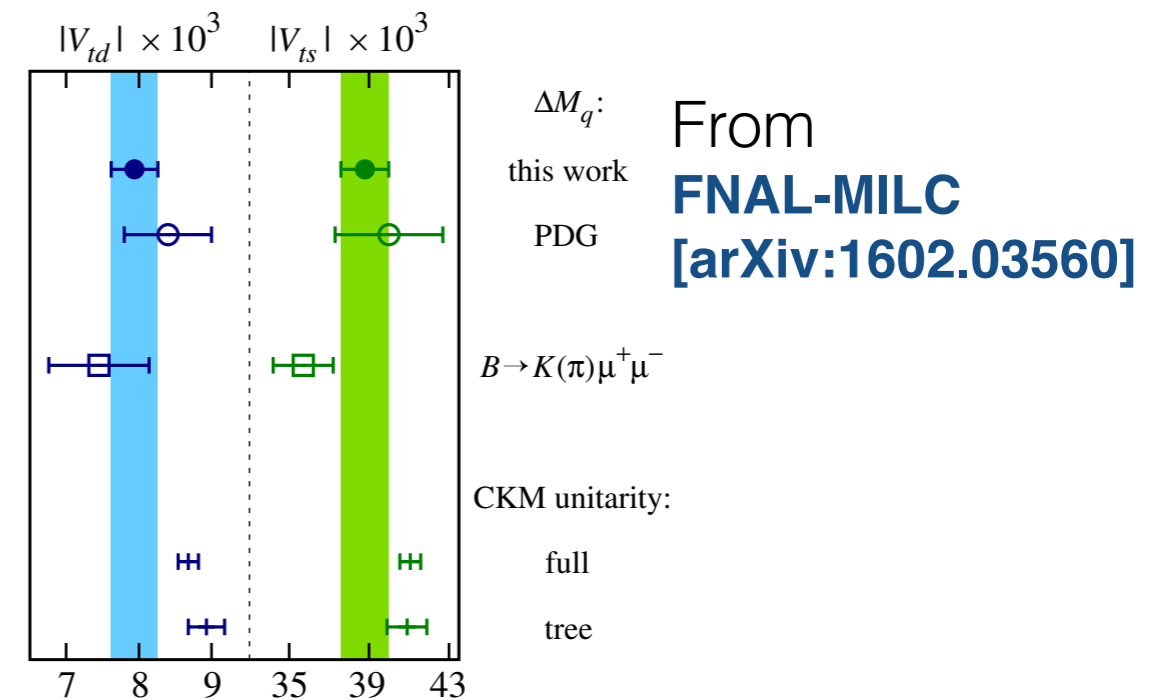
- Determine branching fraction by normalising to $B^+ \rightarrow J/\psi K^+$



Enhancement for $q^2 < 1 \text{ GeV}^2/c^4$ due to light resonances (ρ, ω).

These are included in HKR 15

Can also use and $B^+ \rightarrow K^+ \mu^+ \mu^-$ and $B^+ \rightarrow \pi^+ \mu^+ \mu^-$ to determine the CKM elements V_{ts} and V_{td} (see e.g. [Du et al arXiv:1510.02349])



Ratio consistent with MFV hypothesis.

SM predictions [Ali et al. arXiv:1312.2523], [Hambrock et al. arXiv:1506.07760] and [Bailey et al. arXiv:1507.01618].

Projections

Observable	Run 1 result	8 fb ⁻¹	50 fb ⁻¹	300 fb ⁻¹
Yield $B^0 \rightarrow K^{*0} \mu^+ \mu^-$	2398 ± 57 [74]	9175	70480	435393
Yield $B_s^0 \rightarrow \phi \mu^+ \mu^-$	432 ± 24 [75]	1653	12697	78436
Yield $B^+ \rightarrow K^+ \mu^+ \mu^-$	4746 ± 81 [83]	18159	139491	861709
Yield $B^+ \rightarrow \pi^+ \mu^+ \mu^-$	93 ± 12 [84]	355	2725	16831
Yield $\Lambda_b^0 \rightarrow \Lambda \mu^+ \mu^-$	373 ± 25 [85]	1426	10957	67688
Yield $B^+ \rightarrow K^+ e^+ e^-$ ($1 < q^2 < 6 \text{ GeV}^2/c^4$)	254 ± 29 [76]	972	7465	46118
Yield $B^0 \rightarrow K^{*0} e^+ e^-$ ($1 < q^2 < 6 \text{ GeV}^2/c^4$)	111 ± 14 [77]	425	3262	20154
$d\mathcal{B}(B^+ \rightarrow \pi^+ \mu^+ \mu^-, 1.0 < q^2 < 6 \text{ GeV}^2/c^4)/dq^2 [10^{-9} \text{ GeV}^{-2}c^4]$	0.91 ± 0.21 ± 0.03 [84]	0.11	0.04	0.02
$d\mathcal{B}(B^+ \rightarrow \pi^+ \mu^+ \mu^-, 15 < q^2 < 22 \text{ GeV}^2/c^4)/dq^2 [10^{-9} \text{ GeV}^{-2}c^4]$	0.47 ± 0.12 ± 0.01 [84]	0.06	0.02	0.01
$A_{\text{FB}}(B^0 \rightarrow K^{*0} \mu^+ \mu^-, 1.1 < q^2 < 6 \text{ GeV}^2/c^4)$	-0.075 ± 0.034 ± 0.007 [74]	0.017	0.006	0.003
$A_{\text{FB}}(B^0 \rightarrow K^{*0} \mu^+ \mu^-, 15 < q^2 < 19 \text{ GeV}^2/c^4)$	0.355 ± 0.027 ± 0.009 [74]	0.014	0.005	0.002
$S_5(B^0 \rightarrow K^{*0} \mu^+ \mu^-, 1.1 < q^2 < 6 \text{ GeV}^2/c^4)$	-0.023 ± 0.050 ± 0.005 [74]	0.026	0.009	0.004
$S_5(B^0 \rightarrow K^{*0} \mu^+ \mu^-, 15 < q^2 < 19 \text{ GeV}^2/c^4)$	-0.325 ± 0.037 ± 0.009 [74]	0.019	0.007	0.003
$S_5(B_s^0 \rightarrow \bar{K}^{*0} \mu^+ \mu^-, 1.1 < q^2 < 6 \text{ GeV}^2/c^4)$	-	-	0.087	0.035
$S_5(B_s^0 \rightarrow \bar{K}^{*0} \mu^+ \mu^-, 15 < q^2 < 19 \text{ GeV}^2/c^4)$	-	-	0.064	0.026
$\mathcal{R}_K(1 < q^2 < 6 \text{ GeV}^2/c^4)$	0.745 ± 0.090 ± 0.036 [76]	0.046	0.017	0.007
$\mathcal{R}_{K^*}(1 < q^2 < 6 \text{ GeV}^2/c^4)$	0.69 ± 0.11 ± 0.05 [77]	0.056	0.020	0.008

prepared for Phase II Lol [<https://cds.cern.ch/record/2244311>]

- Large datasets will be available with the LHCb upgrade and Belle 2:
- ➔ We will discuss how to exploit this large dataset as part of the workshop.

Projections

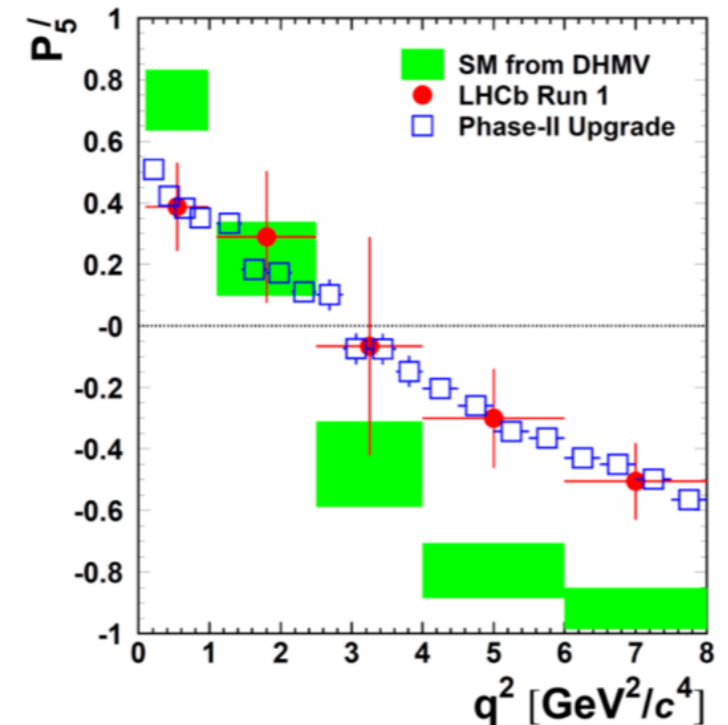
Observable	Run 1 result	8 fb ⁻¹	50 fb ⁻¹	300 fb ⁻¹
Yield $B^0 \rightarrow K^{*0} \mu^+ \mu^-$	2398 ± 57 [74]	9175	70480	435393

With the phase I and phase II upgrades huge samples of “rare” decay modes will become available.

(no, we haven't forgotten the error bars)

Can try to maximise sensitivity to BSM effects by parameterising the full q^2 dependence.

[see talk by Patrick]



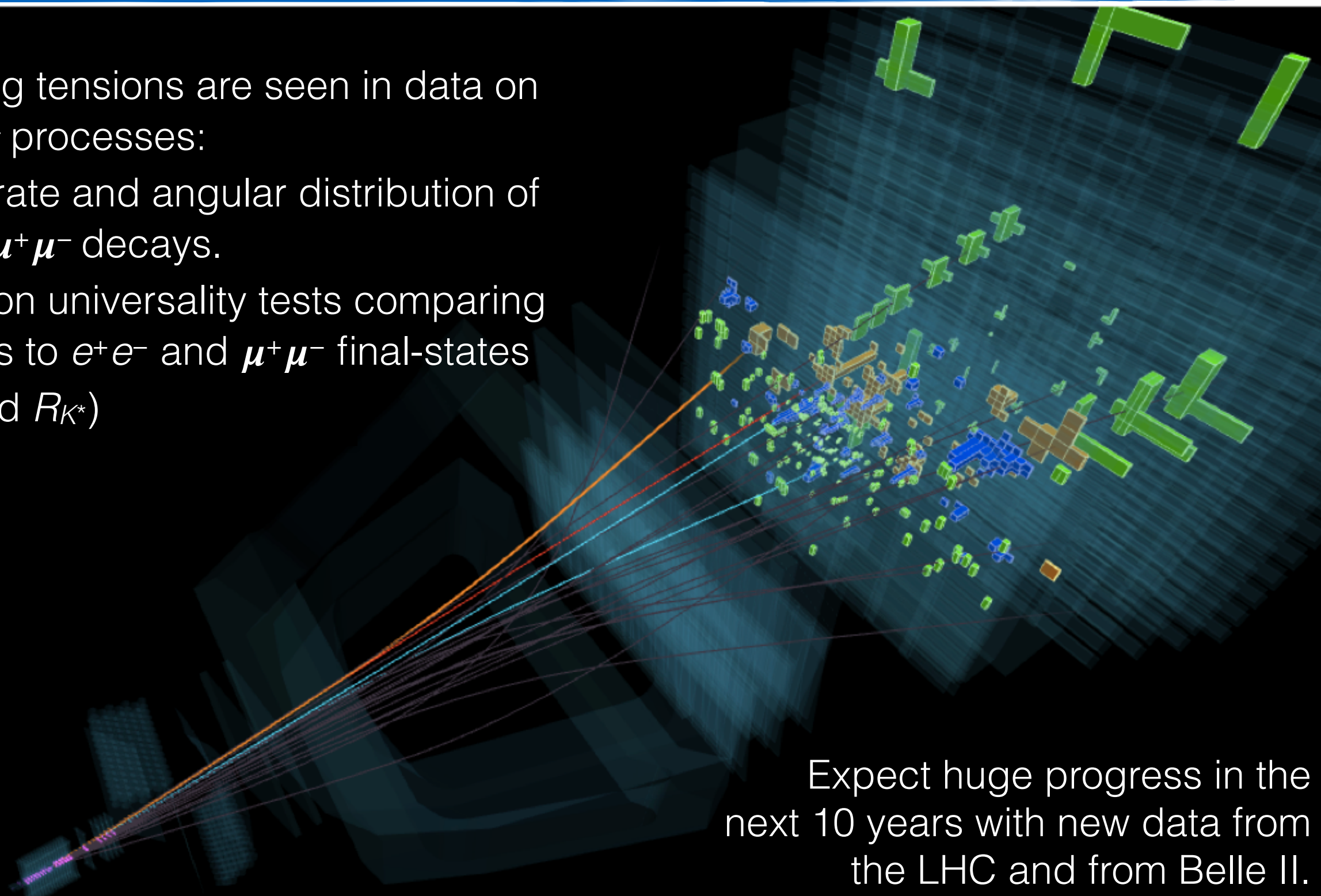
$\mathcal{R}_K(1 < q^2 < 6 \text{ GeV}^2/c^4)$	$0.745 \pm 0.090 \pm 0.036$ [76]	0.046	0.017	0.007
$\mathcal{R}_{K^*}(1 < q^2 < 6 \text{ GeV}^2/c^4)$	$0.69 \pm 0.11 \pm 0.05$ [77]	0.056	0.020	0.008

LHCb will face competition from Belle II in modes with dielectron final-states (e.g. Belle II expects to reach a precision of 3-4% on $R_{K^{(*)}}$ with 50 ab⁻¹).

Summary

Interesting tensions are seen in data on $b \rightarrow s \ell^+ \ell^-$ processes:

1. in the rate and angular distribution of $B \rightarrow X_s \mu^+ \mu^-$ decays.
2. in lepton universality tests comparing decays to $e^+ e^-$ and $\mu^+ \mu^-$ final-states (R_K and R_{K^*})



Expect huge progress in the next 10 years with new data from the LHC and from Belle II.

Effective theory

- Can write a Hamiltonian for an effective theory of $b \rightarrow s$ processes:

Wilson coefficient
(integrating out scales above μ)

Local 4 fermion operators with
different Lorentz structures

$$\mathcal{H}_{\text{eff}} = -\frac{4G_F}{\sqrt{2}} V_{tb} V_{ts}^* \frac{\alpha_e}{4\pi} \sum_i C_i(\mu) \mathcal{O}_i(\mu),$$

c.f. Fermi theory of
weak interaction where
at low energies:

$$\lim_{q^2 \rightarrow 0} \left(\frac{g^2}{m_W^2 - q^2} \right) = \frac{g^2}{m_W^2}$$

$$\Delta \mathcal{H}_{\text{eff}} = \frac{\kappa_{\text{NP}}}{\Lambda_{\text{NP}}^2} \mathcal{O}_{\text{NP}}$$

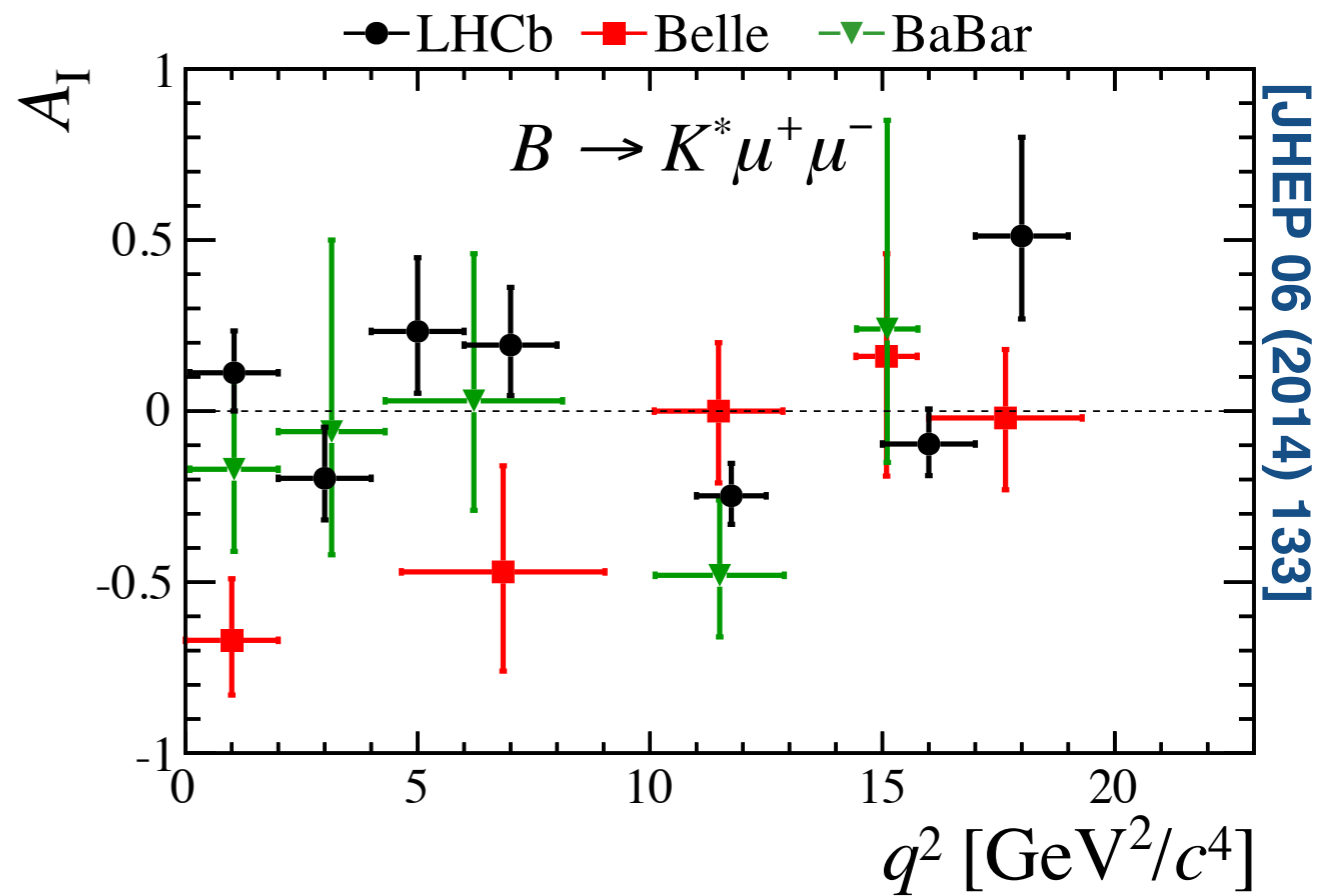
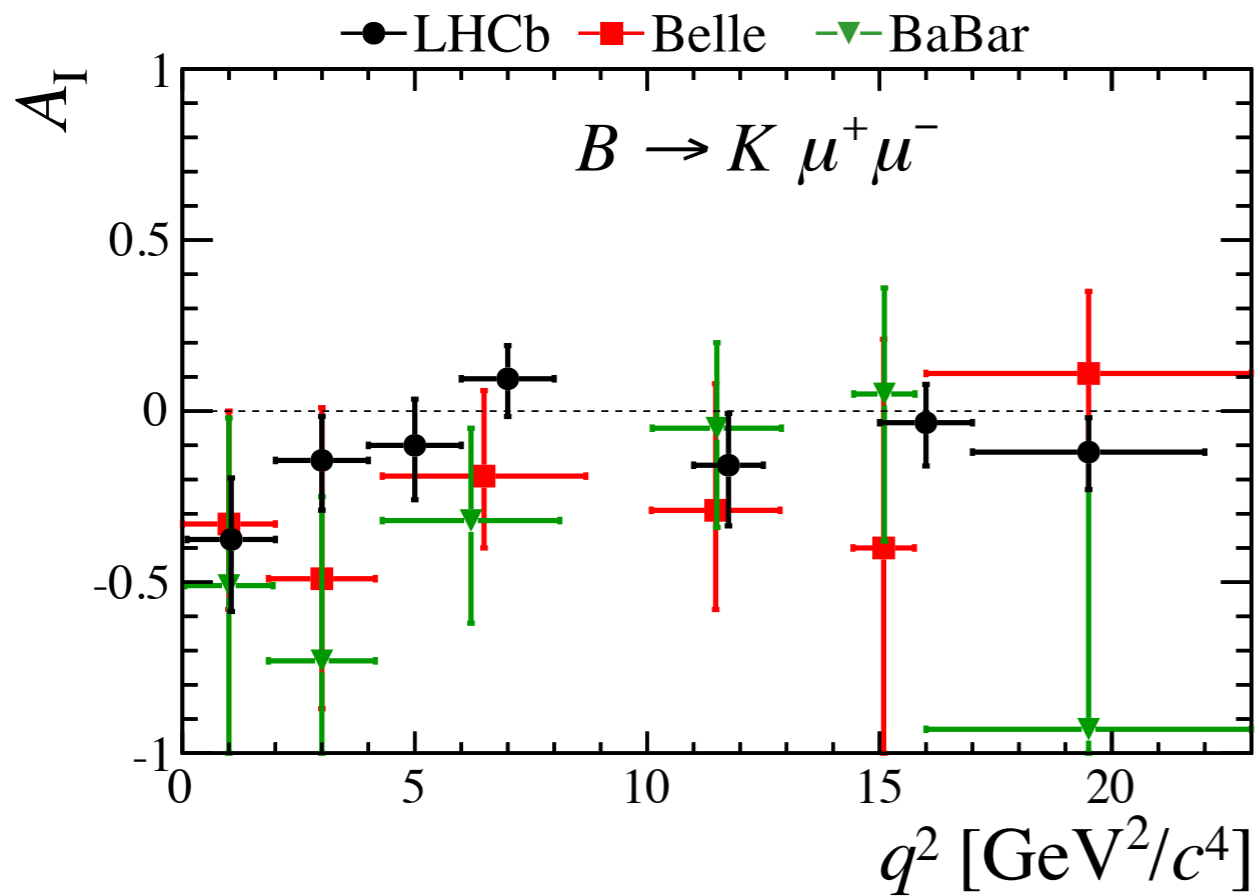
NP scale

NP can modify
SM contribution
or introduce
new operators

i.e. the full theory can
be replaced by a 4-
fermion operator and a
coupling constant, G_F .

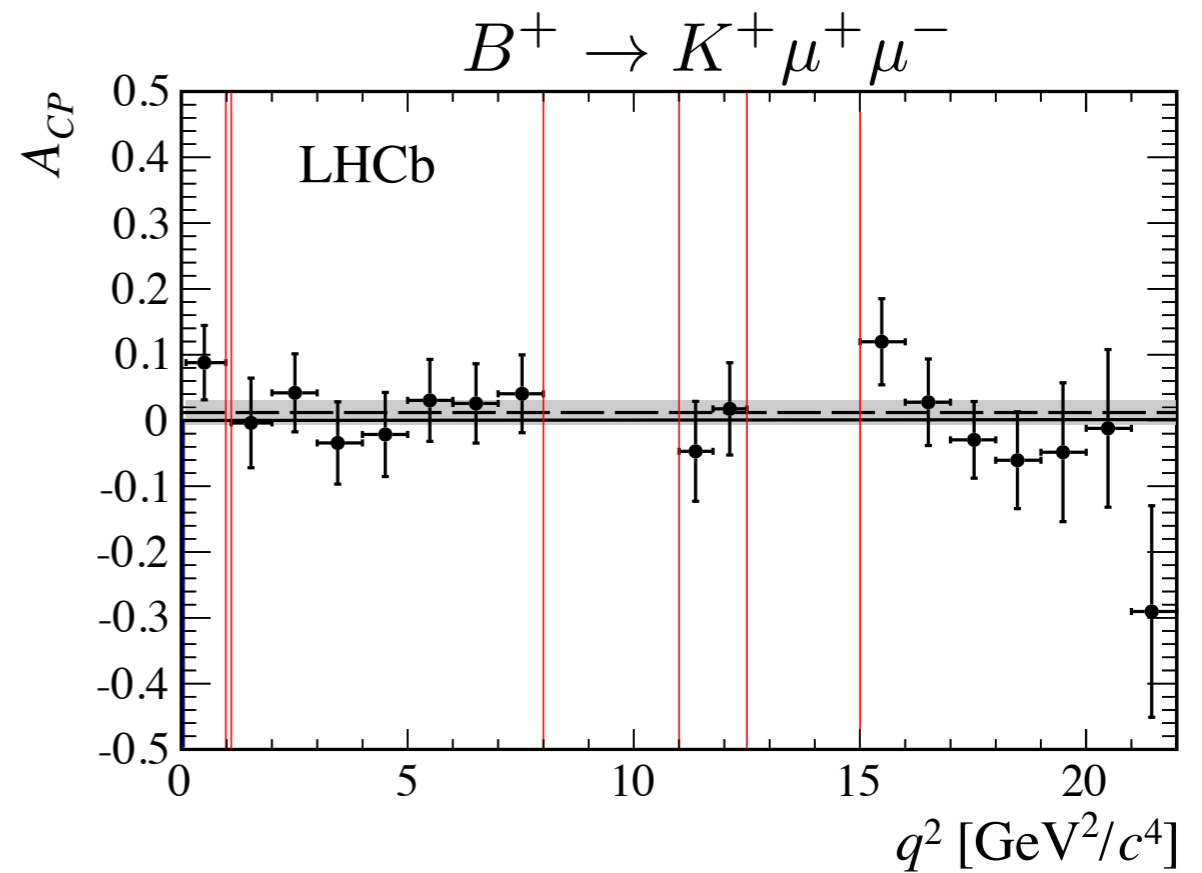
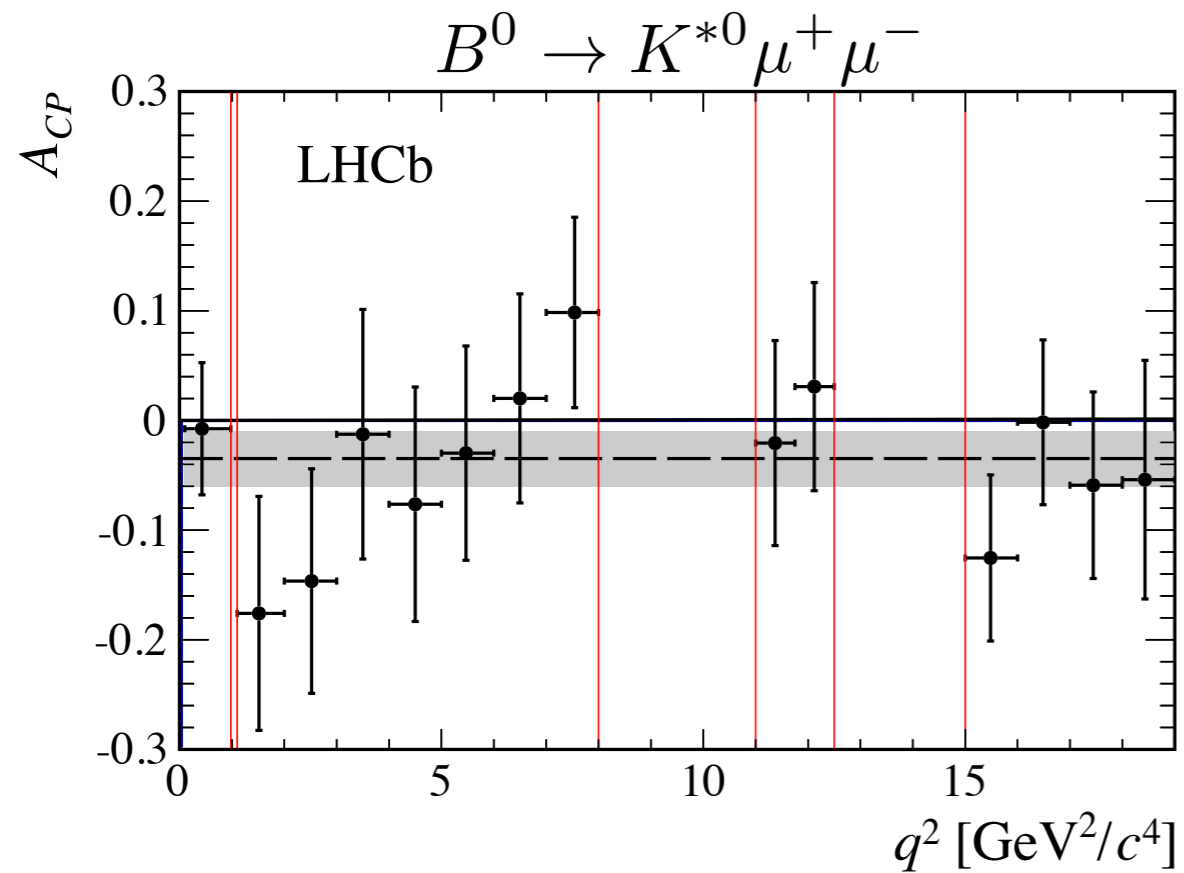
- κ_{NP} can have all/some/none
of the suppression of the SM,
e.g. MFV inherits SM CKM
suppression.

Isospin asymmetries



[JHEP 06 (2014) 133]

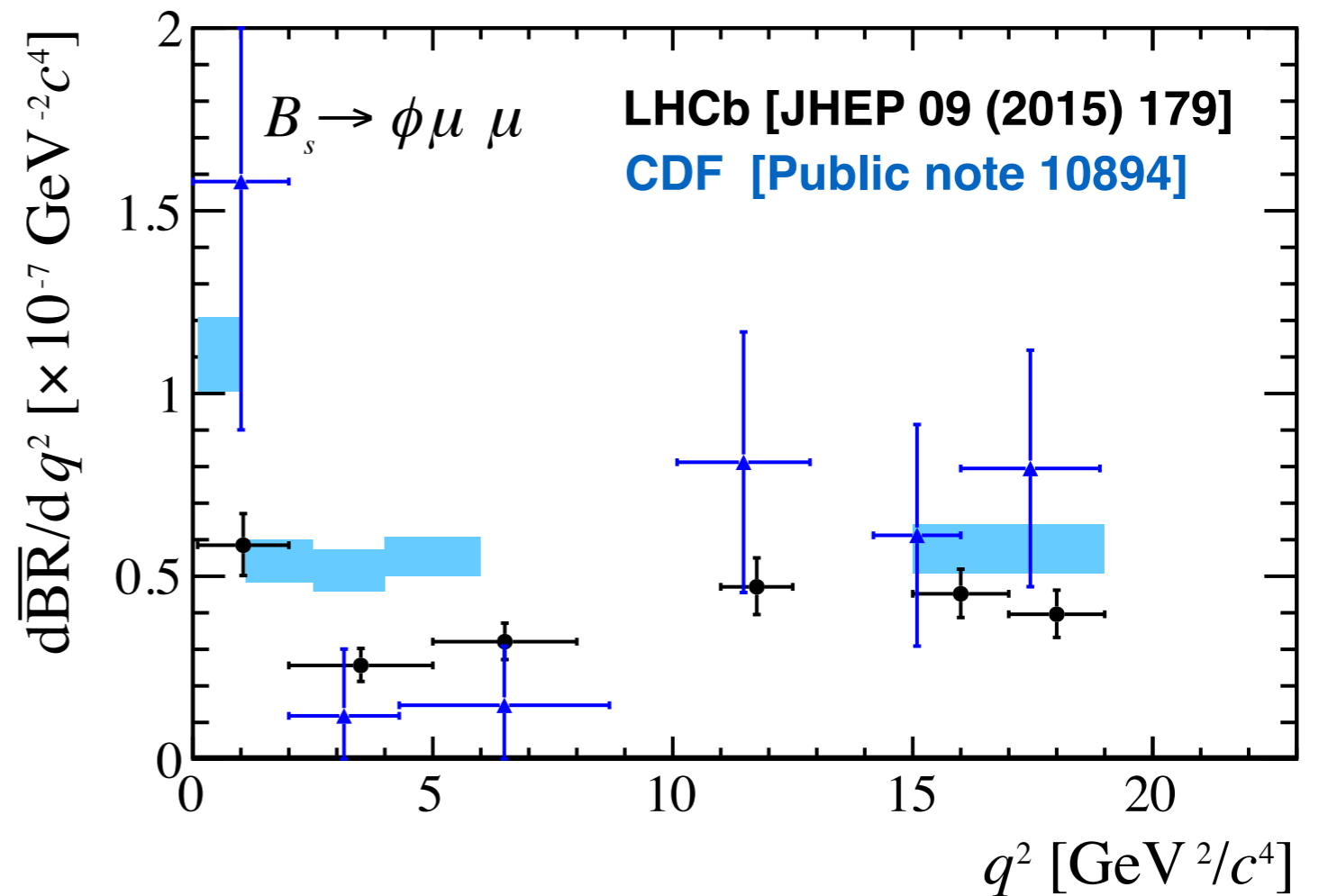
CP asymmetries



[JHEP 09 (2014) 177]

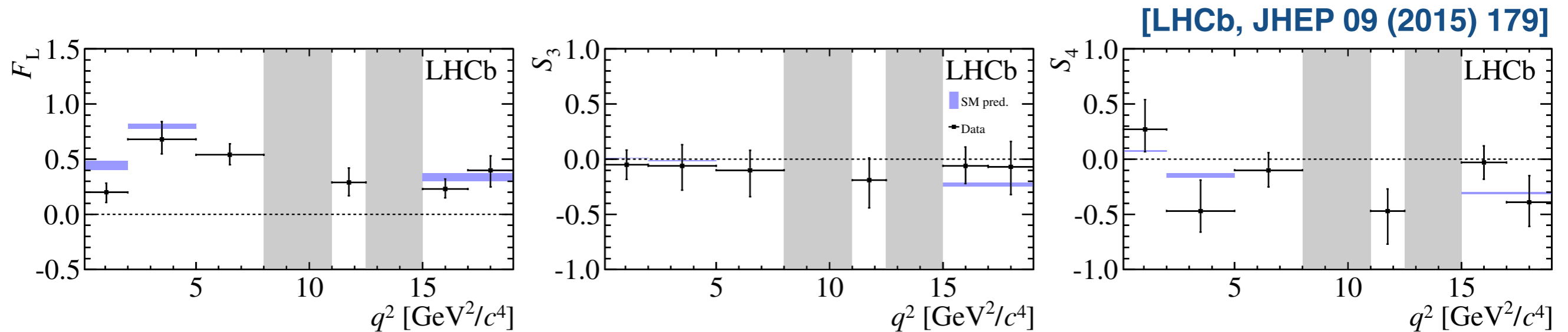
$B_s \rightarrow \phi \mu^+ \mu^-$ decay rate

- Large tension between the SM prediction and the data at low q^2 ($\sim 3\sigma$).
- Angular observables are consistent with SM expectations. However, the final-state is not CP specific (cannot determine A_{FB} or P_5' without flavour tagging).



SM predictions based on
[Altmannshofer & Straub, arXiv:1411.3161]
[LCSR form-factors from Bharucha,
Straub & Zwicky, arXiv:1503.05534]

$B_s \rightarrow \phi \mu^+ \mu^-$ angular distribution



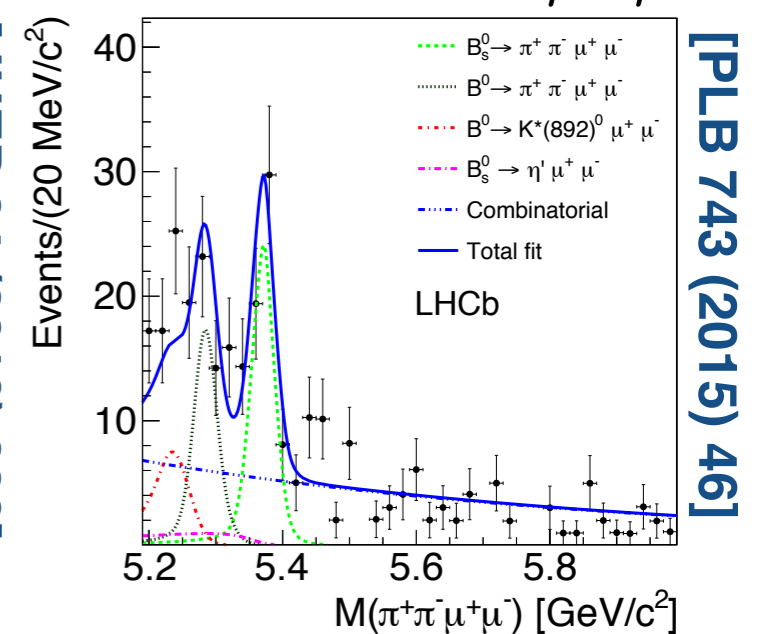
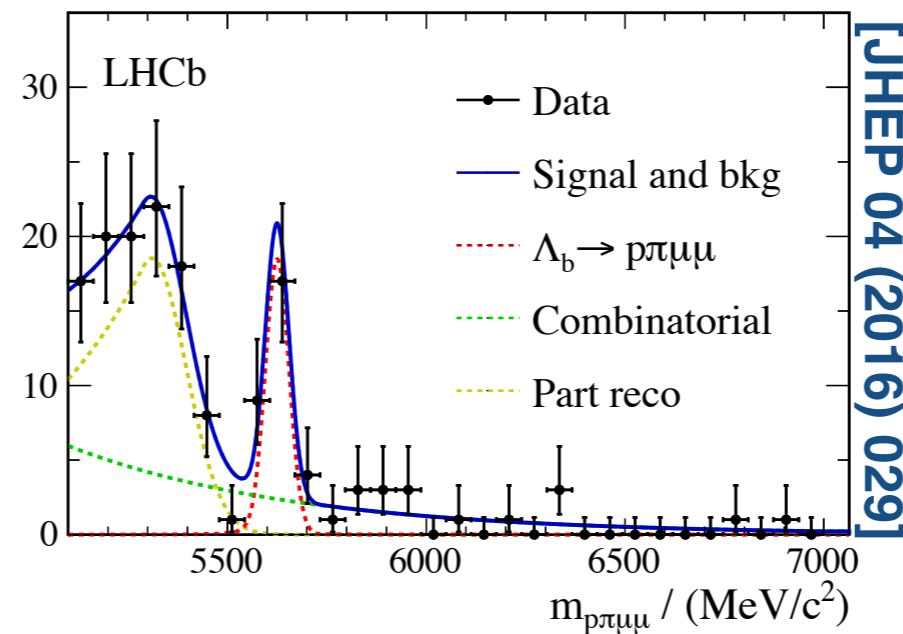
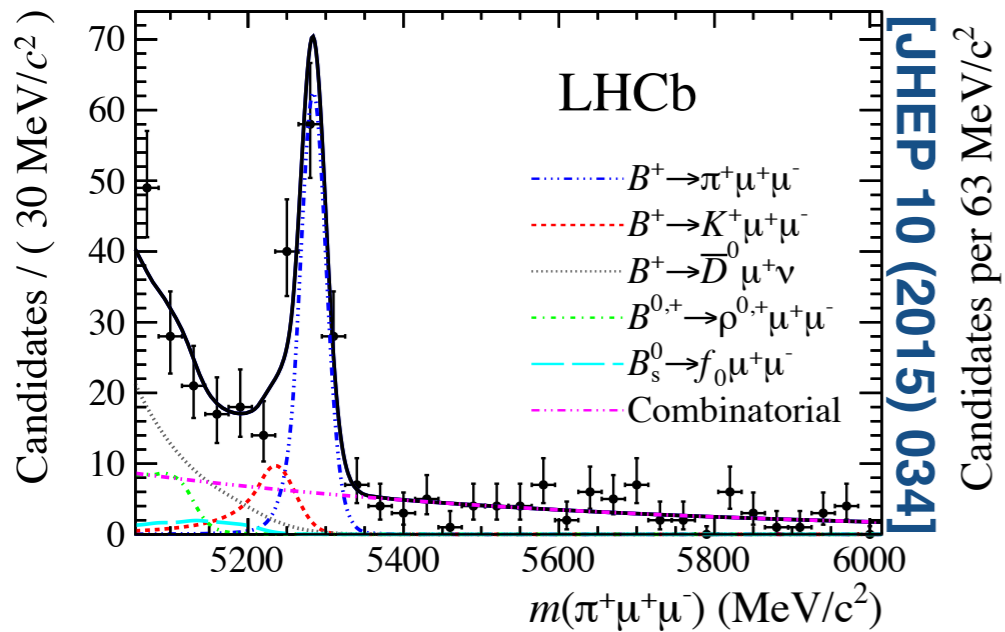
- Angular observables are consistent with SM expectations (but cannot determine A_{FB} or P_5' without flavour tagging).

$b \rightarrow d \ell^+ \ell^-$ processes

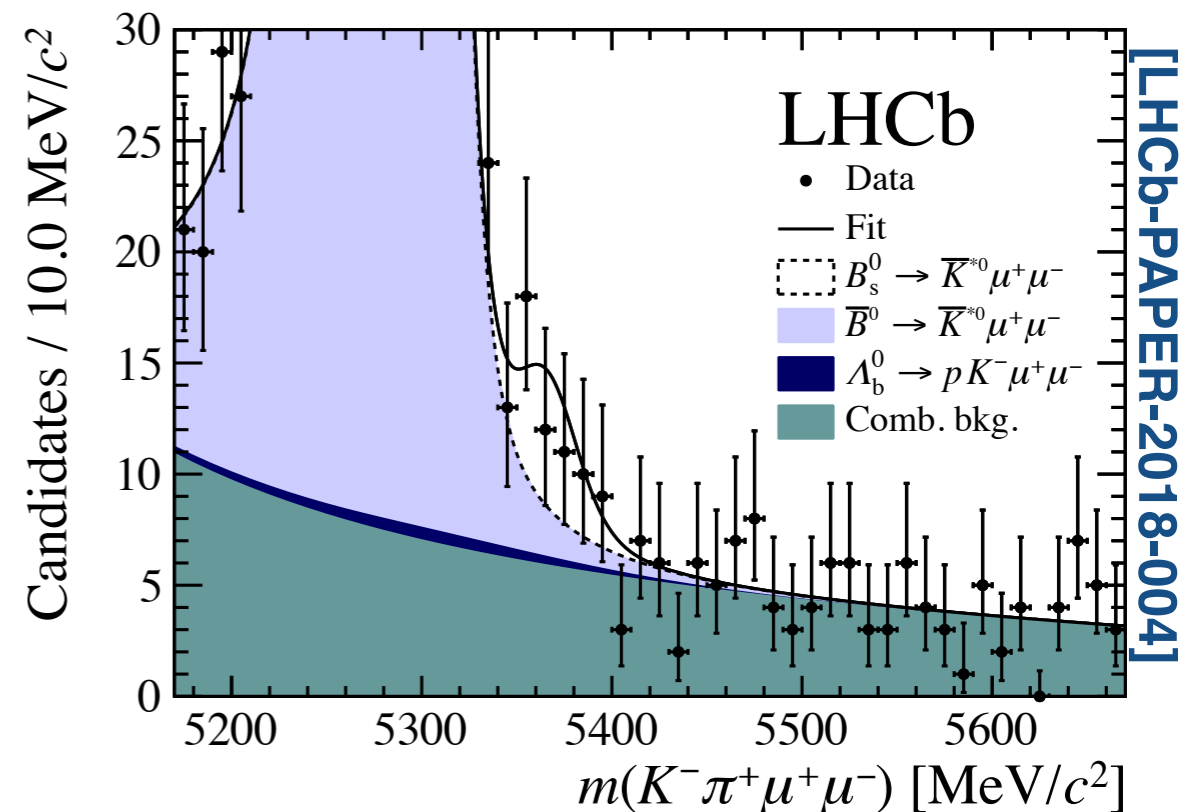
$$B^+ \rightarrow \pi^+ \mu^+ \mu^-$$

$$\Lambda_b \rightarrow N^* \mu^+ \mu^-$$

$$B^0 \rightarrow \pi^+ \pi^- \mu^+ \mu^-$$

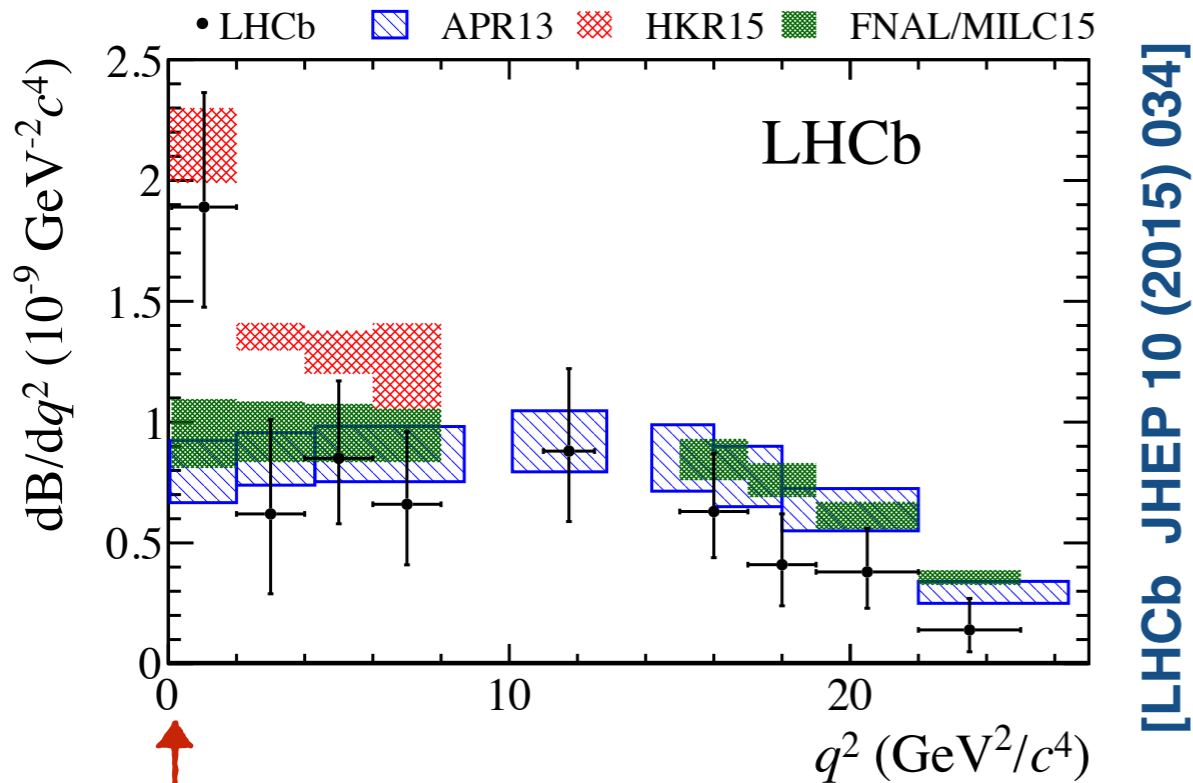


- We have access to $b \rightarrow d \mu^+ \mu^-$ processes in the LHC Run 1 and 2 datasets.
- First observation of $B^+ \rightarrow \pi^+ \mu^+ \mu^-$ and $\Lambda \rightarrow N^* \mu^+ \mu^-$ and first evidence for $B_s \rightarrow K^{*0} \mu^+ \mu^-$ and $B^0 \rightarrow \pi^+ \pi^- \mu^+ \mu^-$ (in the ρ resonance region).



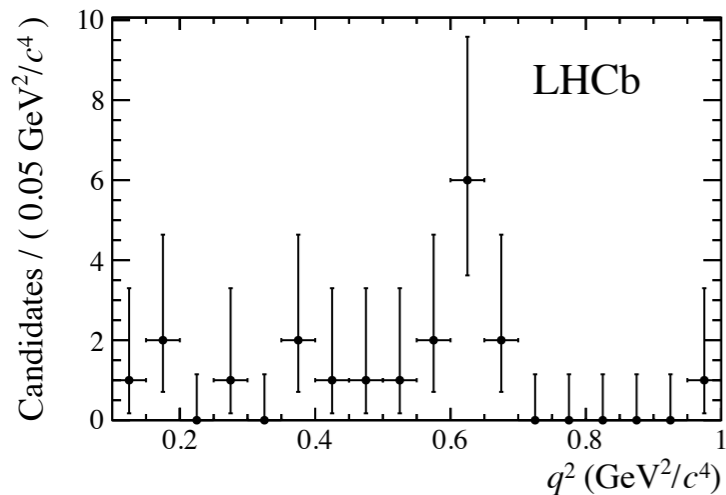
$B^+ \rightarrow \pi^+ \mu^+ \mu^-$ branching fraction

- Determine branching fraction by normalising to $B^+ \rightarrow J/\psi K^+$



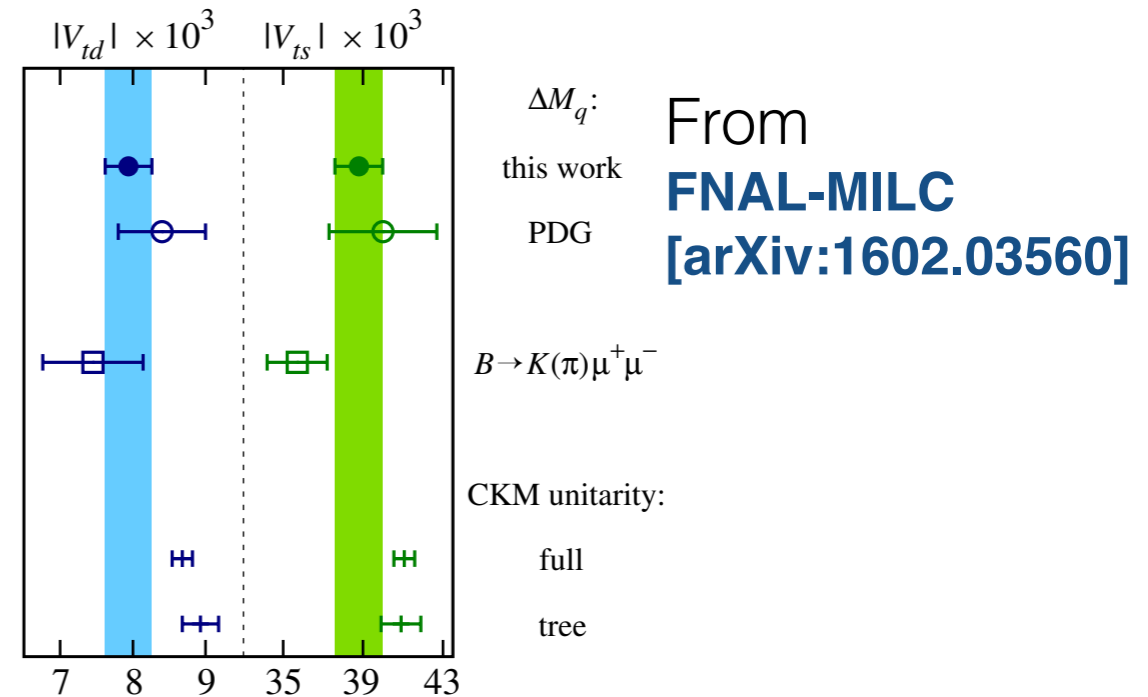
[LHCb JHEP 10 (2015) 034]

Can also use and $B^+ \rightarrow K^+ \mu^+ \mu^-$ and $B^+ \rightarrow \pi^+ \mu^+ \mu^-$ to determine the CKM elements V_{ts} and V_{td} (see e.g. [Du et al arXiv:1510.02349])



Enhancement for $q^2 < 1 \text{ GeV}^2/c^4$ due to light resonances (ρ, ω).

These are included in HKR 15



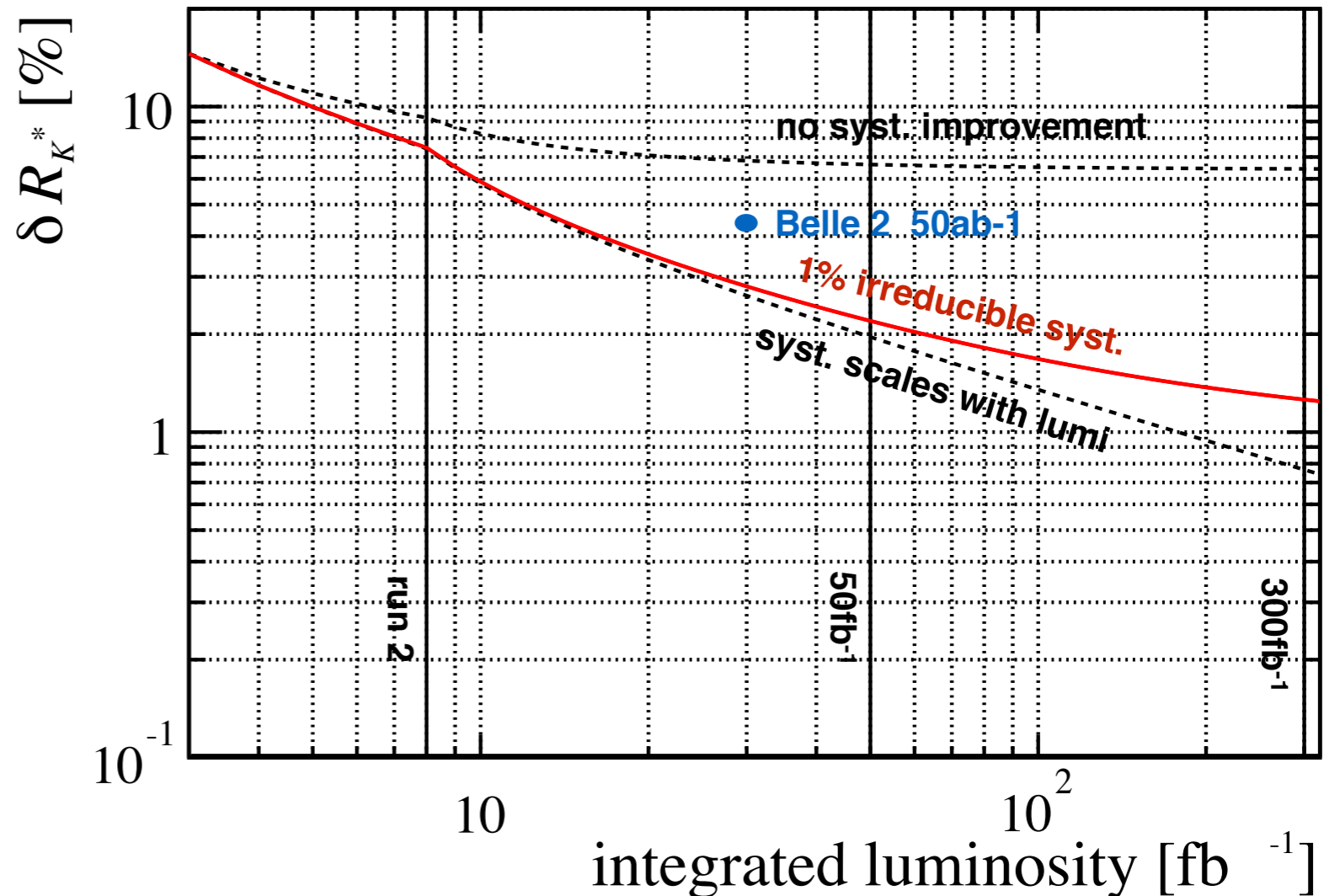
ΔM_q : From **FNAL-MILC [arXiv:1602.03560]**
 PDG
 $B \rightarrow K(\pi) \mu^+ \mu^-$
 CKM unitarity:
 full
 tree

Ratio consistent with MFV hypothesis.

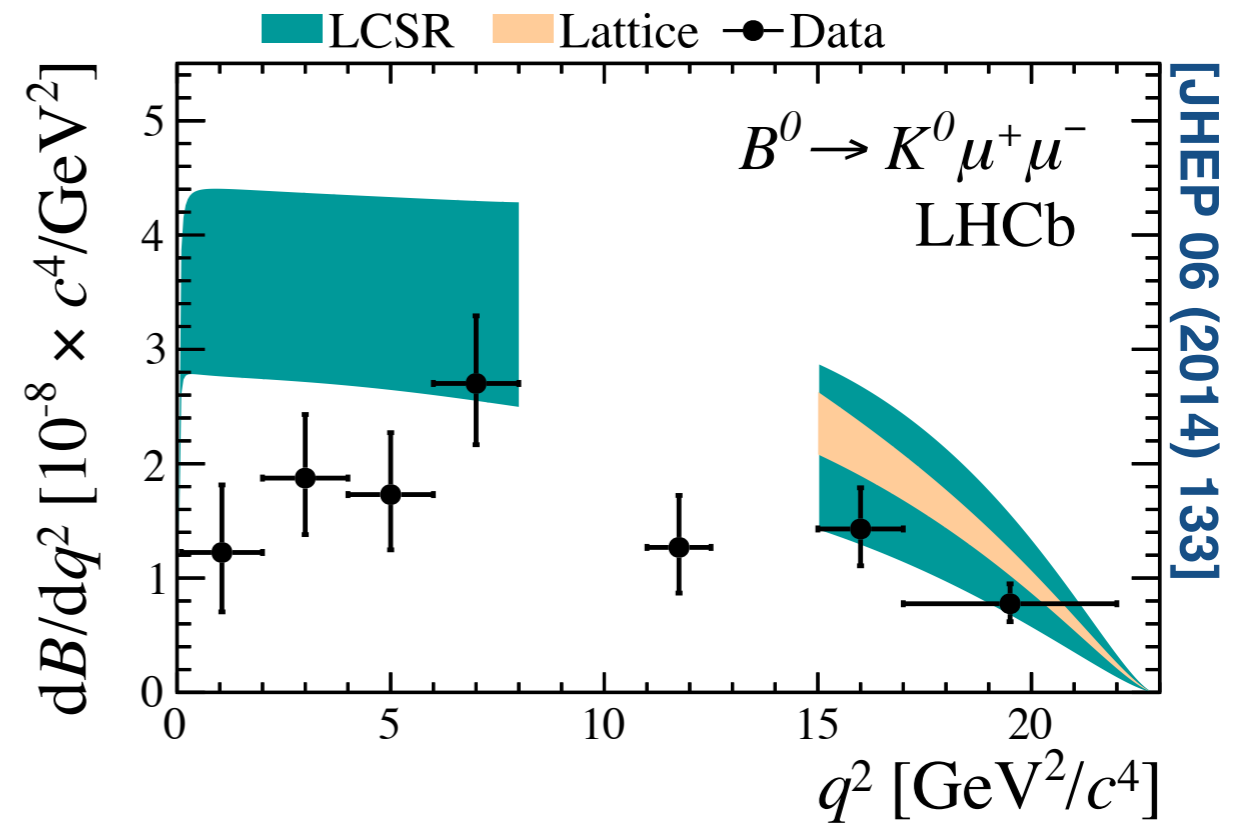
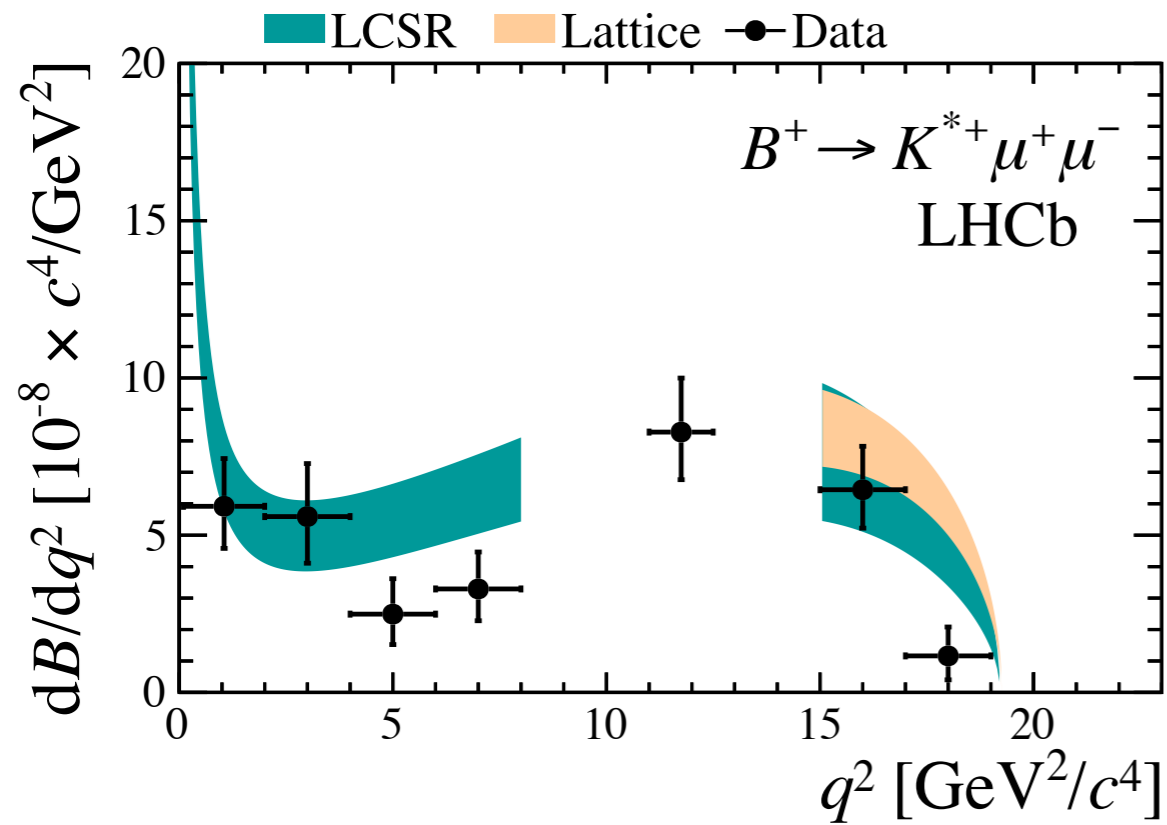
SM predictions [Ali et al. arXiv:1312.2523], [Hambrock et al. arXiv:1506.07760] and [Bailey et al. arXiv:1507.01618].

Projection for R_{K^*}

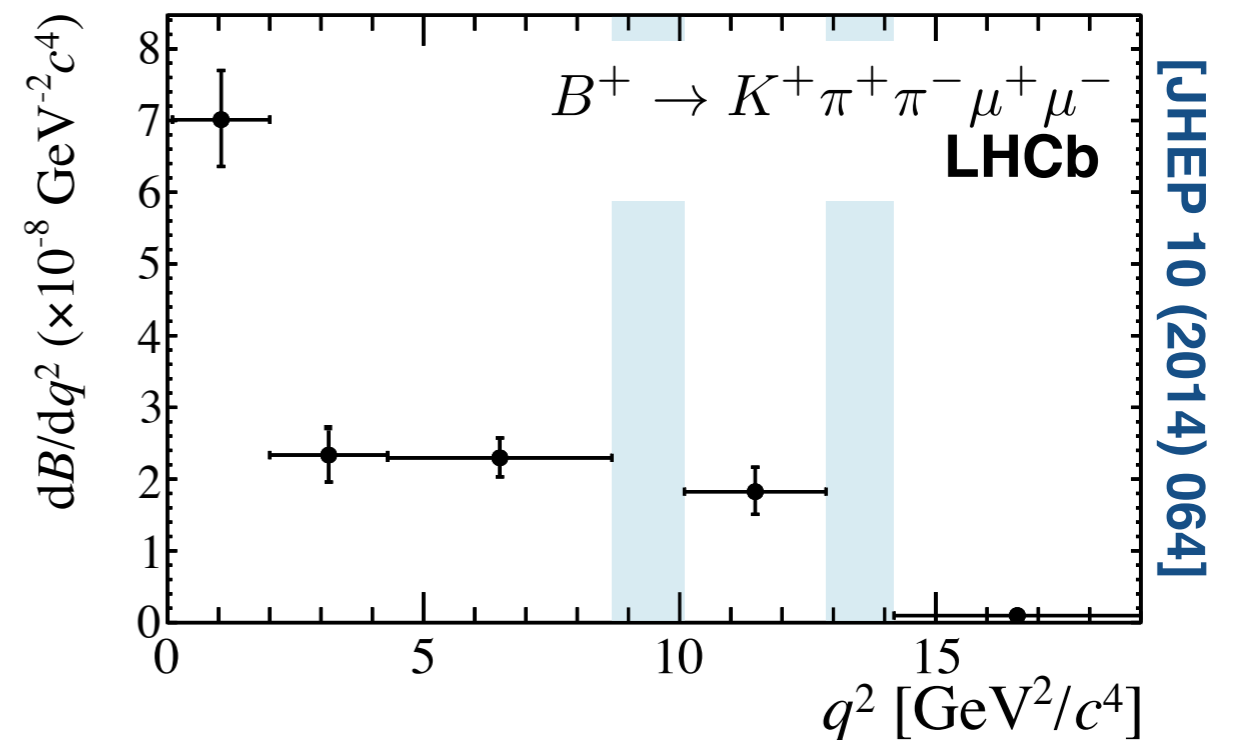
- Assuming an irreducible systematic uncertainty of 1% for R_{K^*} in the range $1 < q^2 < 6 \text{ GeV}^2/c^4$.
- For comparison Belle 2 expects to reach a precision of 4-5% with a systematic uncertainty of 0.4% with a 50ab^{-1} dataset [From talk by S. Sandilya at CKM 2016]



Branching fraction measurements



SM predictions from:
[\[Bobeth et al JHEP 01 \(2012\) 107\]](#)
[\[Bouchard et al. PRL111 \(2013\) 162002\]](#)



Operators

- Different processes are sensitive to different 4-fermion operators.
 - ➔ Can exploit this to over-constrain the system.

$\mathcal{O}_7 = (m_b/e) (\bar{s}\sigma^{\mu\nu} P_R b F_{\mu\nu})$	}	photon (constrained by radiative decays and $b \rightarrow s\ell^+\ell^-$ processes at small q^2)
$\mathcal{O}_9 = (\bar{s}\gamma_\mu P_L b)(\bar{\ell}\gamma^\mu \ell)$		} vector current (constrained by $b \rightarrow s\ell^+\ell^-$ processes)
$\mathcal{O}_{10} = (\bar{s}\gamma_\mu P_L b)(\bar{\ell}\gamma^\mu \gamma_5 \ell)$	}	axial vector current (constrained by leptonic decays and $b \rightarrow s\ell^+\ell^-$ processes)
$\mathcal{O}_S = (\bar{s}P_R b)(\bar{\ell}\ell)$		}
$\mathcal{O}_P = (\bar{s}P_R b)(\bar{\ell}\gamma_5 \ell)$		

e.g.

$$B_s^0 \rightarrow \mu^+ \mu^- \text{ constrains } C_{10} - C'_{10}, C_S - C'_S, C_P - C'_P$$

$$B^+ \rightarrow K^+ \mu^+ \mu^- \text{ constrains } C_9 + C'_9, C_{10} + C'_{10}$$

$$B^0 \rightarrow K^{*0} \mu^+ \mu^- \text{ constrains } C_7 \pm C'_7, C_9 \pm C'_9, C_{10} \pm C'_{10}$$

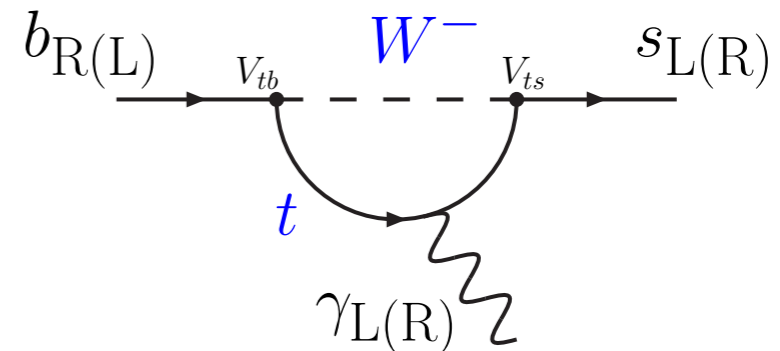
The primes denote right-handed counterparts of the operators whose contribution is small in the SM.

What can we measure?

- Leptonic decay rates, $\Gamma \sim |\text{axialvector}|^2$
 - ➔ Large helicity suppression for e^+e^- and $\mu^+\mu^-$ final-states, which can be lifted in BSM extensions with new (pseudo)scalar operators.
- Semileptonic decay rates, $\Gamma \sim |\text{vector}|^2 + |\text{axialvector}|^2$
 - ➔ Expect large hadronic uncertainties from form-factors.
 - ➔ Expect $\Gamma[B \rightarrow M\mu^+\mu^-] \approx \Gamma[B \rightarrow Me^+e^-]$ due to the universal coupling of the gauge bosons (except the Higgs).
- Angular observables in semileptonic decays:
 - ➔ Can be used to separate vector- and axialvector-currents and left- and right-handed contributions.
 - ➔ Can (partially) cancel hadronic uncertainties.
- Flavour structure of SM implies that the rate of $b \rightarrow d$ processes is suppressed by $|V_{td}/V_{ts}|^2$ compared to $b \rightarrow s$ processes.

Properties of $\Delta F = 1$ processes

- In the SM, photons from $b \rightarrow s \gamma$ decays are predominantly left-handed ($C_7/C'_7 \sim m_b/m_s$) due to the charged-current interaction.
- Flavour structure of SM implies that the rate of $b \rightarrow d$ processes is suppressed by $|V_{td}/V_{ts}|^2$ compared to $b \rightarrow s$ processes.
- In the SM, the rate $\Gamma[B \rightarrow M \mu^+ \mu^-] \approx \Gamma[B \rightarrow M e^+ e^-]$ due to the universal coupling of the gauge bosons (except the Higgs) to the different lepton flavours. Any differences in the rate are due to phase-space.
- Lepton flavour violating FCNC processes are unobservable in the SM at any conceivable experiment due to the small size of the neutrino mass.



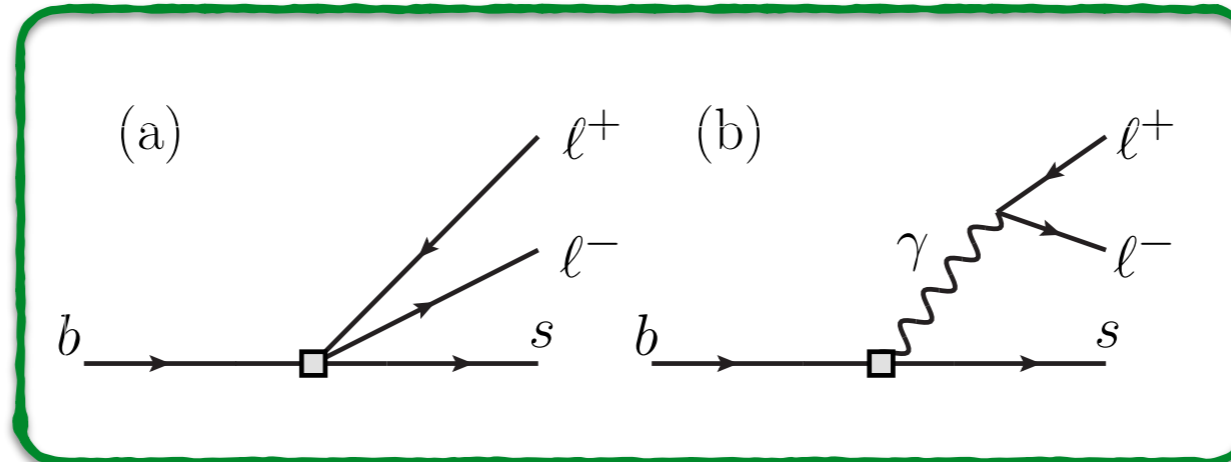
SM contributions

- Interested in new short distance contributions.

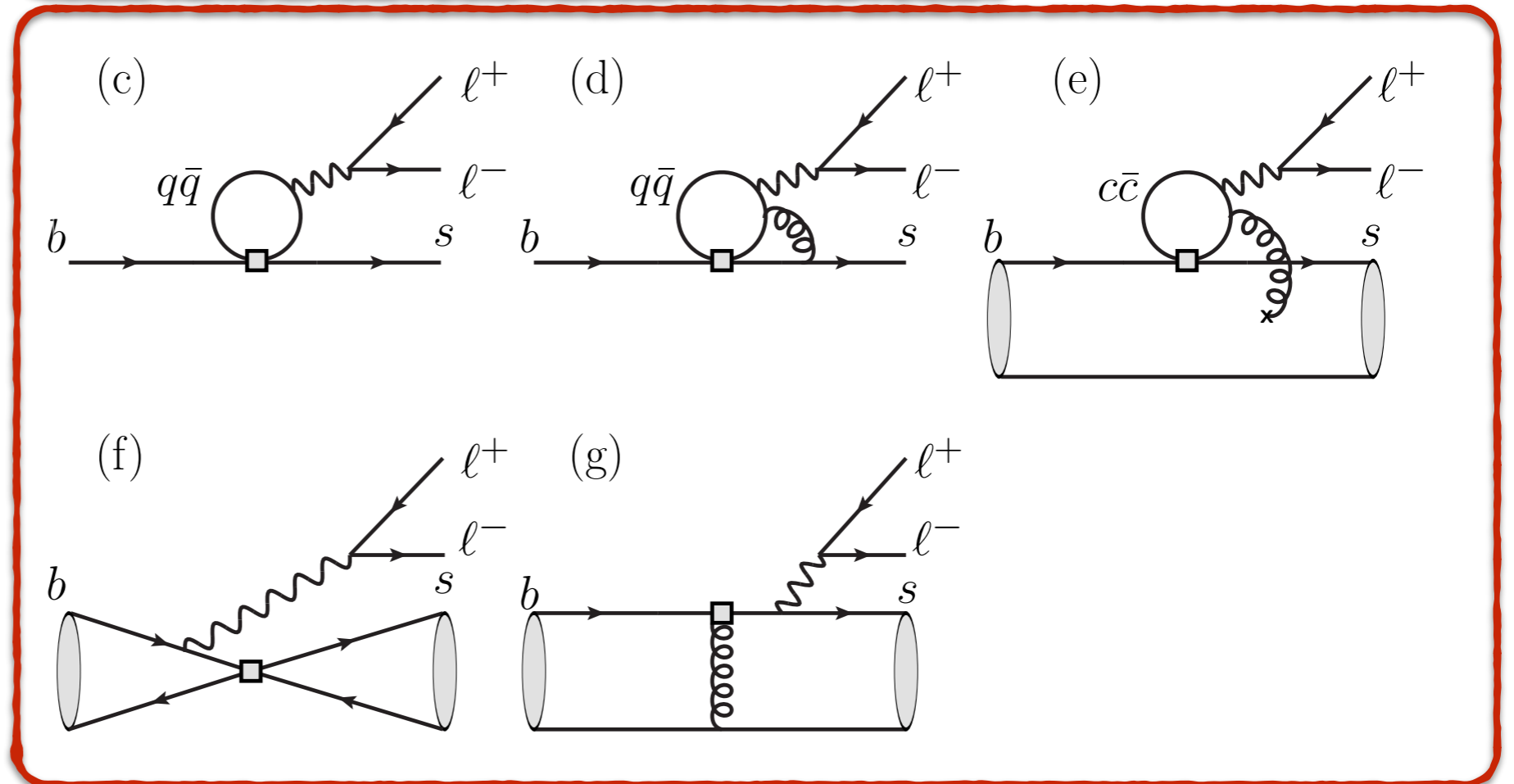
- We also get long-distance hadronic contributions.

- Need estimate of non-local hadronic matrix elements

[Khodjamirian et al. JHEP 09 (2010) 089]

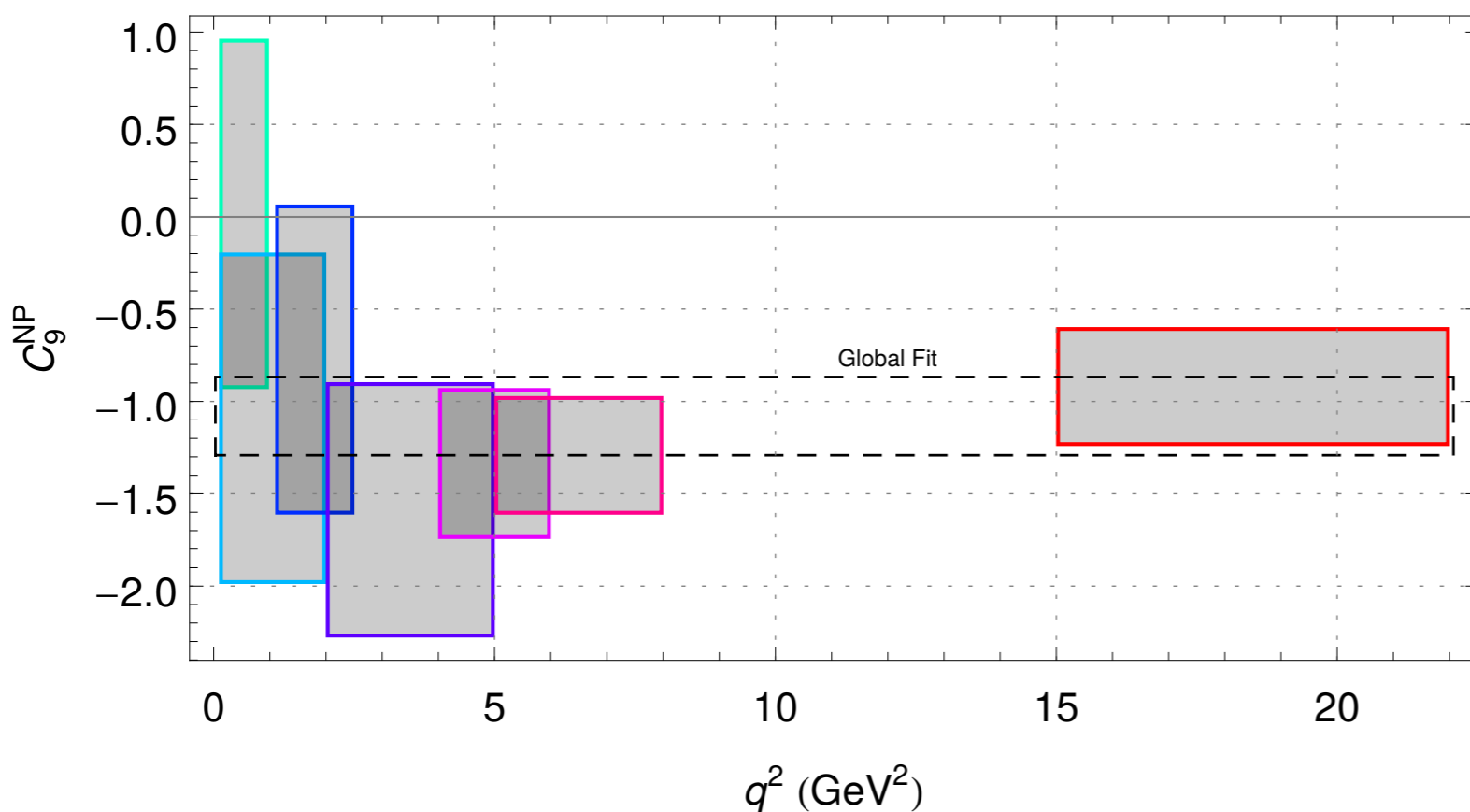


■ Short distance part integrates out (as a Wilson coefficient)



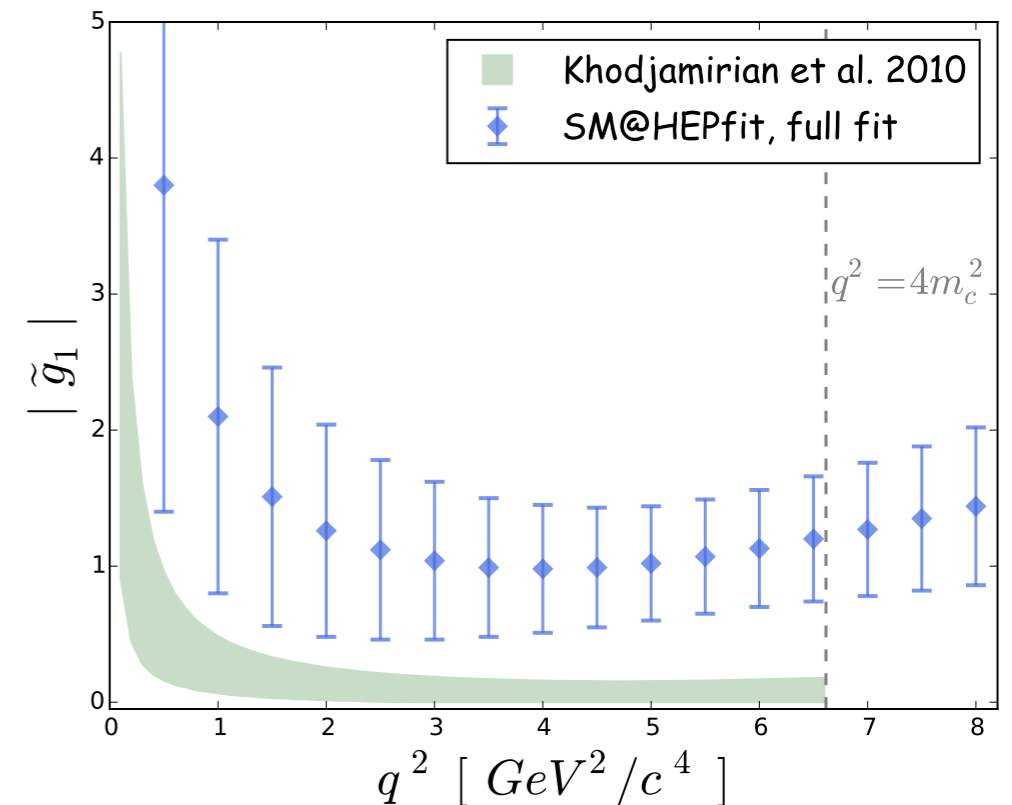
What can we learn from the data?

- If we are underestimating $c\bar{c}$ contributions then naively expect to see the shift in C_9 get larger closer to the narrow charmonium resonances.



[Decotes-Genon et al JHEP 06 (2016) 092]

Fitting separately for C_9 in different q^2 regions.



[M. Ciuchini et al, JHEP 06 (2016) 116]

Parameterised fit for charm contributions in $B^0 \rightarrow K^{*0} \mu^+ \mu^-$ decays with $C_9 = C_9^{\text{SM}}$.

No clear evidence for a rise in the data (but more data is needed).

Theoretical Framework

- In leptonic decays the matrix element for the decay can be factorised into a leptonic current and B meson decay constant:

$$\begin{aligned}\langle \ell^+ \ell^- | j_\ell j_q | B_q \rangle &= \langle \ell^+ \ell^- | j_\ell | 0 \rangle \langle 0 | j_q | B_q \rangle \\ &\approx \langle \ell^+ \ell^- | j_\ell | 0 \rangle \cdot f_{B_q}\end{aligned}$$

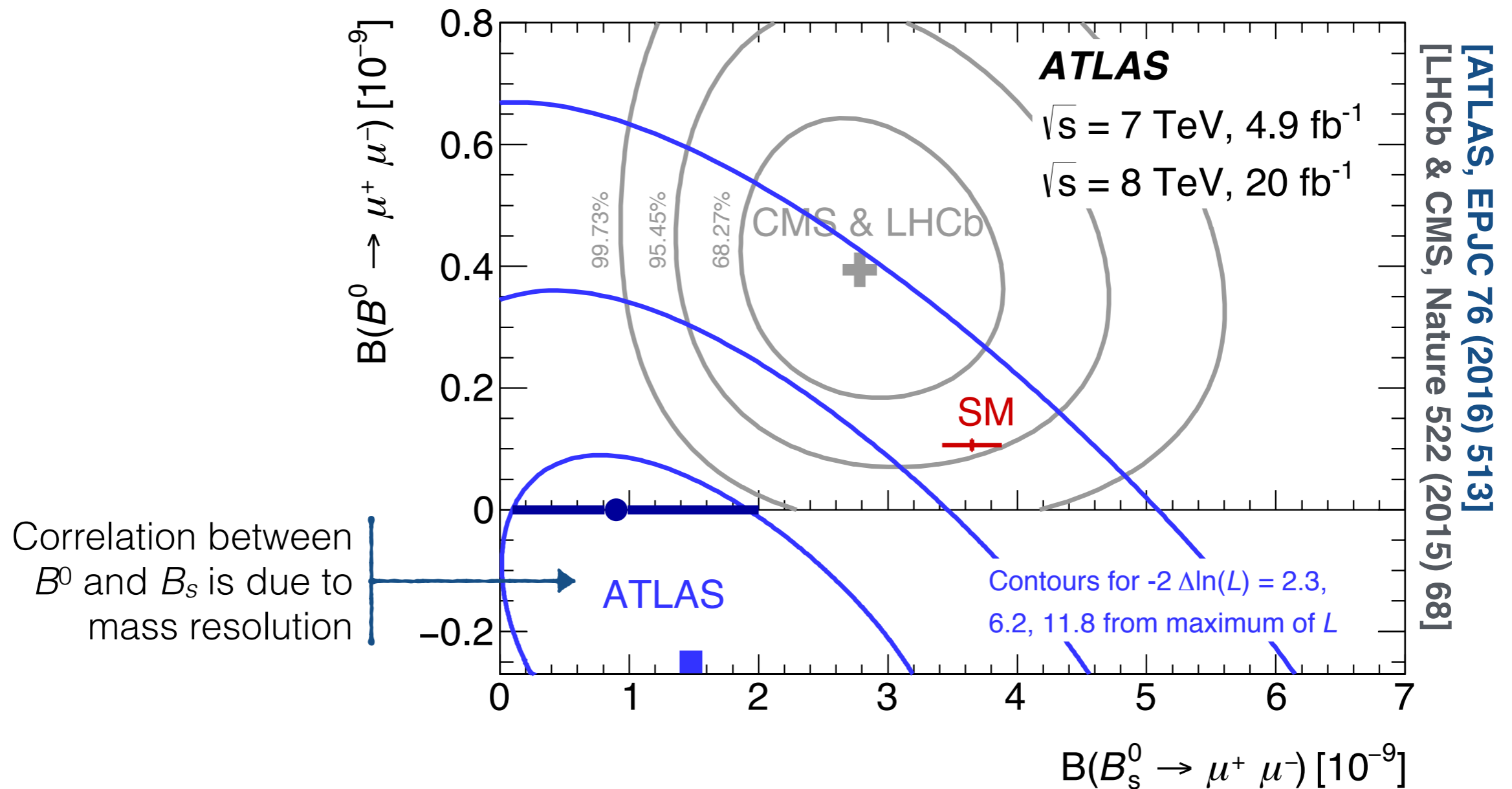
- In semileptonic decays, the matrix element can be factorised into a leptonic current times a form-factor:

$$\begin{aligned}\langle \ell^+ \ell^- M | j_\ell j_q | B \rangle &= \langle \ell^+ \ell^- | j_\ell | 0 \rangle \langle M | j_q | B_q \rangle \\ &\approx \langle \ell^+ \ell^- | j_\ell | 0 \rangle \cdot F(q^2) + \mathcal{O}(\Lambda_{\text{QCD}}/m_B)\end{aligned}$$

however this factorisation is not exact (due to hadronic contributions).

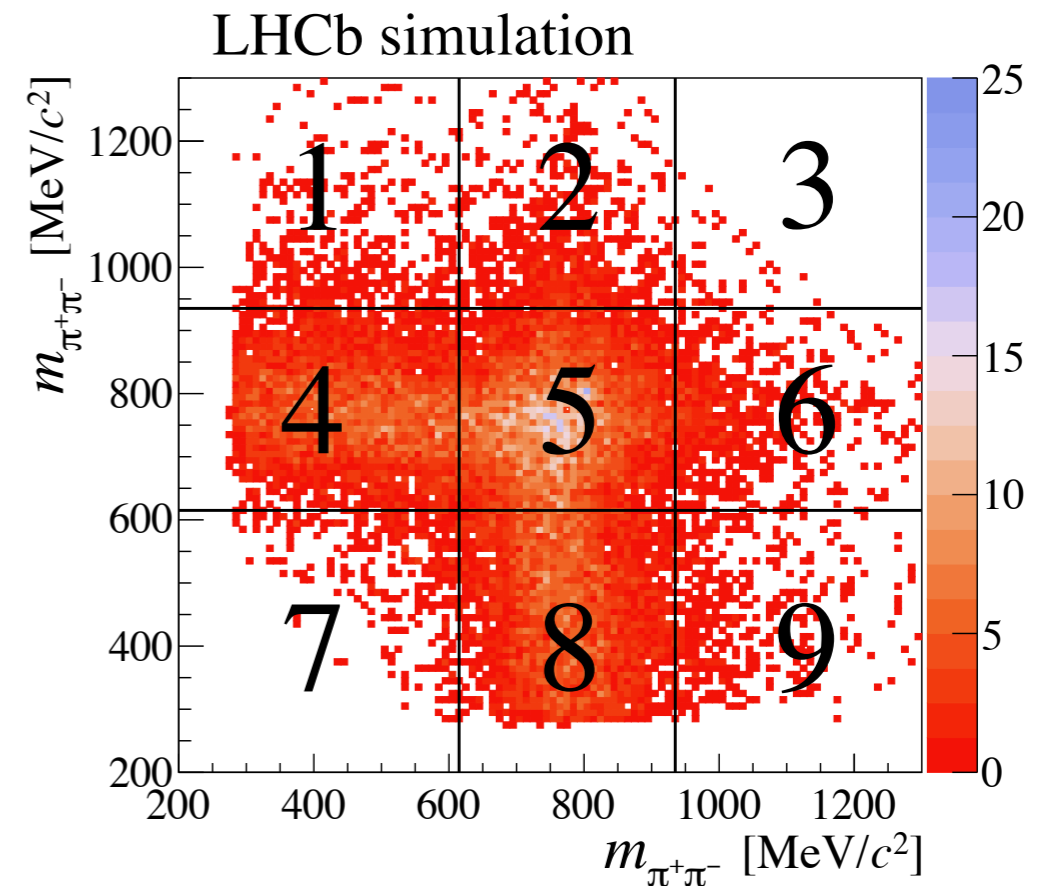
$B_s \rightarrow \mu^+ \mu^-$ fits

- Perform simultaneous fits to the bins of multivariate response to determine the B^0 and B_s branching fractions, e.g. for ATLAS



$$B_{(s,d)} \rightarrow \tau^+ \tau^-$$

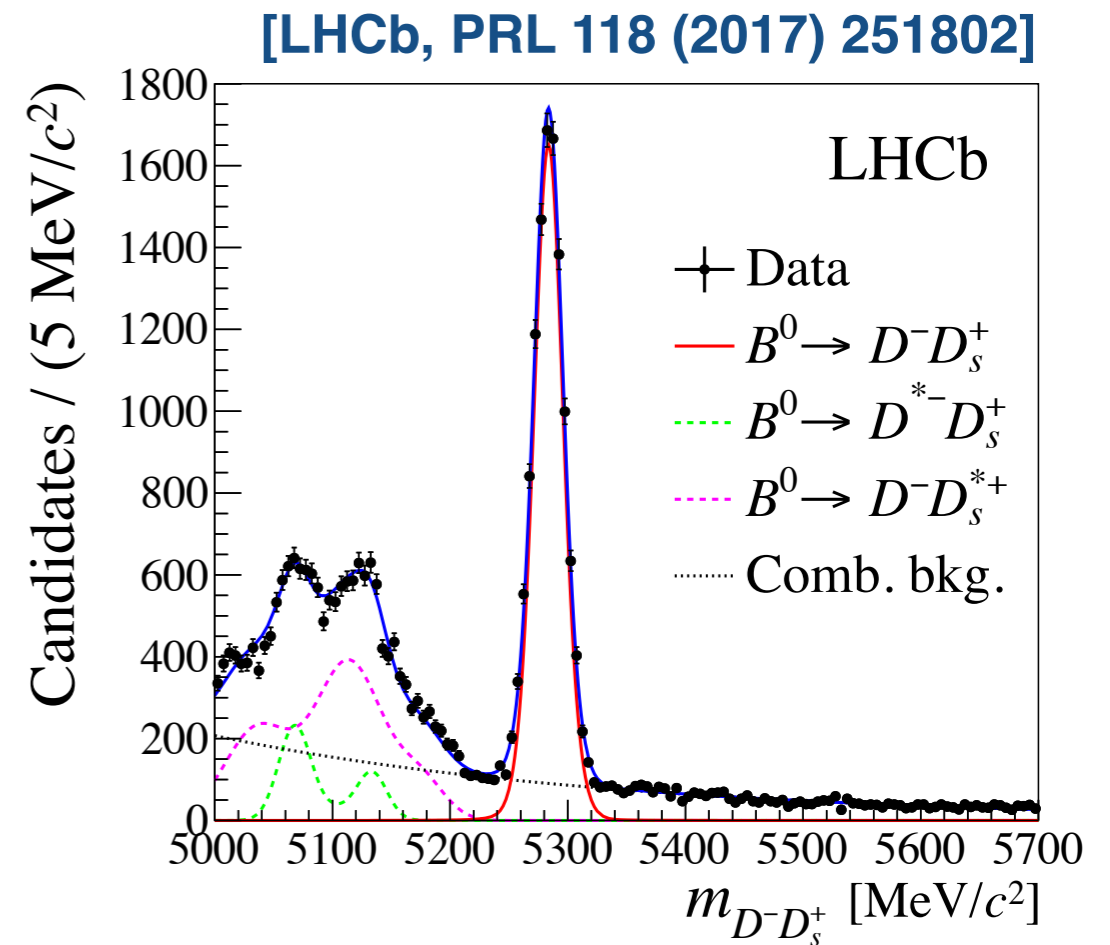
- LHCb performs a search for $B_{(s,d)} \rightarrow \tau^+ \tau^-$ decays using $\tau^- \rightarrow \pi^- \pi^+ \pi^- \nu_\tau$.
 - ➔ Exploit the $\tau^- \rightarrow a_1(1260)^- \nu_\tau$ and $a_1(1260)^- \rightarrow \rho(770)^0 \pi^-$ decays to select signal/control regions of dipion mass.



[LHCb, PRL 118 (2017) 251802]

$$B_{(s,d)} \rightarrow \tau^+ \tau^-$$

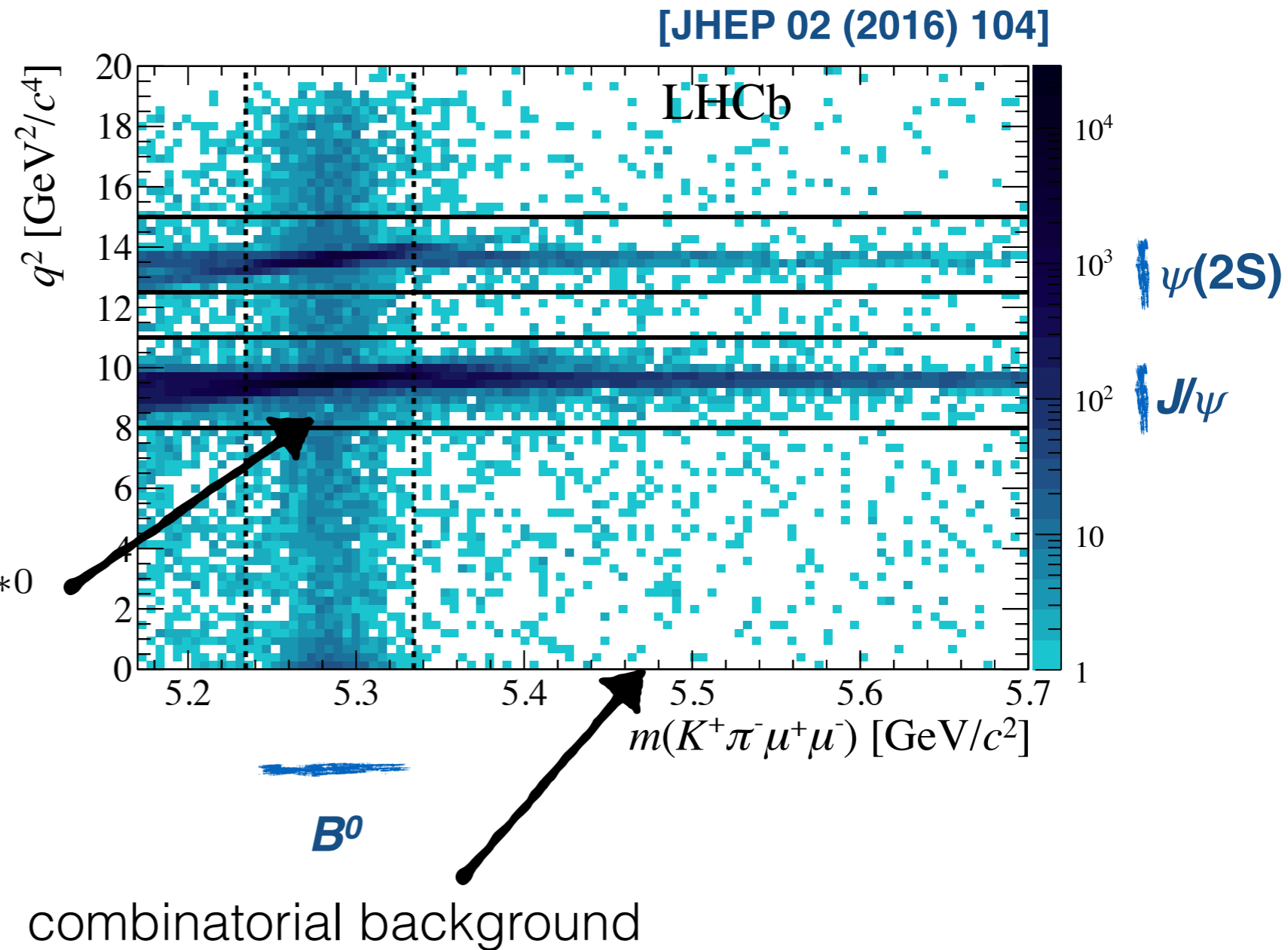
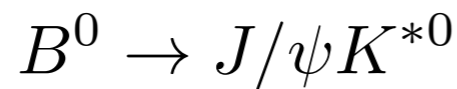
- Normalised the observed yield to $B^0 \rightarrow D^- [\rightarrow K^+ \pi^- \pi^-] D_s^+ [\rightarrow K^+ K^- \pi^+]$ which has a similar topology but no missing energy.



$B^0 \rightarrow K^{*0} \mu^+ \mu^-$ reconstructed candidates

Can select a clean sample of signal events using multivariate classifier.

2398 ± 57 candidates in $0.1 < q^2 < 19 \text{ GeV}^2$ after removing the J/ψ and $\psi(2S)$.



Systematic uncertainty on branching fraction measurements

- Normalise measurements to $B \rightarrow J/\psi X$ control channel.
 - ➔ Cancels luminosity/cross-section/efficiency scale uncertainties.
- Use $B^0 \rightarrow K^{*0} \mu^+ \mu^-$ at LHCb as an example of what systematic uncertainties are important:

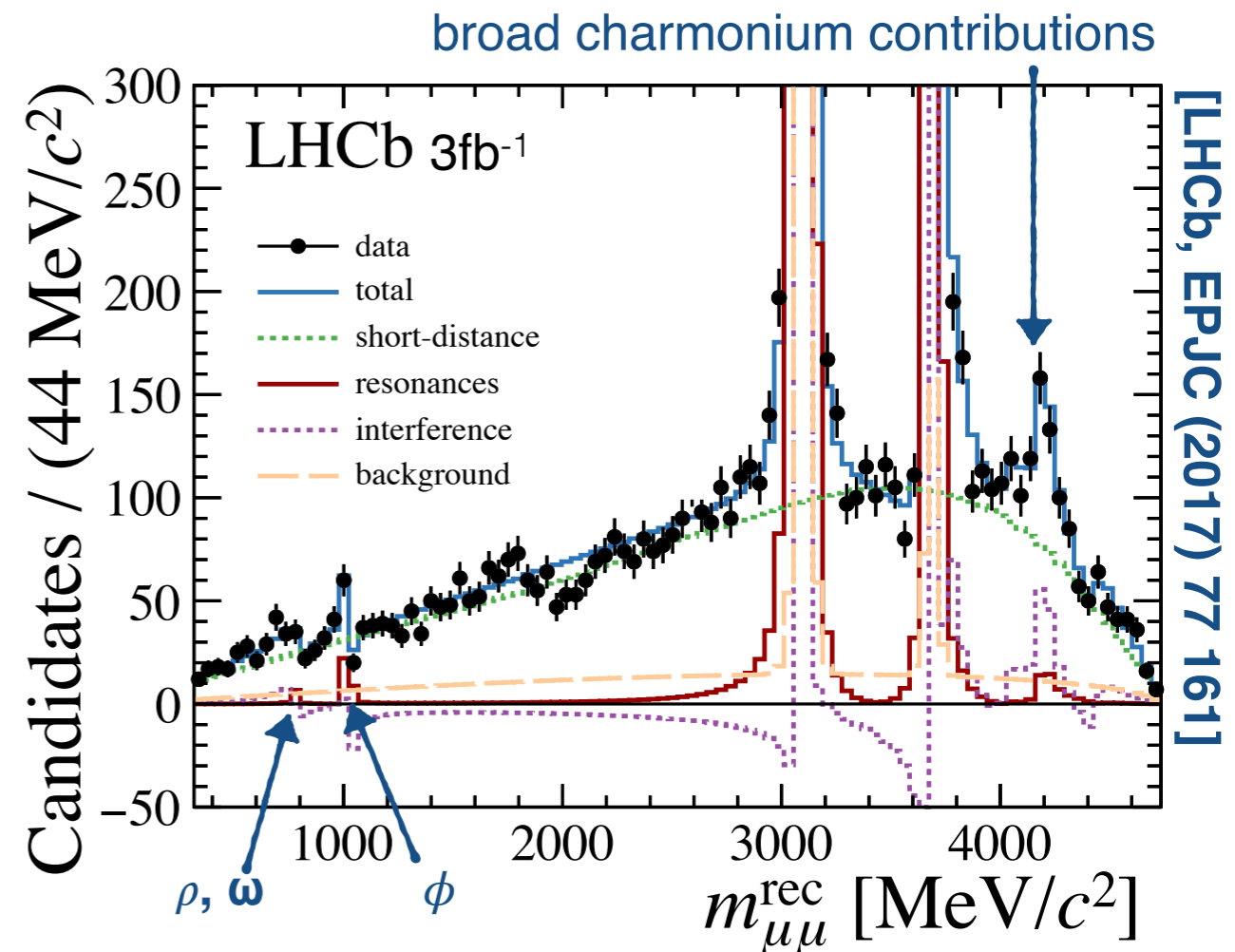
[LHCb, JHEP 12 (2016) 065]

	Source	$F_S _{644}^{1200}$	$d\mathcal{B}/dq^2 \times 10^{-7} (c^4/\text{GeV}^2)$
Need to separate $K^*(892)^0$ from other $K\pi$ contributions	Data-simulation differences	0.008–0.013	0.004–0.021
	Efficiency model	0.001–0.010	0.001–0.012
	S-wave $m_{K\pi}$ model	0.001–0.017	0.001–0.015
	$B^0 \rightarrow K^*(892)^0$ form factors	–	0.003–0.017
	$\mathcal{B}(B^0 \rightarrow J/\psi (\rightarrow \mu^+ \mu^-) K^{*0})$	–	0.025–0.079

Uncertainty on $\mathcal{B}(B \rightarrow J/\psi X)$ normalisation modes is already a limiting factor. Encourage Belle II to update these measurements!

Resonant contributions

- With the large LHC datasets can also explore the shape of the $d\Gamma/dq^2$ spectrum in detail.
- See evidence for broad charmonium states and light quark contributions.
- Can determine relative magnitude/phases of the different contributions.



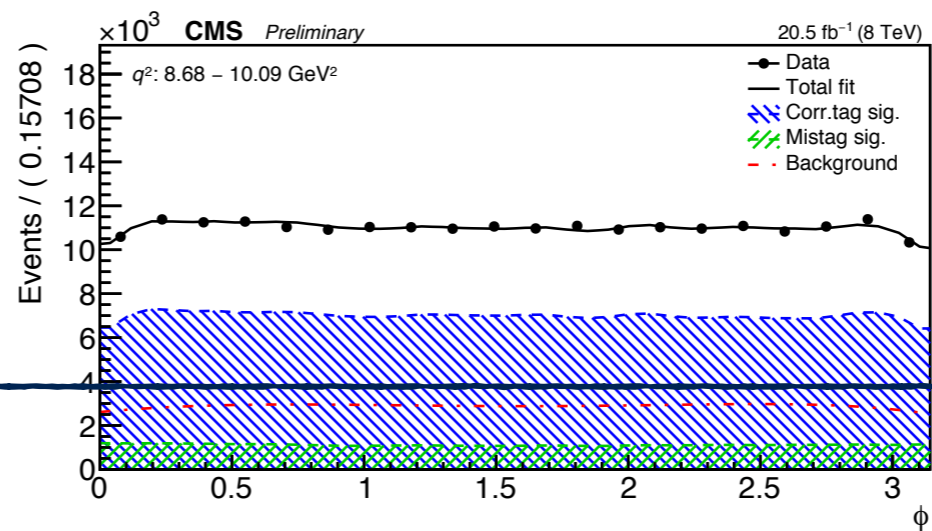
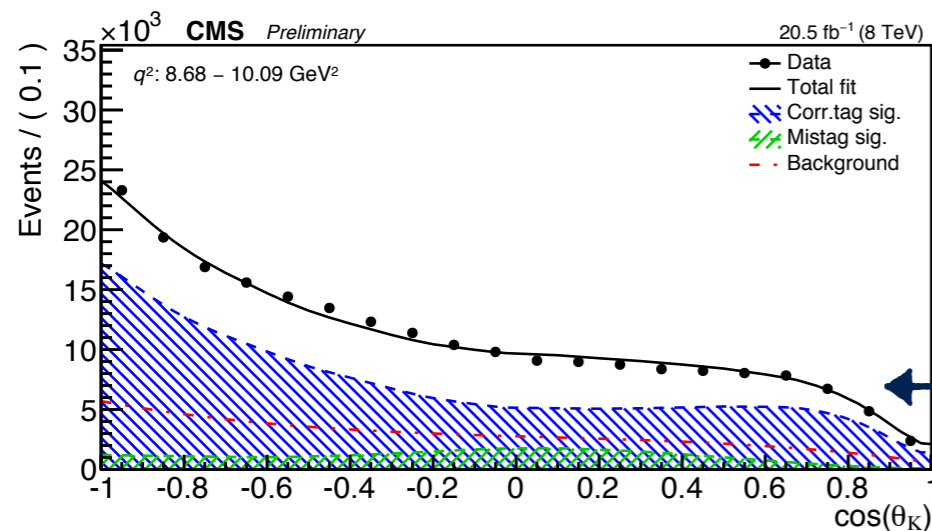
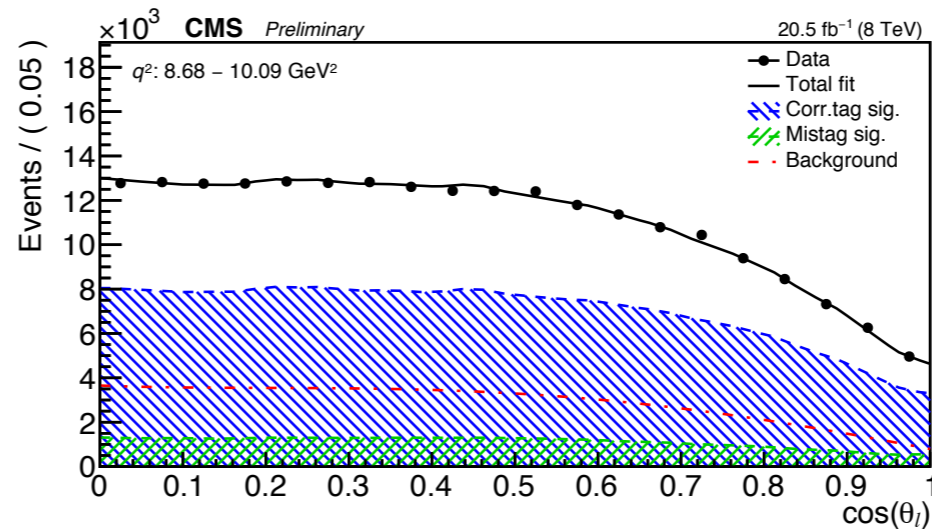
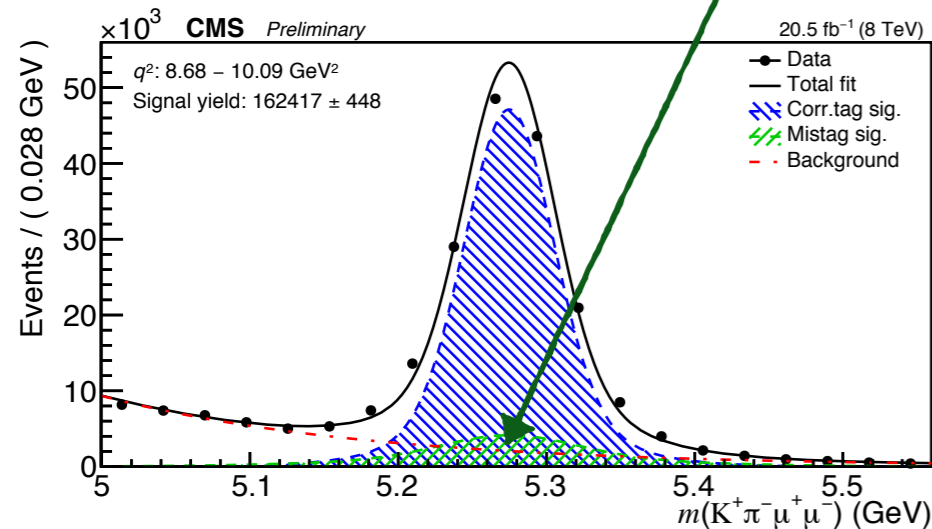
- Data could be used to exclude models proposing new GeV-scale particles as an explanation for R_K/R_{K^*} . [F. Sala & D. Straub, arXiv:1704.06188]

Angular acceptance

- Detector acceptance modelled using MC but can use $B \rightarrow J/\psi K^{*0}$ candidates in data to understand the modelling.

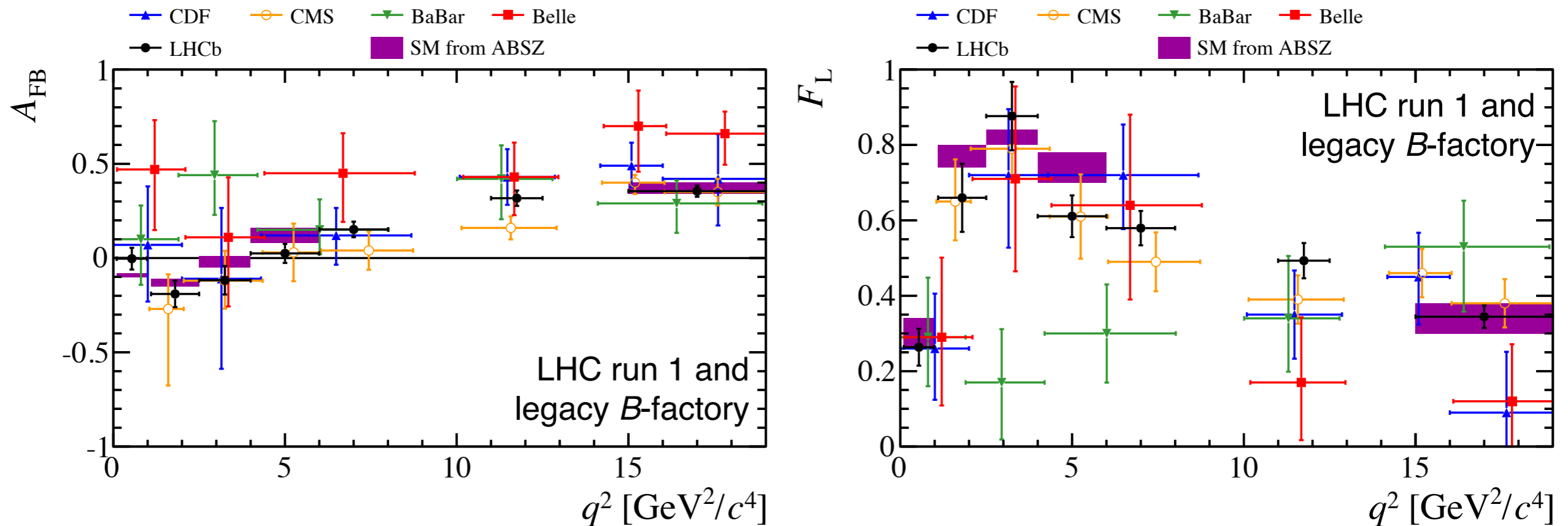
e.g. [CMS-PAS-BPH-15-008]

$K \leftrightarrow \pi$ misid ($\approx 1\%$ of signal in LHCb due to positive PID from RICH detectors)



Parabolic in the absence of any acceptance effects.

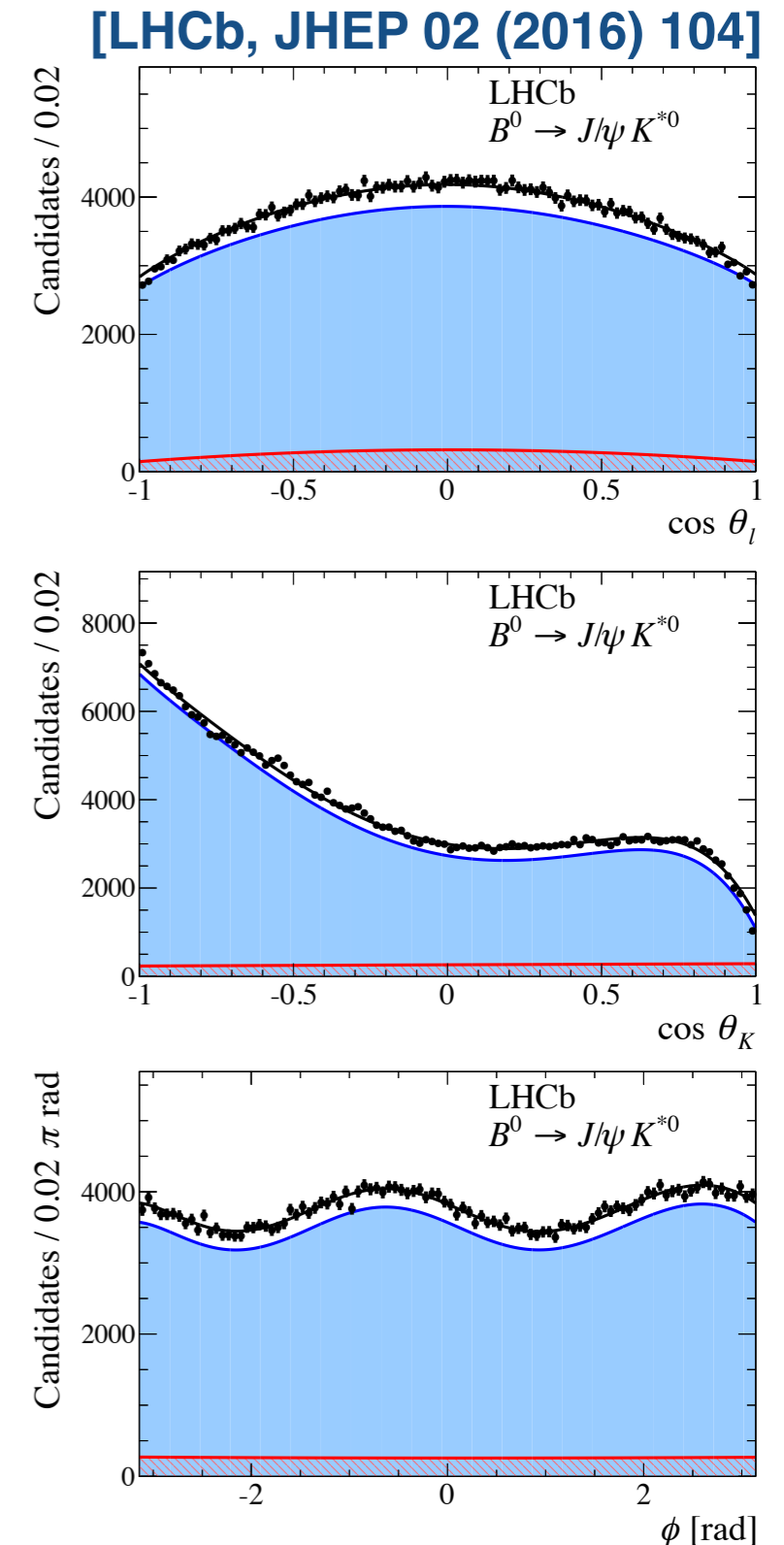
$B^0 \rightarrow K^{*0} \mu^+ \mu^-$ angular observables



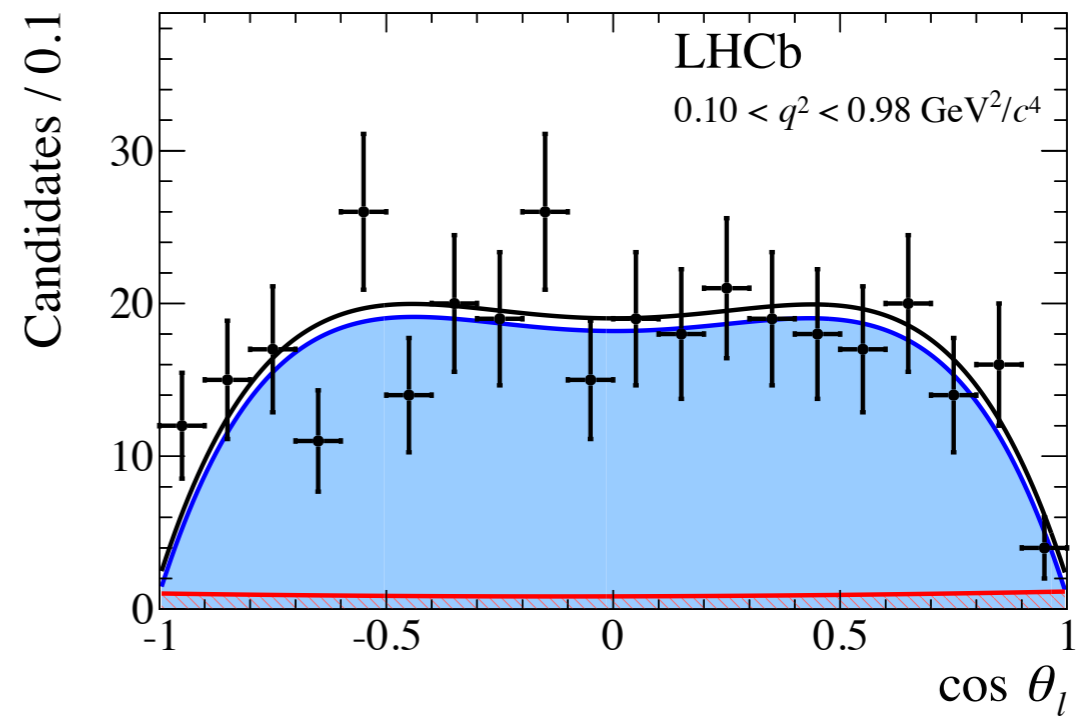
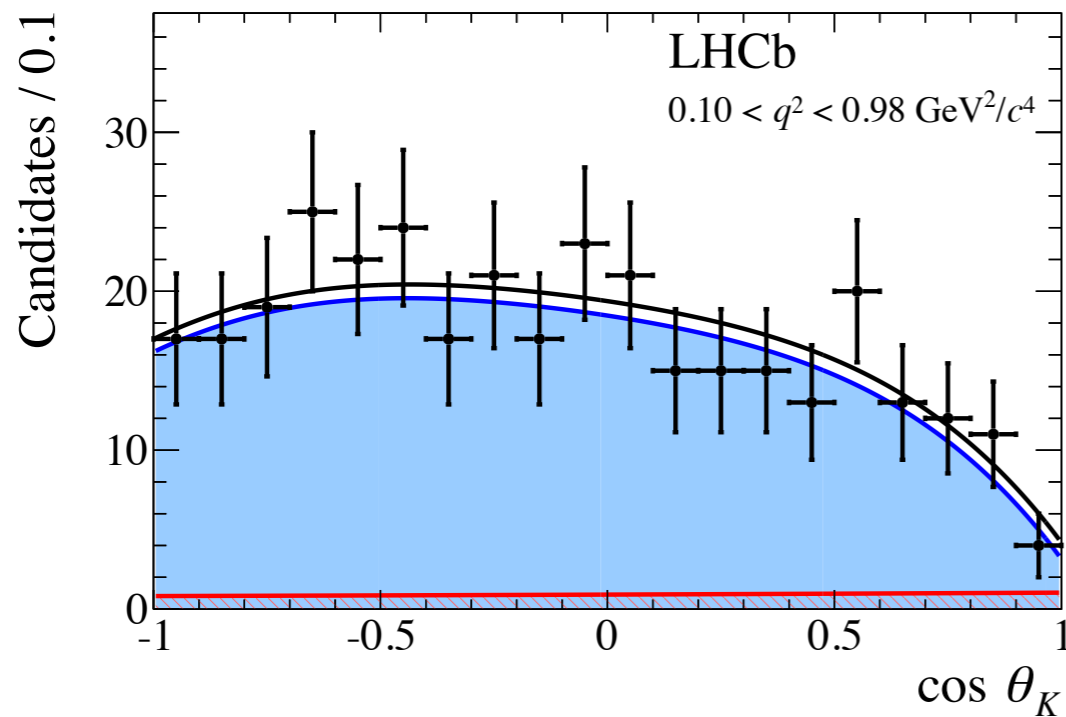
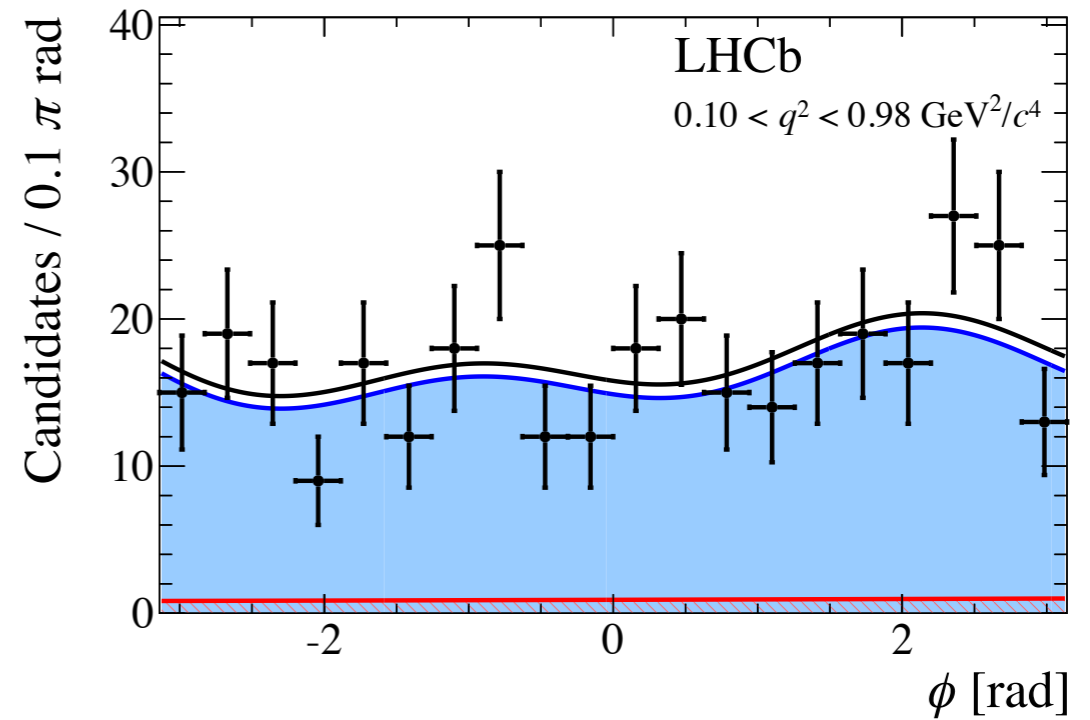
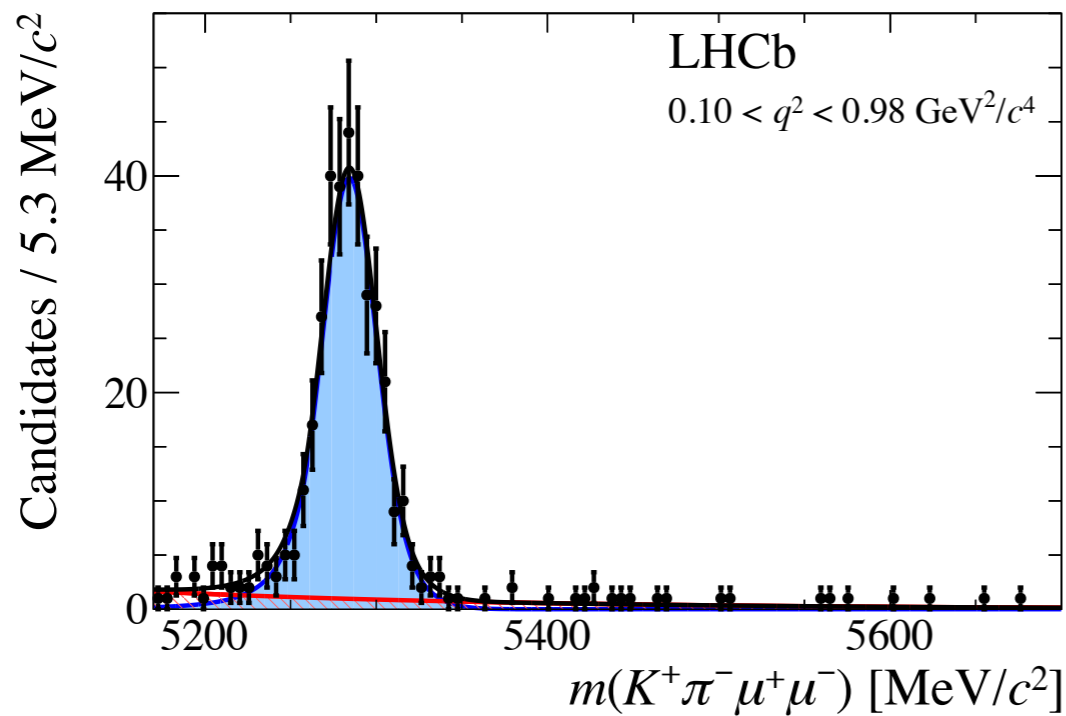
- Overlaying results for F_L and A_{FB} from LHCb [[JHEP 02 \(2016\) 104](#)], CMS [[PLB 753 \(2016\) 424](#)] and BaBar [[PRD 93 \(2016\) 052015](#)] + measurements from CDF [[PRL 108 \(2012\) 081807](#)] and Belle [[PRL 103 \(2009\) 171801](#)].
- SM predictions based on
 - [[Altmannshofer & Straub, EPJC 75 \(2015\) 382](#)]
 - [[LCSR form-factors from Bharucha, Straub & Zwicky, arXiv:1503.05534](#)]
 - [[Lattice form-factors from Horgan, Liu, Meinel & Wingate arXiv:1501.00367](#)]
 } Joint fit performed

$B^0 \rightarrow K^{*0} \mu^+ \mu^-$ angular analysis

- Typically integrate over all but one angle or perform angular folding to reduce the number of observables.
- **LHCb has performed the first full angular analysis of the decay.**
 - ➔ **Access the full set of angular observables and their correlations.**
- Experiments need good control of detector efficiencies and to understand background from decays where the $K\pi$ is in an S-wave configuration.
- Use $B^0 \rightarrow J/\psi K^{*0}$ as a control channel to understand the acceptance of the detector.

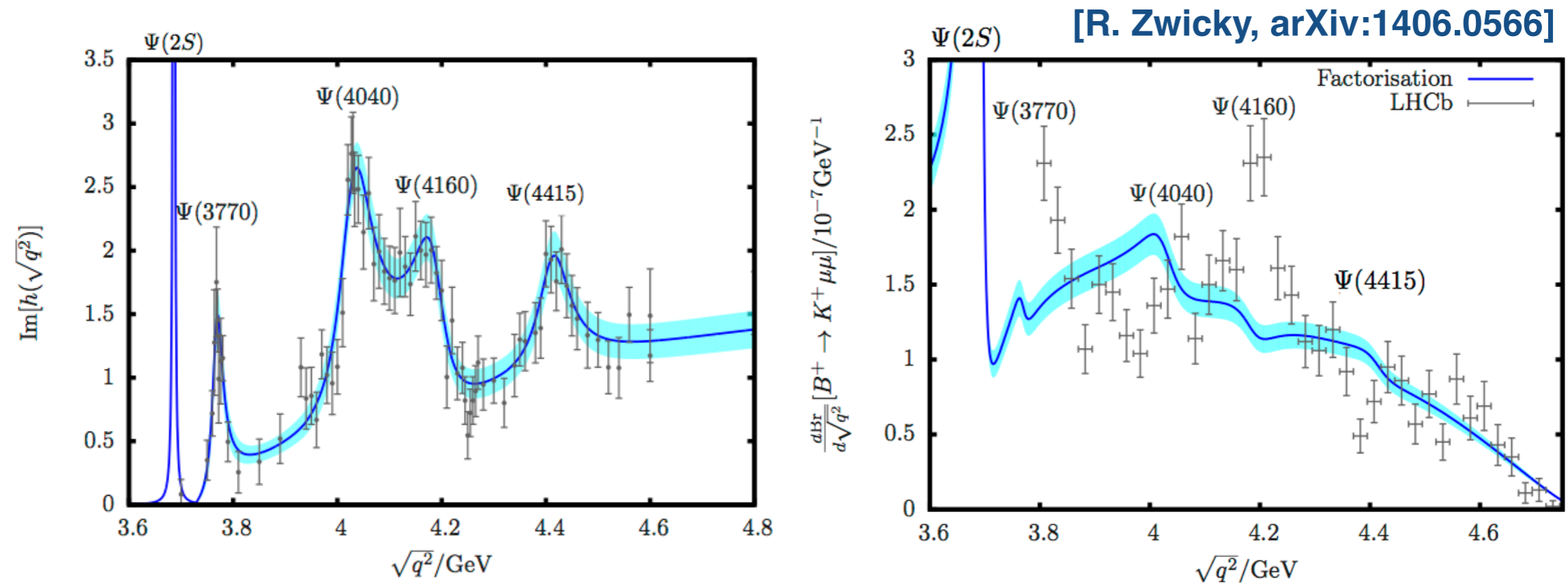


$B^0 \rightarrow K^{*0} \mu^+ \mu^-$ example fit



Resonance structure

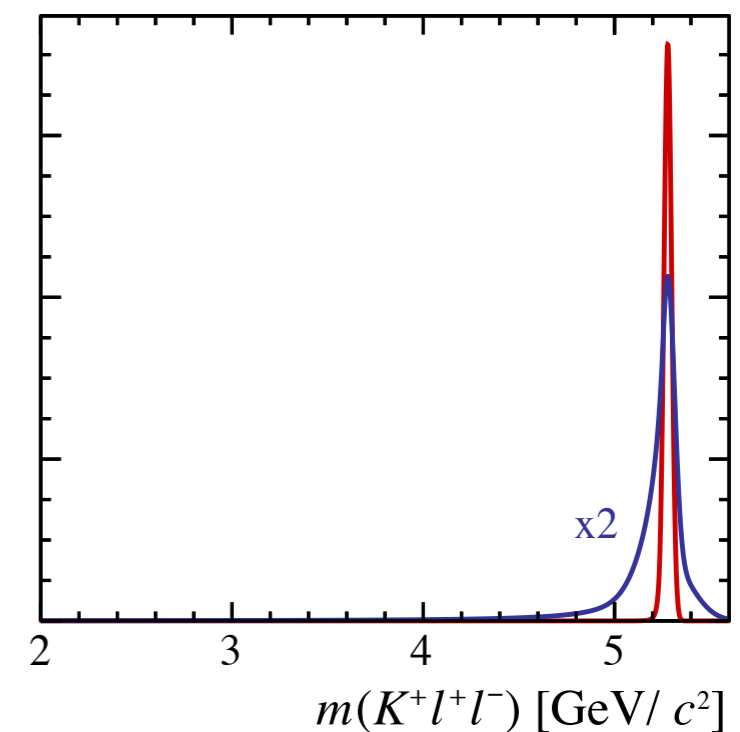
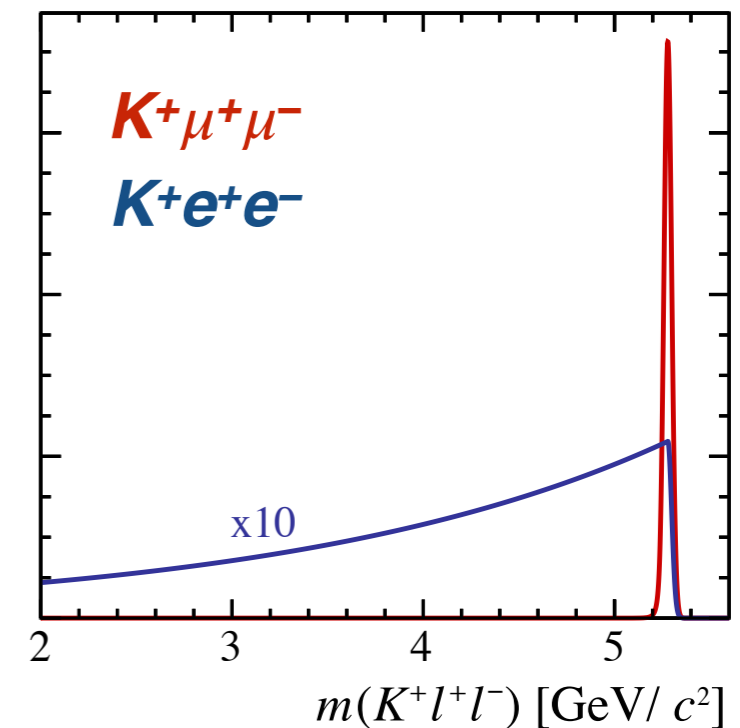
- Can try determine the factorisable charm loop contribution from vacuum polarisation data , i.e. from $\sigma(e^+e^- \rightarrow \text{hadrons})$



- Large difference between prediction and observed spectrum seems to imply that there are huge non-factorisable effects.

Bremsstrahlung recovery

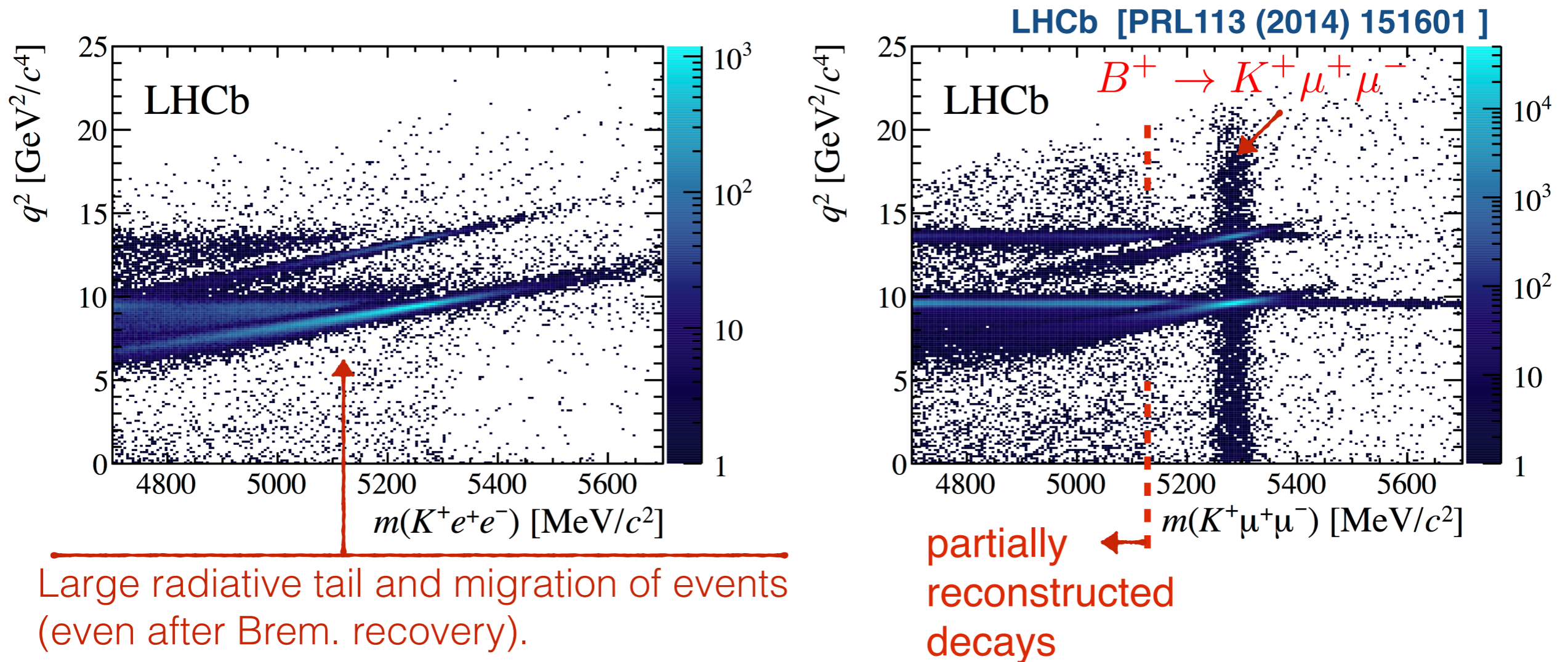
- Two big experimental differences between electrons/muons:
 - ➔ Bremsstrahlung/FSR from the electrons.
 - ➔ Typically require higher trigger thresholds for electrons than muons ($E_T > 3$ GeV c.f. $p_T > 1.76$ GeV/c in 2012) and have a lower tracking efficiency (factor 2 per track).
- Bremsstrahlung causes migration of events in q^2 and in reconstructed B mass.
 - ➔ Recover clusters with $E_T > 75$ MeV/c² to correct for Bremsstrahlung.



↕ Applying brem. recovery

$B^+ \rightarrow K^+ \ell^+ \ell^-$ candidates

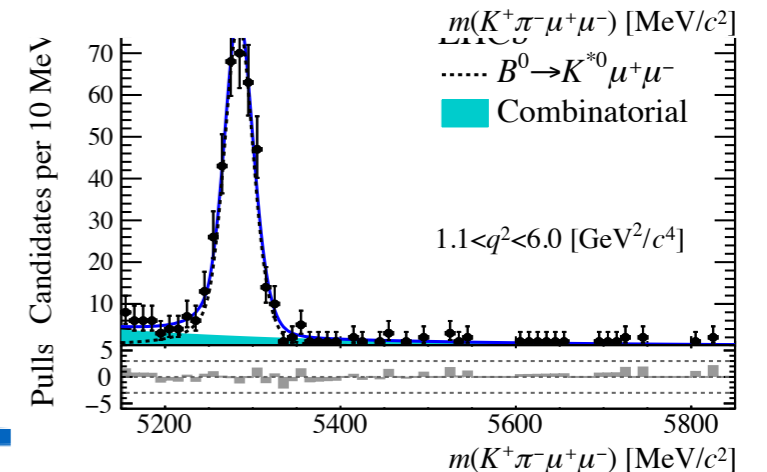
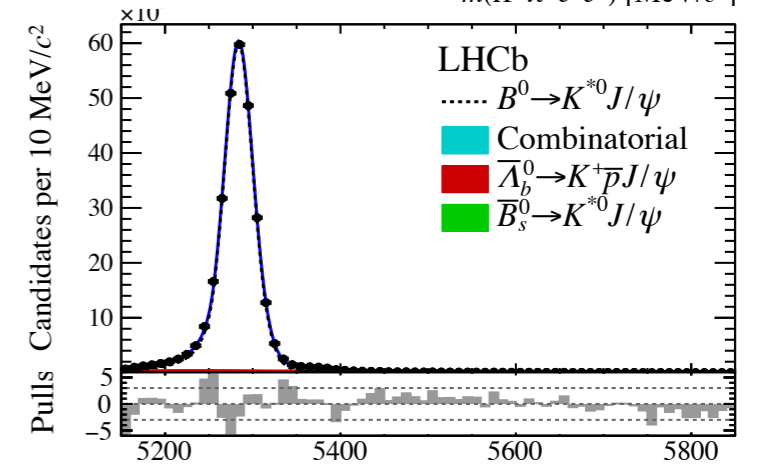
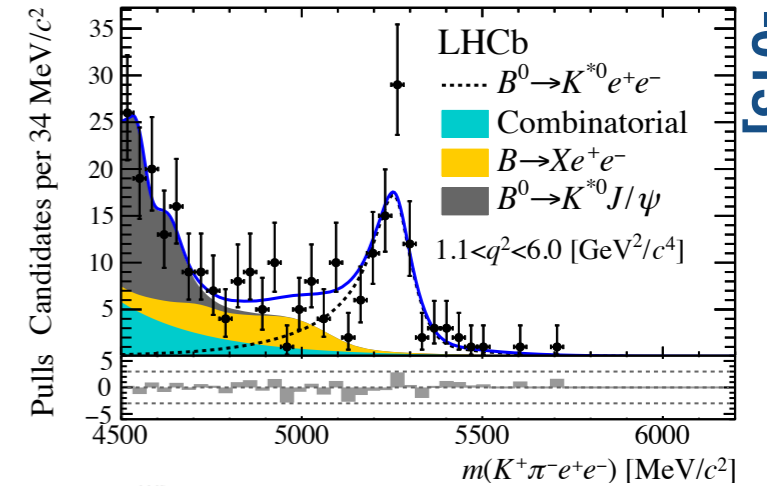
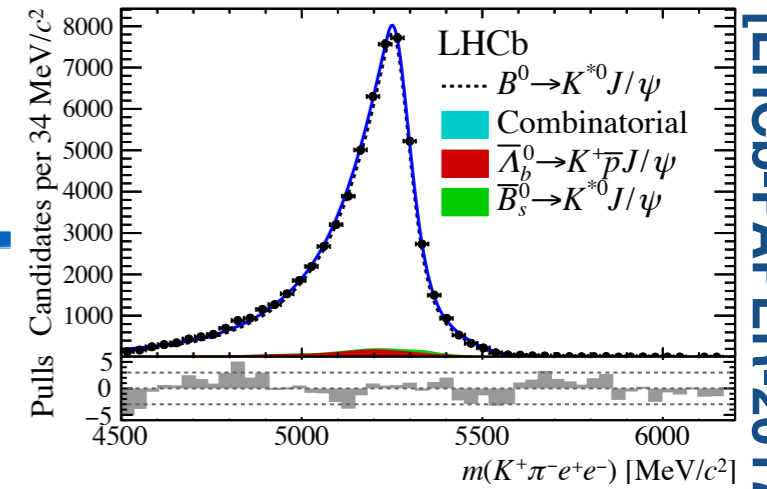
- Even after Bremsstrahlung recovery there are significant differences between dielectron and dimuon final states:



Evaluating R_K and R_{K^*}

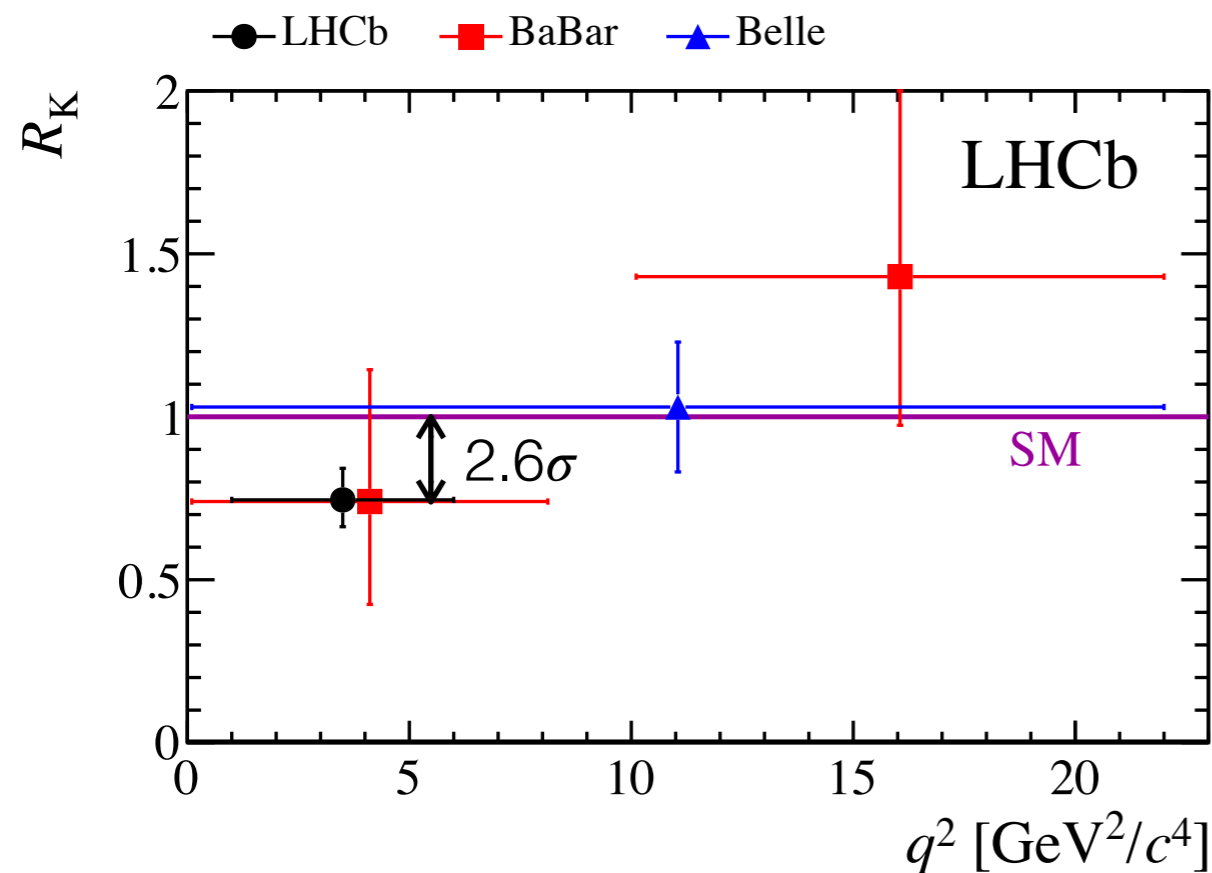
- Simultaneous analysis of three categories of events:
 1. Events triggered by one or both electrons.
 2. Events triggered by the kaon or pion.
 3. Events triggered by the other b -hadron in the event.
- Measure a double ratio to cancel out large reconstruction differences, e.g.:

$$R_{K^*} = \frac{N[B^0 \rightarrow K^{*0} \mu^+ \mu^-] / \epsilon[B^0 \rightarrow K^{*0} \mu^+ \mu^-]}{N[B^0 \rightarrow K^{*0} e^+ e^-] / \epsilon[B^0 \rightarrow K^{*0} e^+ e^-]} \times \frac{N[B^0 \rightarrow K^{*0} J/\psi(e^+ e^-)] / \epsilon[B^0 \rightarrow K^{*0} J/\psi(e^+ e^-)]}{N[B^0 \rightarrow K^{*0} J/\psi(\mu^+ \mu^-)] / \epsilon[B^0 \rightarrow K^{*0} J/\psi(\mu^+ \mu^-)]}$$

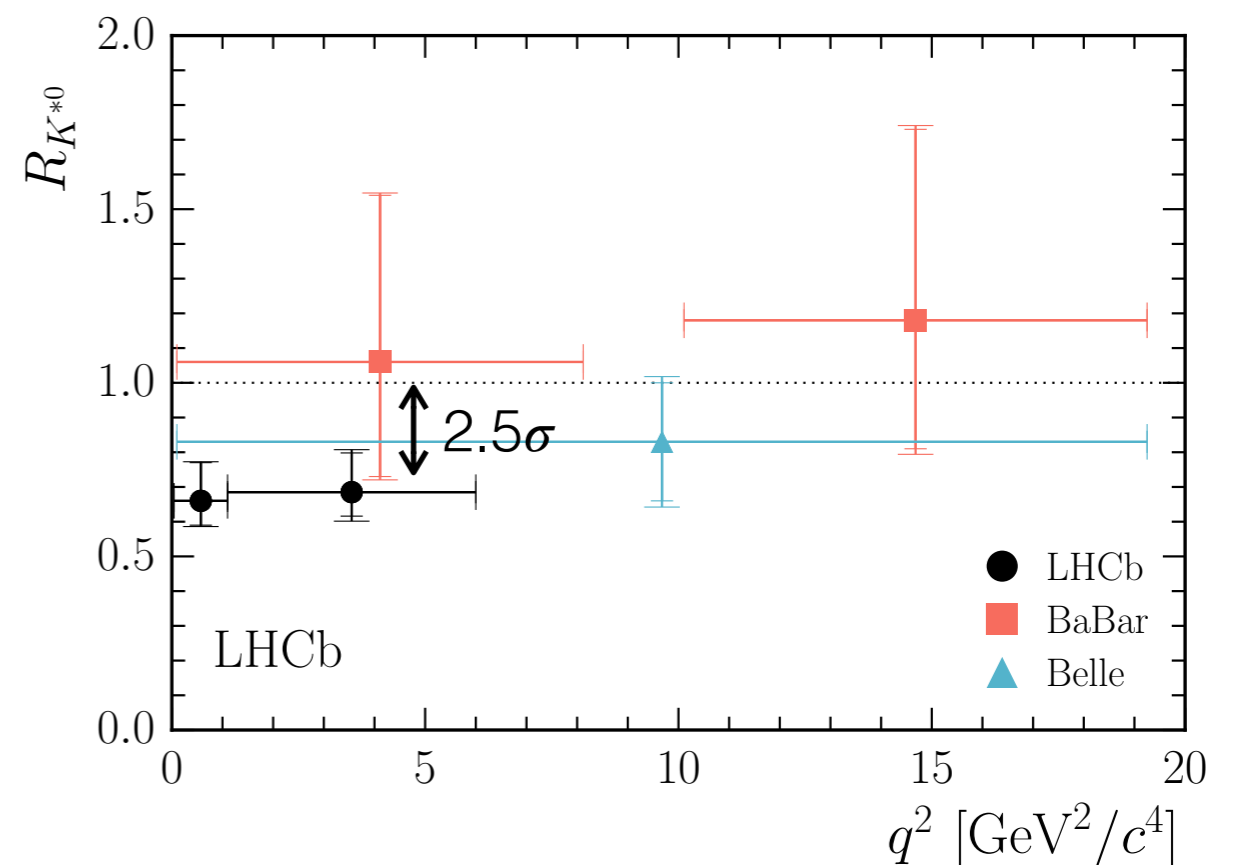


Lepton universality tests

- We have interesting hints of non-universal lepton couplings in LHCb run 1 dataset:



[LHCb, PRL113 (2014) 151601]
 [LHCb, LHCb-PAPER-2017-013]
 [BaBar, PRD 86 (2012) 032012]
 [Belle, PRL 103 (2009) 171801]



NB $R_K \approx 0.8$ is a prediction of one class of model explaining the $B^0 \rightarrow K^{*0} \mu^+ \mu^-$ angular observables, see $L_\mu - L_\tau$ models
W. Altmannshofer et al. [PRD 89 (2014) 095033]

R_X results

$$R_{K^{*0}} = \begin{cases} 0.66 \pm_{-0.07}^{+0.11} (\text{stat}) \pm 0.03 (\text{syst}) & \text{for } 0.045 < q^2 < 1.1 \text{ GeV}^2/c^4, \\ 0.69 \pm_{-0.07}^{+0.11} (\text{stat}) \pm 0.05 (\text{syst}) & \text{for } 1.1 < q^2 < 6.0 \text{ GeV}^2/c^4. \end{cases}$$

[LHCb, LHCb-PAPER-2017-013]

$$R_{K^+} = 0.745 \pm_{-0.07}^{+0.09} (\text{stat}) \pm 0.04 (\text{syst}) \quad \text{for } 1.0 < q^2 < 6.0 \text{ GeV}^2/c^4.$$

[LHCb, PRL113 (2014) 151601]

- QED effects are well modelled by PHOTOS. They enter as R_K and R_{K^*} as

$$\frac{\alpha_{\text{EM}}}{\pi} \log \left(\frac{m_\mu^2}{m_e^2} \right)$$

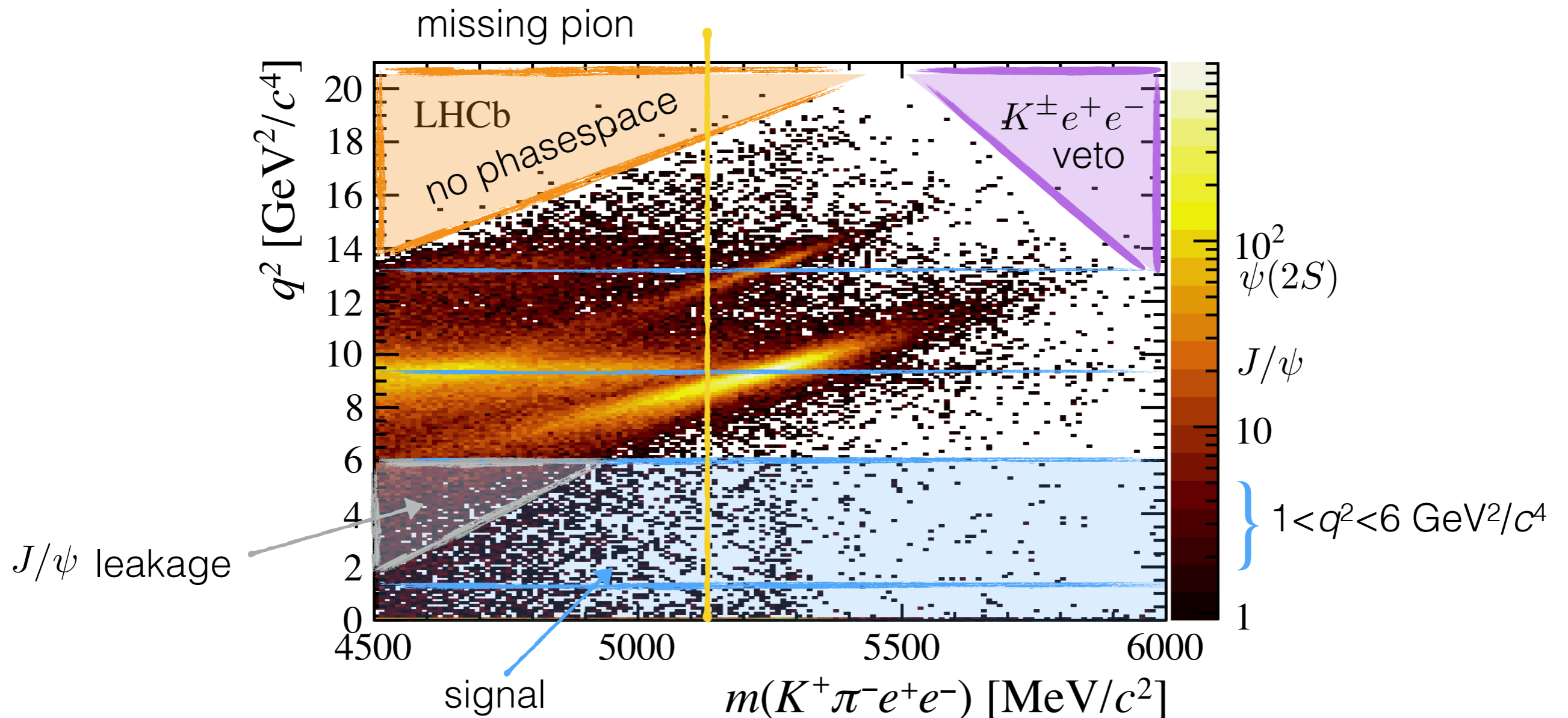
see **[Isidori et al. EPJC 76 (2016)]**.

These effects are accounted for in the analysis.

- Can also consider decays to other hadronic systems as the prediction is (almost) independent of mass/spin of hadronic final state.
- Await results from LHCb run II dataset/first data from Belle II.

R_{K^*} backgrounds

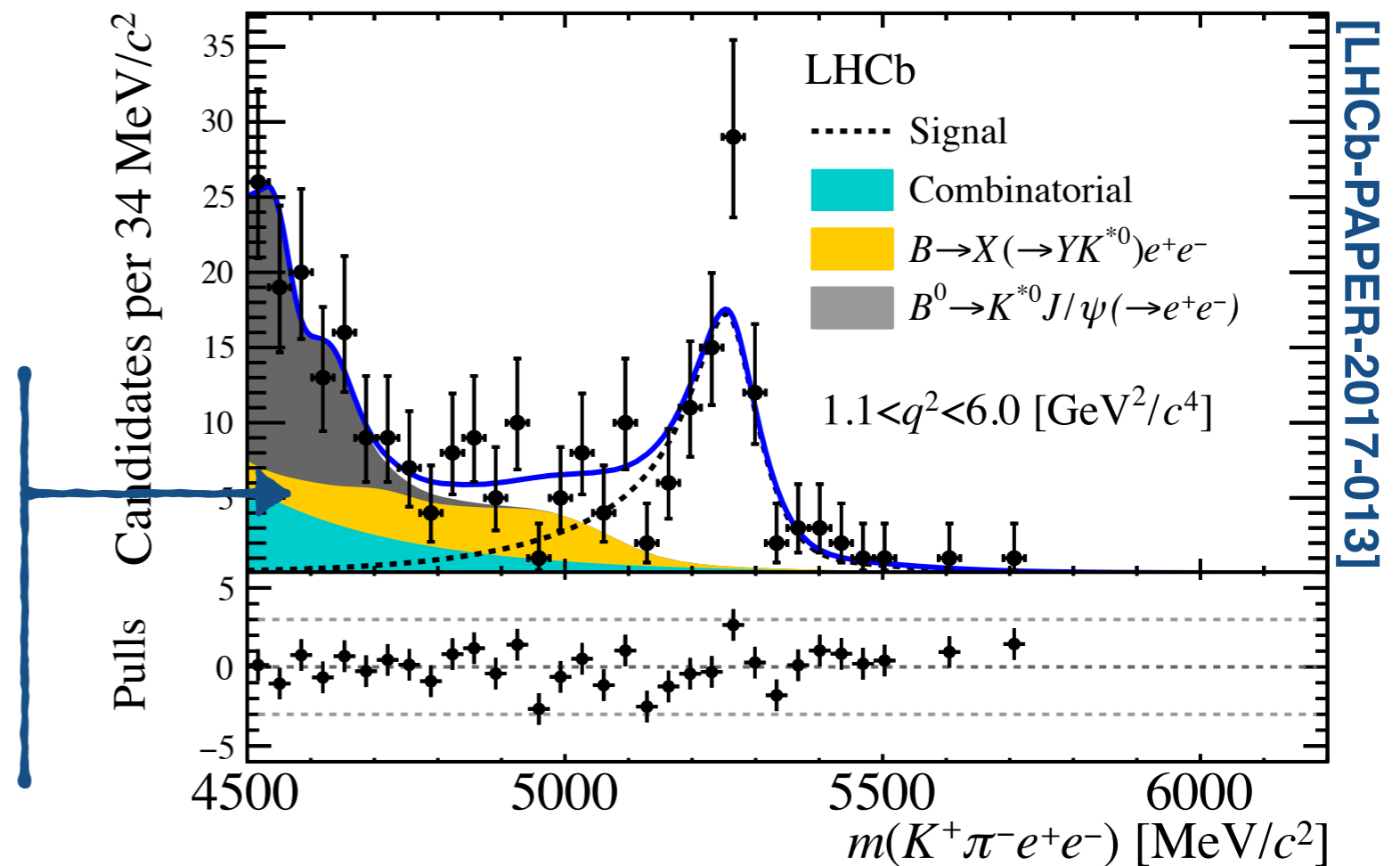
- It is much more difficult to separate dielectron final-state from physics backgrounds.



R_{K^*} mass fit

- Example fit for the L0Electron trigger category:

Partially reconstructed background is poorly known and comprises the largest source of systematic uncertainty

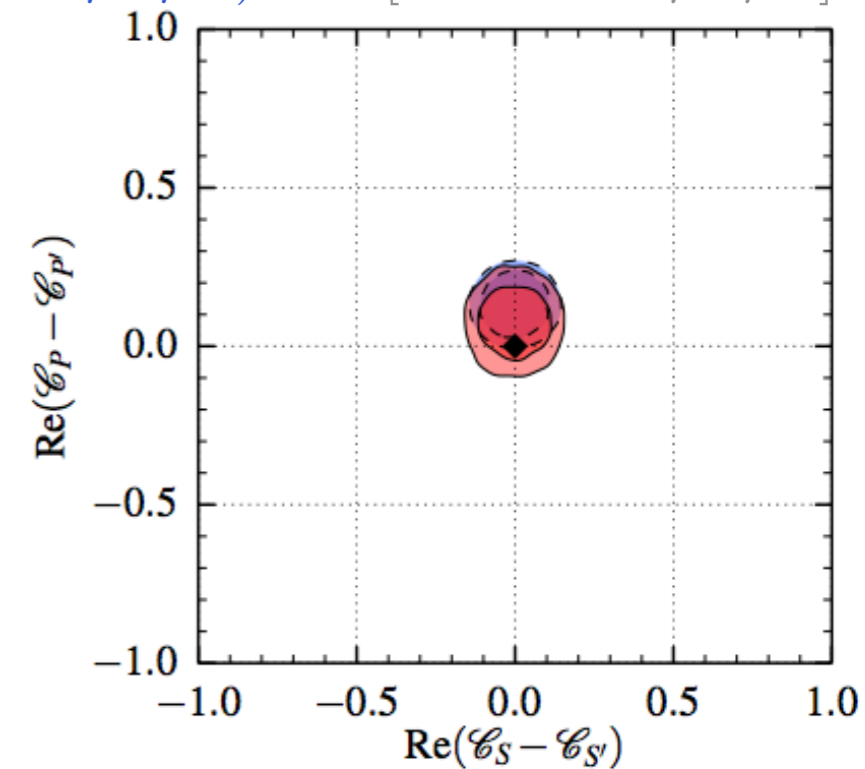
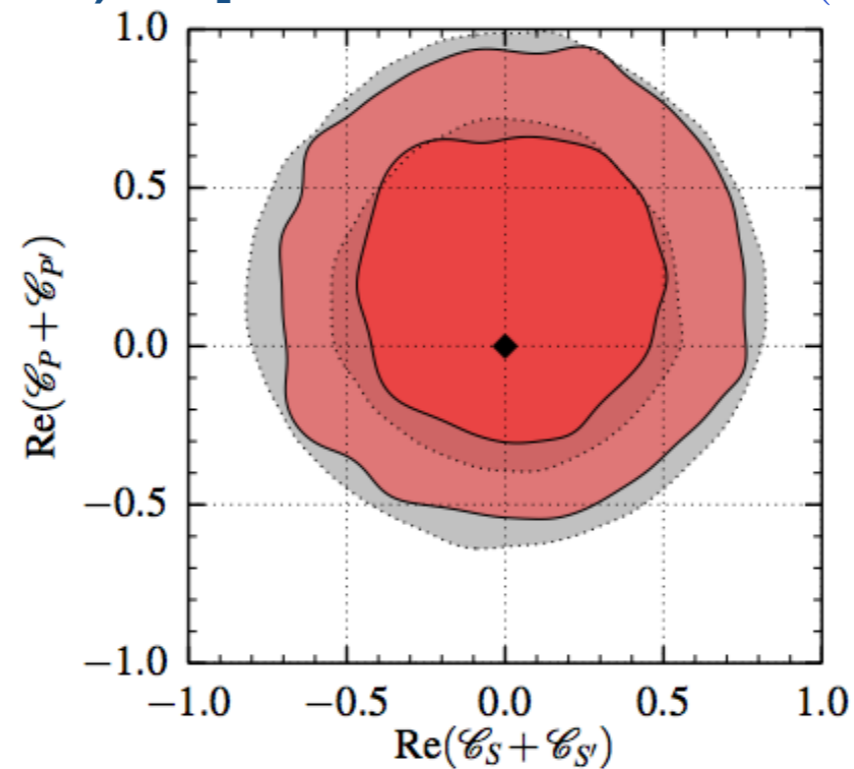
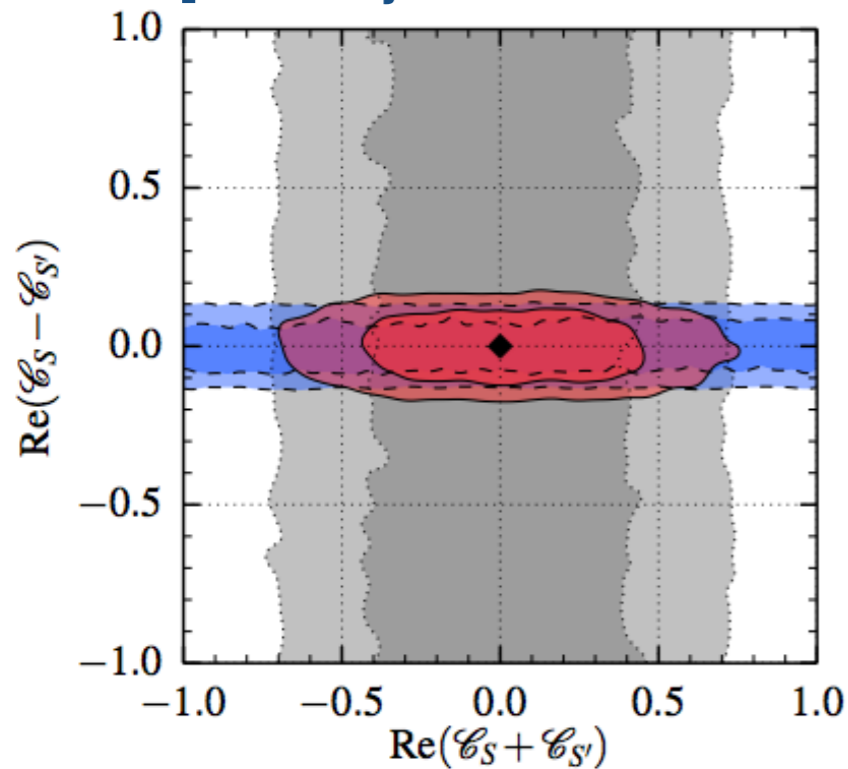


$B^+ \rightarrow K^+ \ell^+ \ell^-$

- Angular distribution of $B^+ \rightarrow K^+ \ell^+ \ell^-$ is a null test of SM, but can be sensitive to new scalar/pseudoscalar/tensor contributions, e.g.

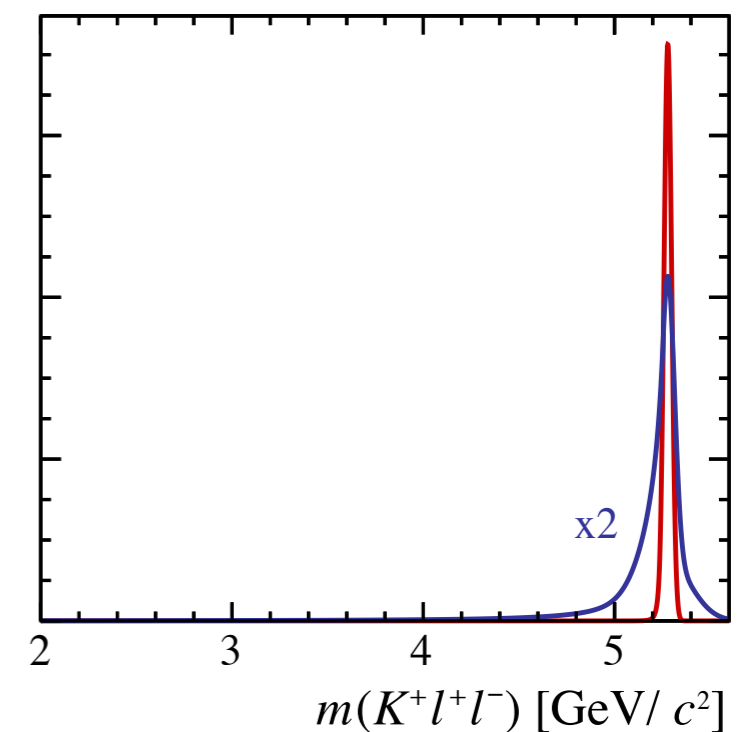
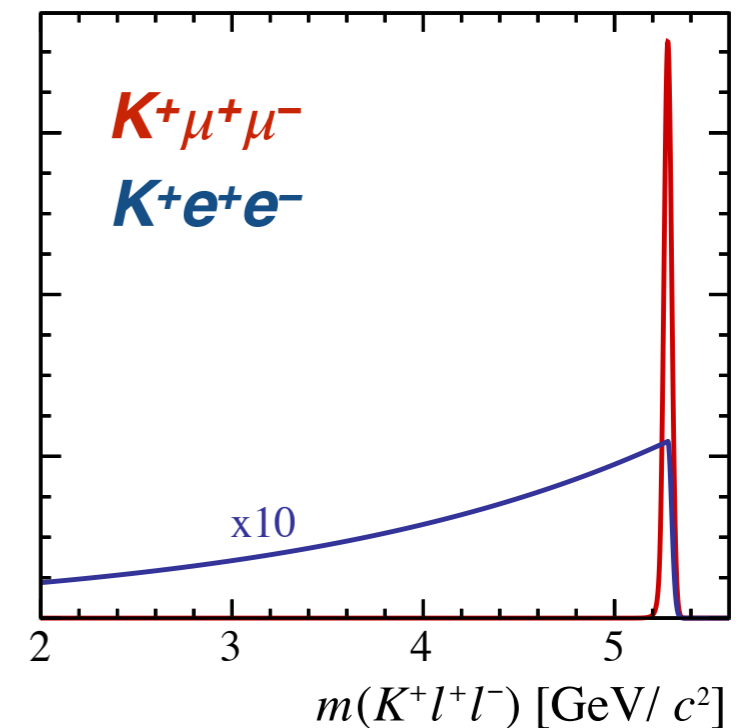
[F. Beaujean et al. EPJC 75 (2015) 456]

Combination $\mathcal{B}(B_s \rightarrow \mu^+ \mu^-)$ $F_H[B^+ \rightarrow K^+ \mu^+ \mu^-]$



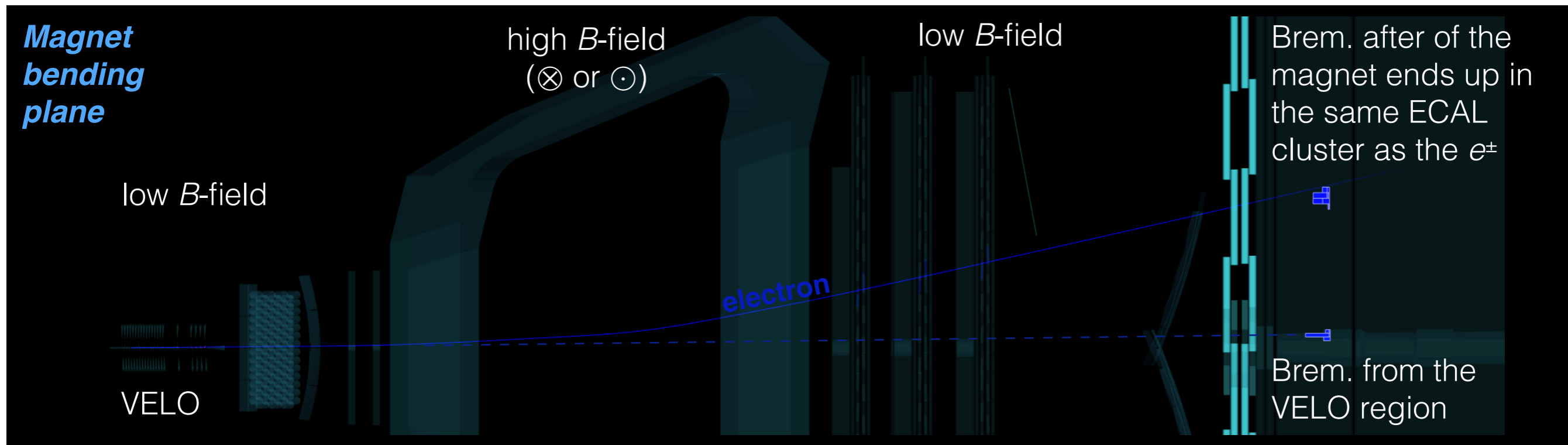
Bremsstrahlung recovery

- Two big experimental differences between electrons/muons:
 - ➔ Bremsstrahlung/FSR from the electrons.
 - ➔ Typically require higher trigger thresholds for electrons than muons ($E_T > 3$ GeV c.f. $p_T > 1.76$ GeV/c in 2012) and have a lower tracking efficiency.
- Bremsstrahlung causes migration of events in q^2 and in reconstructed B mass.
 - ➔ Recover clusters with $E_T > 75$ MeV/c² to correct for Bremsstrahlung.

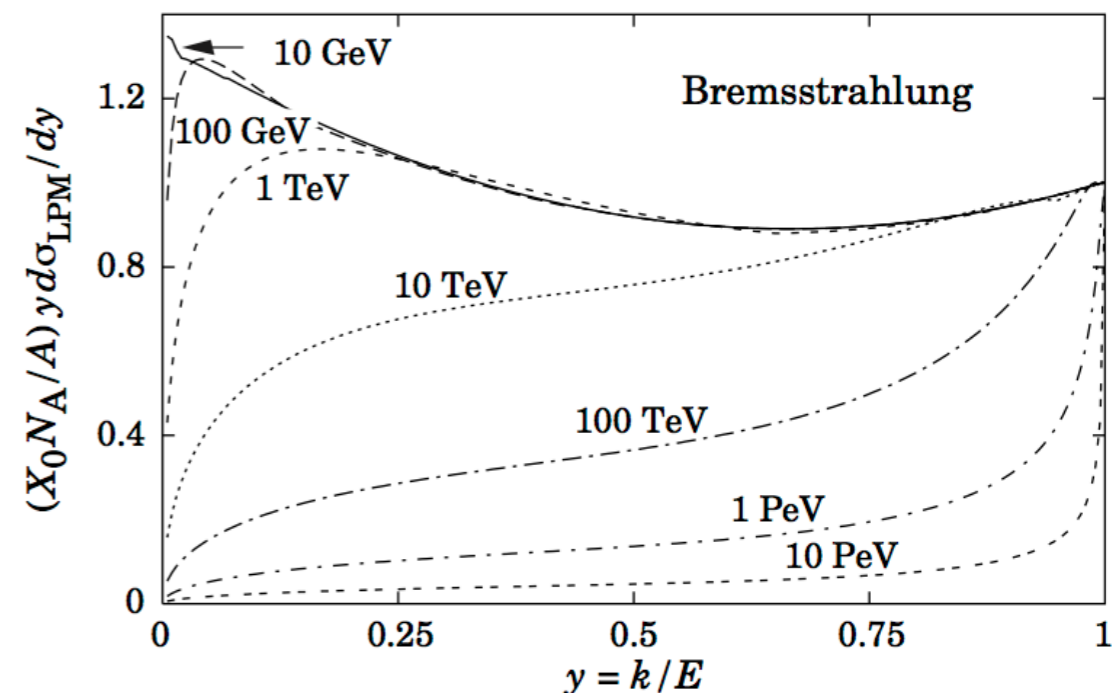


↕ Applying brem. recovery

Bremsstrahlung recovery



- Large energy loss through Bremsstrahlung in the detector (significant fraction of the e^\pm energy).
- Recover clusters with $E_T > 75 \text{ MeV}/c^2$ to correct for Bremsstrahlung emission.



[<http://pdg.lbl.gov/2017/reviews/rpp2016-rev-passage-particles-matter.pdf>]

$R(K^*)$ comparison

